Collection of Severe Weather Event articles from ECMWF Newsletters 2014-2019

Linus Magnusson

This document contains a collection of severe weather event articles from ECMWF Newsletters 139-158, spanning the period 2014-2019. Each case was selected from ECMWF Severe Event Catalogue (https://confluence.ecmwf.int/display/FCST/Severe+Event+Catalogue) and extended into a Newsletter article. The aim of each article has been to illustrate predictability on different time-scales, raise awareness of limitations of the forecasting system, highlight recent and ongoing model developments and show suitable forecast products of the events.

I am extremely grateful to all the authors contributing to the articles, to Georg Lentze and Bob Riddaway for editing the articles, to Anabel Bowen for editing the figures and to David Richardson for reviewing the contents of all articles.

Newsletter Issue	Title
139	Windstorms in northwest Europe in late 2013
140	Forecasting the severe flooding in the Balkans
141	Recent cases of severe convective storms in Europe
142	Forecasts for a fatal blizzard in Nepal in October 2014
143	Forecasts for US east coast snow storm in January 2015
144	ECMWF forecasts for tropical cyclone Pam
145	Predicting this year's European heat wave
146	Forecasting flash floods in Italy
147	Wind and wave forecasts during Storm Gertrude/Tor
148	Forecasts showed Paris flood risk well in advance
149	Predicting heavy rainfall in China
150	Flash floods over Greece in early September 2016
151	The cold spell in eastern Europe in January 2017
152	ECMWF supports flood disaster response in Peru
153	Predictions of tropical cyclones Harvey and Irma
154	Two storm forecasts with very different skill
155	Predicting extreme snow in the Alps in January 2018
156	Forecasting convective rain events in late May
157	Forecasting the 2018 European heatwave
158	Predicting multiple weather hazards over Italy

Windstorms in northwest Europe in late 2013

TIM HEWSON, LINUS MAGNUSSON, OYVIND BREIVIK, FERNANDO PRATES, IVAN TSONEVSKY, HANS (J.W.) DE VRIES

The winter period of 2013/14 has been very active in terms of windstorms affecting northwest Europe. This article provides a short summary of two such storms, from 28 October (Christian) and 5 December (Xaver), and the handling thereof by the ECMWF IFS (Integrated Forecasting System). It is shown that for both storms IFS output provided an indication of high winds 5 to 6 days in advance. This is important because a key component of ECMWF's strategy is to provide Member States' National Meteorological Services with reliable forecasts of severe weather across the medium range.

Figure 1 shows a model-based estimate of areas where the 5-year return period of 24-hour maximum wind gust was exceeded for Christian and for Xaver. Here we have used ERA-Interim forecasts as a proxy for observations, with red squares denoting those grid points where maximum wind gust in the short-range (0–24 hour) forecast from ERA-Interim exceeded the 5-year return period value. Return period values were first estimated by fitting the generalised extreme value distribution to a 20-year block of annual maximum wind gust (again using 0–24 hour ERA-Interim forecasts). The results in Figure 1 suggest that in some locations these were indeed very rare events.

Whilst the representation of extreme gusts in windstorms in ERA-Interim suffers from resolution limitations, this issue can to some extent be circumvented by comparing model climate with model forecast, as we have done here. Indeed similar results are seen in real observations exceeding the 5-year event for Christian over Germany and the Netherlands, as computed by the 'European Climate Assessment and Dataset' (ECA&D).

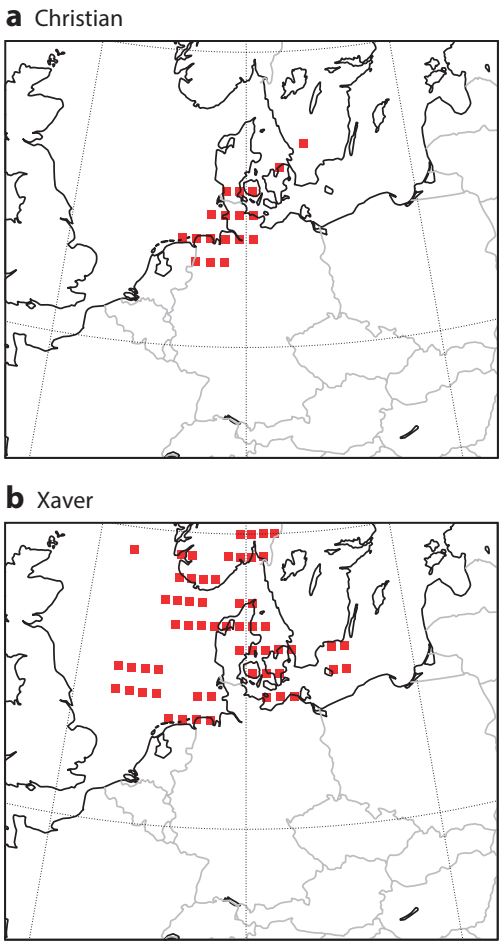

Figure 1 Areas exceeding the 5-year return period of 24-hour maximum wind gust for windstorms (a) Christian and (b) Xaver as diagnosed using the ERA-Interim reanalysis as a proxy for observations.

28 October (Christian)

On 28 October a small but vicious windstorm hit northwest Europe, killing 19 people (8 in Germany, 5 in UK, 3 in the Netherlands, 2 in Denmark and 1 in France) and causing extensive disruption. The highest ever wind gust for Denmark was measured at Kegnäs on Als (53 ms^{-1}). The storm was named Christian by the Institute of Meteorology at Berlin's Free University, though other institutions have used alternative names including St Jude and Simone.

The cyclone first appeared, as a cold front wave, south of Nova Scotia late on 25 October. It then transferred rapidly east-northeast and deepened, with the centre moving into southern Sweden late on the afternoon of the 28th. According to the Met Office surface synoptic charts the 6-hour period of most rapid deepening was 06 to 12 UTC on the 28th (fall of 9 hPa), between eastern England and the eastern North Sea. It was during this period, and the subsequent few hours, that the strongest surface gusts were recorded, south of the track.

Figure 2e shows observed maximum wind gusts during the 28th (24-hour period). The band of very strong gusts started in Brittany in France and followed the English Channel and southern England, up through the southern North Sea and on towards Denmark, but with exceptional values reserved for northern parts of The Netherlands, northernmost Germany and southern Denmark. Strong wind gusts were also experienced along the Baltic Sea coasts. The surface pressure field around the storm at 12 UTC on 28th can be seen on Figure 2d (this is actually a 12-hour forecast, but is quite accurate).

AFFILIATIONS

Tim Hewson, Linus Magnusson, Oyvind Breivik, Fernando Prates, Ivan Tsonevsky: ECMWF, Reading, UK

Hans (J.W.) de Vries: KNMI, De Bilt, The Netherlands

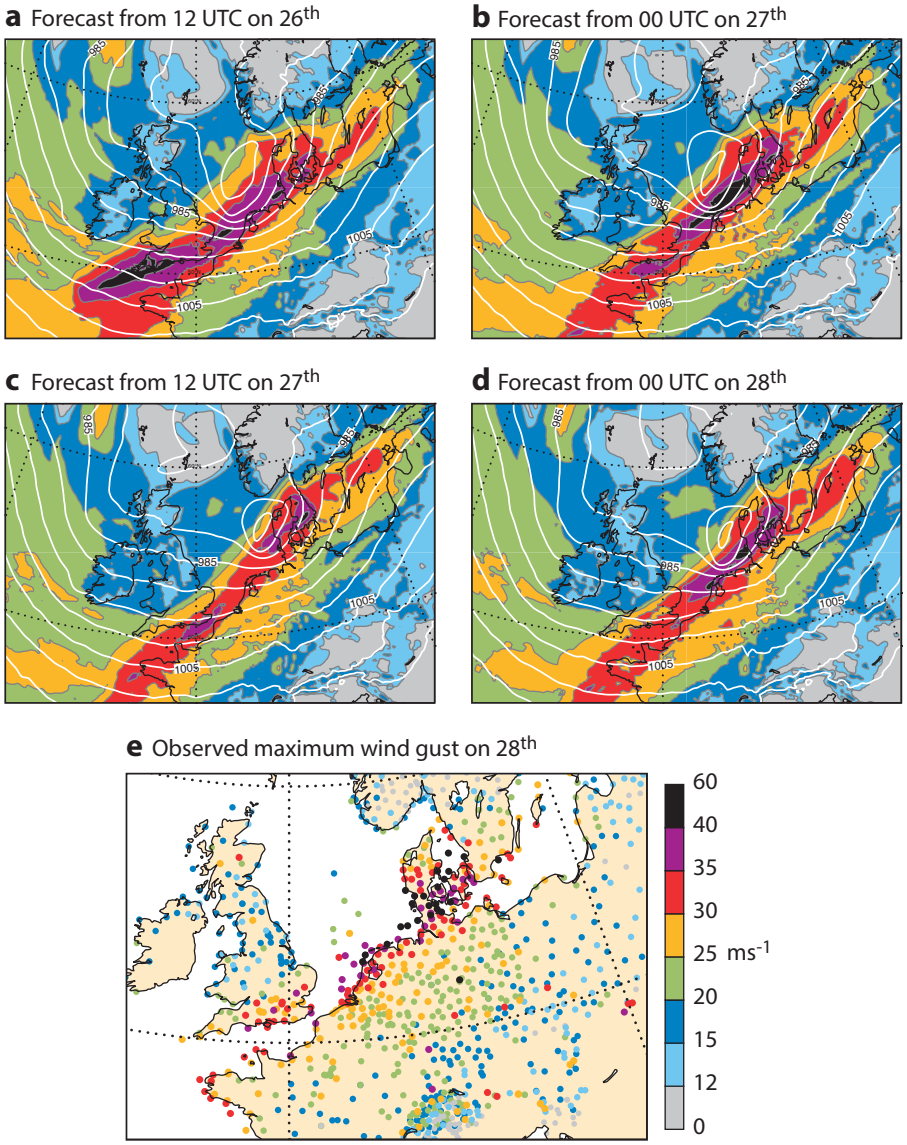

Figure 2 Forecasts of 24-hour maximum wind gust between 00 and 24 UTC on 28 October (shading) with the mean-sea-level pressure for 12 UTC on the 28th (contours) from HRES from data times (a) 12 UTC on 26 October, (b) 00 UTC on 27 October, (c) 12 UTC on 27 October and (d) 00 UTC on 28 October 2013. Panel (e) shows verifying data from observations.

High-resolution forecast

Figures 2a to 2d show the 24-hour maximum wind gust for the 28th from the high-resolution forecasts (HRESs) starting at 48, 36, 24 and 12 hours before 12 UTC on the 28th. HRES from 00 UTC on the 28th (Figure 2d) and 00 UTC on the 27th (Figure 2b) both agree well with observations. However, the forecast from in-between, from 12 UTC on the 27th (Figure 2c), is less good, showing less strong gusts in general, notably over the far north of the Netherlands. Meanwhile, forecasts from data times before 00 UTC on the 27th, whilst capturing peak intensity quite well, tended to develop the storm too soon, and as a result placed the strongest winds too far to the southwest, and often over the sea. The forecast from 12 UTC on the 26th (Figure 2a) is one such example – note the peak over and southwest of southwest England.

Preliminary investigations of observational data suggest that the most extreme winds associated with this windstorm were probably attributable to a 'sting jet' (after *Browning*, 2004). This is a very rare phenomenon comprising a pulsing stream of strong winds that can descend rapidly from within the cyclone's cloud head region. When this stream of strong winds hits the surface, very strong gusts can arise for short periods, with inland locations being especially vulnerable to major impacts. In numerical experiments it has been shown that high spatial resolution is necessary to predict this phenomenon. Thus this case provided a stern test for the ECMWF IFS.

Only a small subset of rapidly-deepening extratropical cyclones exhibits the sting jet phenomenon. This is an ongoing area of research but evidence to date suggests that in order for a cyclone to possess a sting jet, the cyclone's

cloud head region must, as a minimum, be unstable to slantwise convection, and should contain warm air from a relatively low-latitude source. Conventional observations have also been shown to exhibit hallmarks of the sting jet in past cases; these include evaporating cloud filaments emanating from the tip of the cloud head (in imagery), and surface observations that show gusts that peak downwind of the gaps between these filaments. It is on the basis of observational evidence of this type that we think Christian was probably a sting jet storm.

The sting jet phase likely terminated over eastern Denmark. Note how wind gust strength in Figure 2e is generally maintained across the landmasses of Denmark, but dies away much more rapidly inland over southern Sweden. This behaviour over Sweden is more typical of strong winds in the 'cold conveyor belt' (CCB) zone of a cyclone, which tend to follow and overlap any sting jet phase. In this CCB phase the forced descent of high momentum air is lacking, so unless there is an alternative mechanism for bringing the high momentum air downwards, such as convective overturning, gusts tend to not be as strong.

Ensemble forecast

At lead times of 7–10 days, the ensemble forecasts (ENSs) generally provided cyclonic solutions for northwest Europe, but with the more extreme cyclones mostly located west of the UK. Figure 3 encapsulates the ENS handling at shorter leads, showing the Extreme Forecast Index (EFI) and shift of tails (SOT) for 24-hour maximum wind gusts for (a) 5–6, (b) 3–4 and (c) 1–2 day forecasts, all valid on 28 October, as well as 24-hour maximum wind gust CDFs (cumulative distribution functions) for Leeuwarden in the north of the Netherlands. By 5–6 days before the event, the EFI (indicating, broadly, the likelihood of high gusts) and SOT (signifying how extreme the gusts might be) were pointing to the potential for a major windstorm (Figure 3a). Closer to the event the signal increased (Figures 3b and 3c). The most noteworthy feature of these plots is perhaps the fact that the SOT reaches a value of 5 over Denmark in the 1–2 day forecast. For *very extreme* events the EFI saturates, as it is unaffected by changes in forecasts beyond the maximum of the model climate. The SOT on the other hand can be more useful here, as it is designed to focus on the domain beyond the model climate maximum, telling the forecaster how extreme an extreme event might really be (*Zsótér*, 2006).

The wind gust CDFs for Leeuwarden (Figure 3d) confirm that many forecast outcomes, at different lead times, lay above the maximum of the model climate (shown here for lead time 24–48 hours). Also one can see 'jumpiness' in the

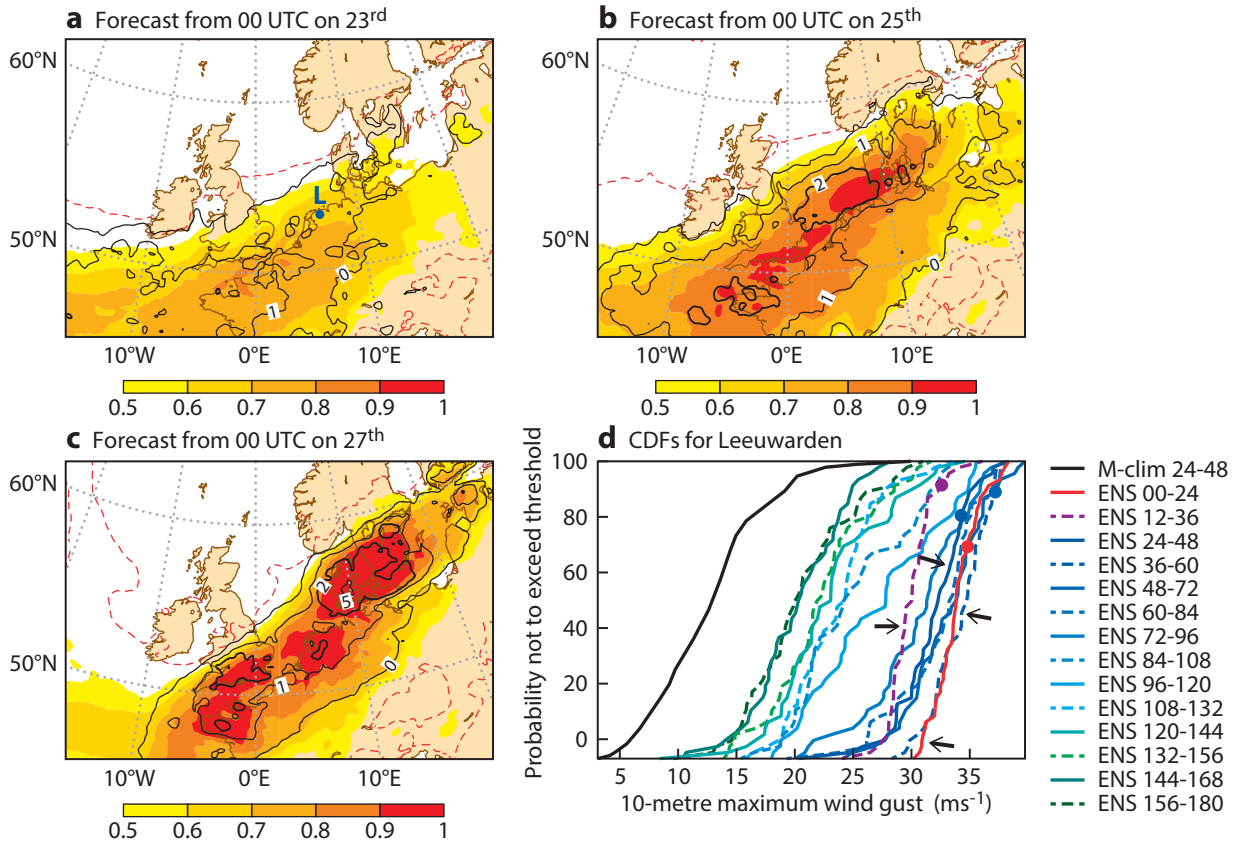

Figure 3 Maximum gust forecasts from ENS represented as the EFI (shading as on legend, and red contours = 0.3) and SOT (black contours = 0, 1, 2, 5) for 00 to 24 UTC on 28 October 2013 from data times (a) 00 UTC on the 23rd, (b) 00 UTC on the 25th and (c) 00 UTC on the 27th. Panel (d) shows, for the same 24-hour period, maximum wind gust CDFs for Leeuwarden in the Netherlands (location 'L' marked on panel (a)) from 14 ENS runs (see legend), with spots denoting the corresponding HRES from the last four runs (colours as on legend). Arrows highlight CDFs referred to in the text. M-clim (black line) is the 20-year model climate distribution based on 500 realisations.

ENS probabilities at short leads, that roughly mirrors HRES behaviour discussed above (for the Leeuwarden grid point, the corresponding HRES values are shown with spots on Figure 3d). Following the last four forecast sets, highlighted with arrows, one sees a steady reduction in maximum gusts (a movement of the CDFs to the left, dashed blue to solid blue to purple) until the very last forecast (red) which jumps back to stronger values.

To explain the changes depicted in Figure 3d in spatial, synoptic terms, one can reference ECMWF extratropical cyclone products (see *Hewson*, 2009), as illustrated in 'dalmatian chart' format in Figure 4. These charts show the positions of all synoptic-scale cyclonic features from all IFS runs. Forecasts from 12 UTC on the 26th (a, b) commonly showed intense solutions, as denoted by bright colours, but also highlighted uncertainty. In the runs from 00 UTC on the 27th (c, d) uncertainty seems to have increased, at least for 12 UTC on the 28th (d), when the storm turned out to be near to its peak. The 'maximum 1 km wind' represented ranges from 55–60 knots (dark green, equivalent to an ordinary winter cyclone) to 80–85 knots (light magenta, equivalent to a once in a lifetime event!). The positions of these cyclones also varied, the weaker cyclones having progressed further east, commensurate with less interaction with upper levels; this is a common feature of dalmatian charts in potentially cyclogenetic situations.

For the forecasts from 12 UTC on the 27th (e, f) the spatial range of the outcomes had narrowed, and intensities had weakened, to lie generally between 60 and 70 knots. The short-range forecast then jumped back, to show outcomes of mostly 70–75 knots (h). This final change seems to relate, in turn, to the analysis at 00 UTC on 28th (g) being on the edge of the range of the previous 12-hour forecast (e) – i.e. the surface cyclone being a little slower and therefore perhaps interacting a little more favourably with upper-level forcing.

One can thus see how finely balanced the situation was and, if this is added to the related difficulties of modelling mesoscale structures (e.g. the sting jet), it starts to become apparent why we may occasionally see unwanted jumps in ECMWF forecasts in such situations. Intertwined with all this is the issue of initial condition uncertainty, which other studies have shown is the major factor leading to jumpy forecasts.

5 December (Xaver)

On 5 December a large and violent cyclonic storm hit the North Sea region and several adjacent countries. Problems were caused both by high wind speeds and a related storm surge. The surge reached 6 metres on the Elbe in Hamburg for example, and along the east coast of England and in the south of the Netherlands it was the highest for 60 years. In the cold air outbreak following the storm a blizzard hit Sweden. The storm system was name Xaver by Berlin's Free University; other names assigned elsewhere include Bodil, Sven and St. Nicholas.

The cyclone first developed around 00 UTC on the 4th as a warm front wave/diminutive wave, northeast of

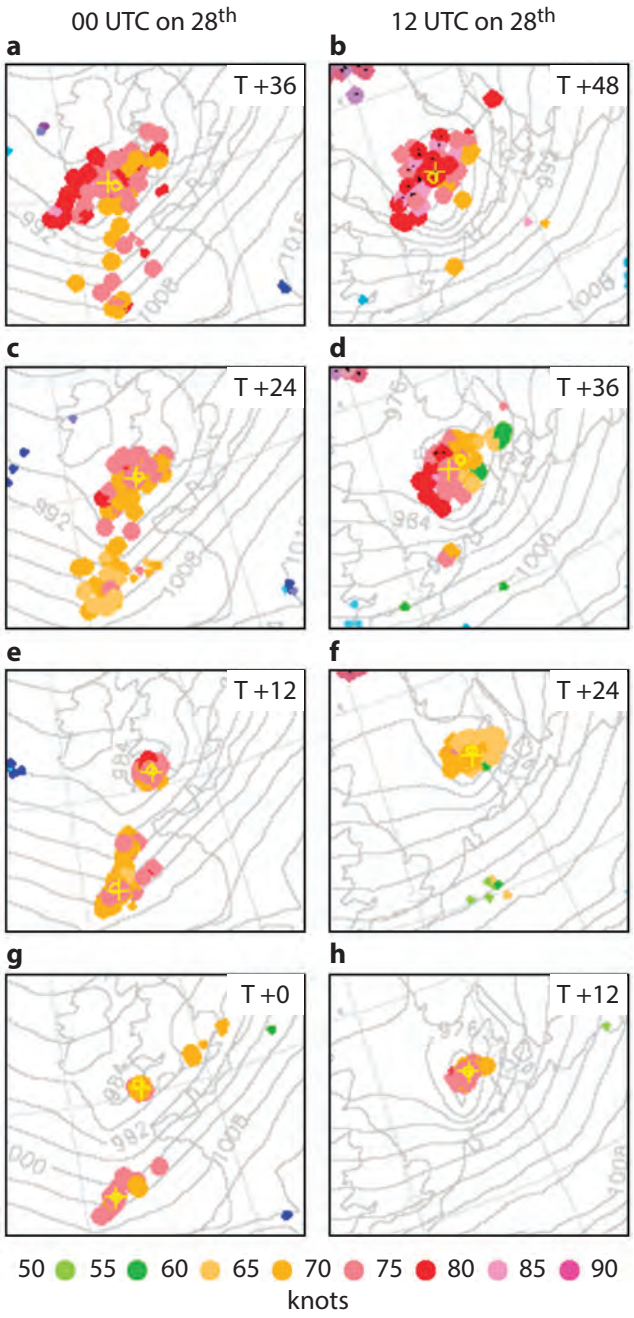

Figure 4 'Dalmatian max wind attribute' charts from the ECMWF extratropical cyclone tracking system, for two validity times: 00 UTC on 28 October (left side) and 12 UTC on 28 October 2013 (right side) from forecasts with data times of (a, b) 12 UTC on the 26th, (c, d) 00 UTC on the 27th, (e, f) 12 UTC on the 27th and (g, h) 00 UTC on the 28th. Each spot denotes a cyclonic feature (frontal wave, barotropic low or diminutive frontal wave) identified in one of 52 IFS runs. A small spot means that the feature lies on a front that is thermally weak. Black dots denote barotropic low centres. Colours signify a 'maximum 1 km wind' attribute: this is the maximum of all the grid point mean wind speed values lying within a 300 km radius of the feature point, on a level that is everywhere 1 km above the Earth's surface, in the relevant model run. Legend below is in knots (1 knot ≈ 0.5 ms^{-1}); the limits of a colour's range are the values either side. Contours show mean-sea-level pressure from the control run. Yellow circles/crosses denote respectively control/deterministic run features; these features are plotted last.

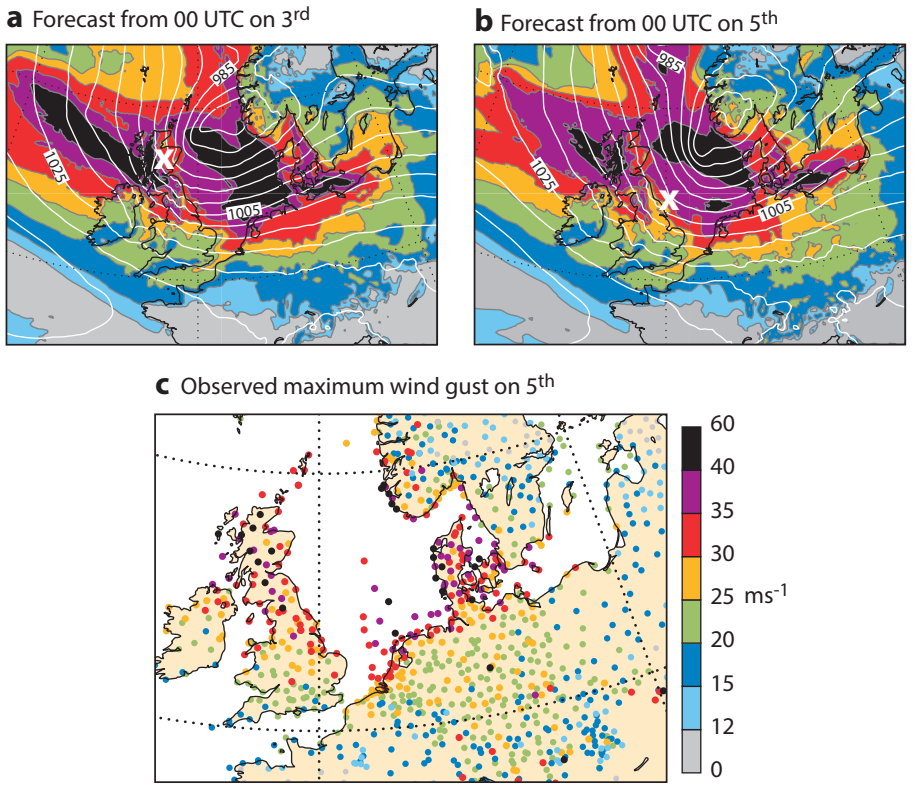

Figure 5 Forecasts, of 24-hour maximum wind gust between 00 and 24 UTC on the 5th (shading) with mean-sea-level pressure for 12 UTC on the 5th (contours) from data times of (a) 00 UTC on 3 December and (b) 00 UTC on 5 December 2013. White crosses denote the remnants of a meso-vortex discussed in the text. Panel (c) shows verifying data from observations.

Newfoundland. In common with many formative North Atlantic windstorms, the cyclone was then situated between converging northerly and southerly airstreams, convergence which in turn gave rise to substantial increases in the strength of both the low-level thermal gradient and the upper-level westerly jet. Subsequently, under the influence of the accelerated jet stream, the cyclone sped northeast, then east along latitude 60°N, deepening explosively and attaining its minimum central pressure of 961 hPa near Oslo around 18 UTC on the 5th. The maximum 6-hour deepening (from Met Office surface charts and ECMWF analyses) was about 13 hPa, north of Scotland, between 00 and 06 UTC on the 5th, whilst the maximum 24-hour deepening was about 44 hPa, which is extreme. The cyclone had a more complex structure than storm Christian, with an intense meso-vortex hanging back to the west of the main low for a time, and this enhanced the strong wind swathe running into western Scotland (see observations and model forecasts of 24-hour maximum gust in Figure 5). The barely discernible remnants of this meso-vortex (at 12 UTC on the 5th) are marked with white crosses in Figures 5a and 5b.

High-resolution and ensemble forecasts

The main band of very strong gusts extended from the northern North Sea, around the coasts of southwest Norway and on into Denmark and the coastal fringes of the Netherlands, Germany and Sweden (Figure 5c). HRES in the lead up to this event generally captured the maximum wind gusts well (two examples are shown on Figure 5), albeit with an over-estimation inland over northern Germany, and with some timing errors (cyclone progress is too slow in the 60-hour forecast of surface pressure in Figure 5a).

The cause of the very strong winds appears to have been CCB flow around the southern flank of the cyclone. On imagery sequences, unlike for Christian, there was no signature of a sting jet. Indeed the cloud head, which should be the source region for any sting jet, was barely present, being very ragged and ill-defined. Note also how wind gust strength dies away downstream of coastlines for the Xaver case, both in observations and model output (e.g. compare the west coast of Jutland with other parts of Denmark in Figure 5). This relates to the CCB being the synoptic scale cause of the gusts, and not the sting jet, as discussed above for storm Christian. Meanwhile the wind gust CDFs for Torsminde (Figure 6d) show a signal for extreme winds that grows and then stabilises. This all contrasts with the more jumpy forecasts for storm Christian. CCB windstorms tend to cover larger areas and be more predictable than sting jet windstorms.

At longer lead times of 7 and 8 days (not shown) some ENS runs had produced vigorous cyclones in about the right location, though few if any of these were sufficiently extreme. As with Christian, the EFI and SOT products from the ENS provided an indication for the event from

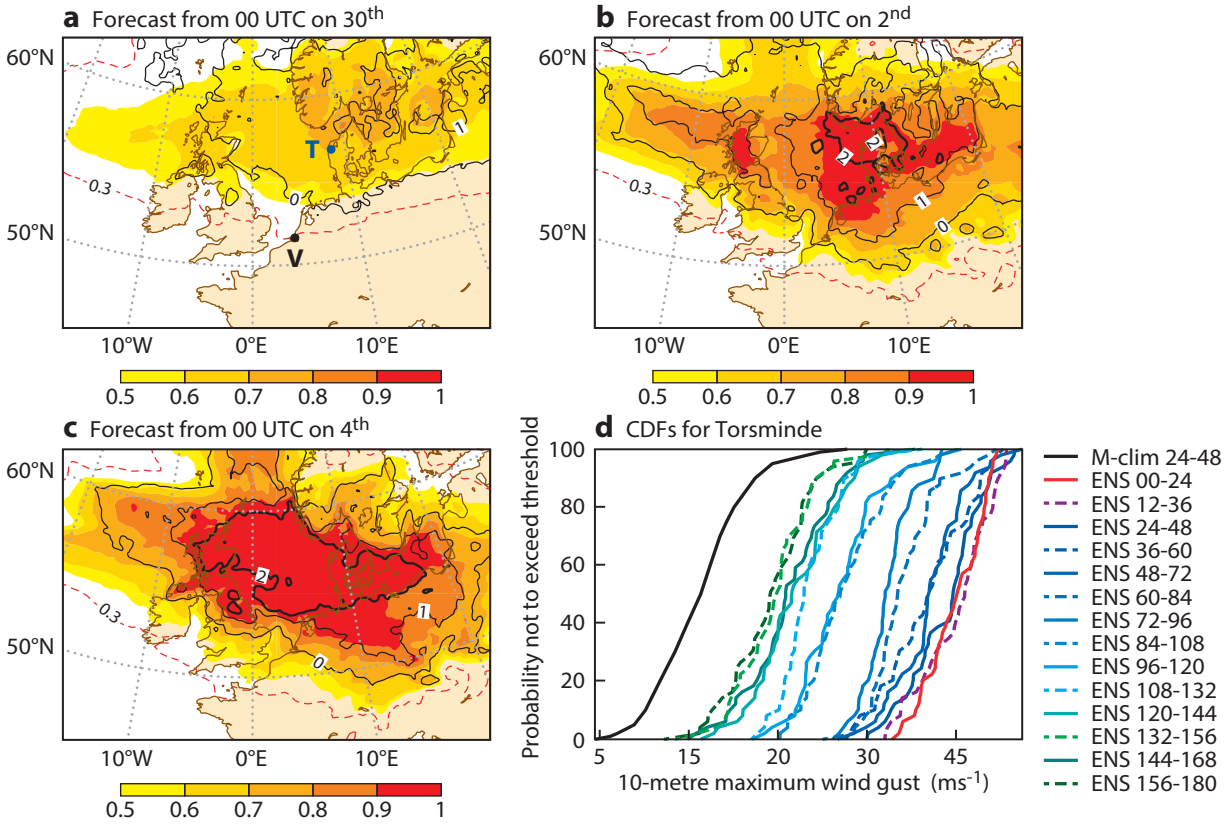

Figure 6 Maximum gust forecasts from ENS represented as the EFI (shading as on legend, and red contours = 0.3) and SOT (black contours = 0, 1, 2, 5) for 00 to 24 UTC on 5 December 2013 from data times (a) 00 UTC on 30 November, (b) 00 UTC on 2 December and (c) 00 UTC on 4 December 2013. Panel (d) shows, for the same 24-hour period, maximum wind gust CDFs for Torsminde in northwest Denmark (location 'T' marked on panel (a) from 14 ENS runs (see legend). M-clim (black line) is the model climate, as in Figure 3.

about 5–6 days in advance, and this signal strengthened in later forecasts (Figures 6a, 6b and 6c). The area with large values of EFI (>0.9 say) and SOT (>2 say) was greater than for Christian, though the maximum SOT was not as high (compare Figures 3c and 6c). These differences are consistent with the larger size of Xaver compared to Christian, and the different causes of the strong winds (CCB versus sting jet).

Ensemble storm surge forecast

The most significant impacts to have occurred in connection with Xaver were arguably related to the associated storm surge. Record surges were set up by the windstorm along the east coast of Britain, the coasts of the Netherlands and in the German Bight.

The atmosphere influences the sea surface elevation in two distinct, but related, ways:

- There is the inverse barometric effect where, as a rule-of-thumb, a 1 hPa reduction in surface pressure leads to a 1 cm increase in water level.
- Due to the Earth's rotation, winds will push water away at right angles, and to the right of the airflow direction, through what is known as Ekman transport.

In turn, a pulse of piled-up water will travel forwards as a Kelvin wave, with the coast to its right, as a consequence of the Coriolis effect. The North Sea is prone to such storm surges when the wind is blowing from the north or northwest. By piling up water along the east coast of Scotland, a pulse (the aforementioned Kelvin wave) is set off which travels southward before turning northward in the direction of Denmark.

Although storm surge forecasting is not performed by ECMWF, the 10-metre wind fields and surface pressure fields from our ensemble forecasts are put to use by KNMI and Rijkswaterstaat, who are jointly responsible for issuing ensemble storm surge forecasts for Dutch waters. The barotropic WAQUA/DCSM98 (Dutch Continental Shelf Model), which covers the northwest European Continental Shelf, including the North Sea, is run at 8 km resolution. A 51-member ensemble is integrated to 240 hours twice daily. The destructive potential of a storm surge depends on whether it coincides with the astronomical tide or not, and the Dutch system includes all the major tidal constituents (see *de Vries*, 2009).

Figure 7 shows the ensemble storm surge forecast for Vlissingen (location marked on Figure 6a), based on a data time of 00 UTC on 2 December. Box-and-whisker symbols denote water levels in the 51 ensemble members. Evidently the peak of the storm surge coincided quite closely with the fortnightly spring tide which will occur

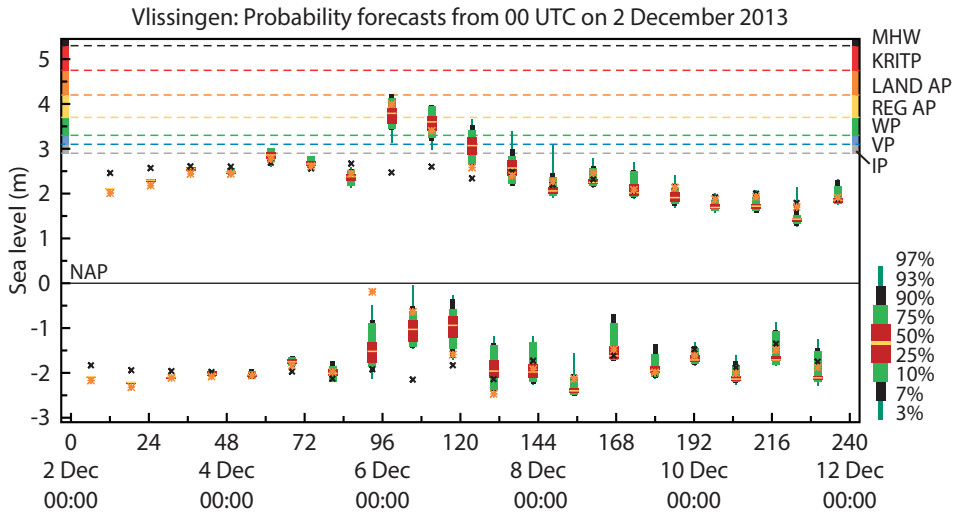

Figure 7 The ensemble storm surge forecast for Vlissingen (location marked on Figure 6a), from 00 UTC on 2 December 2013. Box-plots show water level probabilities for high and low waters as derived from the 51 ENS inputs. Marked with black through to grey dashed lines are various risk levels for the coastal district. The semi-diurnal tide is clearly visible as the box-plots jump between high and low water roughly every six hours. The fortnightly spring-neap tidal cycle is less visible, but reaches its peak on 4 December, 1.5 days before the peak of the storm surge. Orange asterisks are the observed water levels and grey crosses show, as a reference point, the pure astronomical tides.

two or three days after the moon is new or full. There was a new moon on 3 December.

The Dutch forecasting system highlights the value of ensemble forecasts in planning and preparing for events with high destructive potential. The storm surge is but one of the hazards that storms bring to European coasts. Cyclones can also bring high waves (wind wave and swell) and large amounts of rain. The multi-hazard scenario of flooding, waves and surge can be a highly destructive mix for coastal Europe. Forecasting the joint probability of two or even all three of these events is within reach of the present suite of ensemble forecast products.

Importance of case studies

In this study we have evaluated forecasts for the extreme windstorms Christian and Xaver, which both hit northwest Europe in late 2013. For both storms the EFI and SOT provided an indication of extreme wind gusts 5–6 days in advance. However, the finer details regarding timing and strength of Christian were not well forecast even one day before the event. These uncertainties probably relate to the sting jet, a small-scale phenomenon that presents resolution difficulties for models, and to a simultaneous and probably related high sensitivity to subtle differences in synoptic-scale forcing. For the larger storm Xaver, the strongest gusts were instead connected to the cold conveyor belt, and were more consistently and accurately predicted.

To make a robust evaluation of a forecasting system, verification should be aggregated over many cases, not just two. This type of multi-case evaluation has been undertaken in a companion article in this issue of the *ECMWF Newsletter* starting on page 29. However, for such an evaluation, one has to include less extreme cases in order to obtain reliable statistics. Therefore, we need always to complement statistical assessments with case studies, such as those presented here, to obtain a more complete picture of IFS performance for severe weather, and to get pointers to weaker aspects that should be further explored.

FURTHER READING

Browning, **K.A.**, 2004. The sting at the end of the tail: Damaging winds associated with extratropical cyclones. *Q. J. R. Meteorol. Soc.* **130**: 375–399.

Vries, **J.W. de**, 2009. Probability forecasts for water levels at the coast of The Netherlands. *Marine Geodesy*, **32**,100–107, doi:10.1080/01490410902869185.

Hewson, **T.D.**, 2009: Tracking fronts and extra-tropical cyclones. *ECMWF Newsletter No. 121*, 9–19.

Zsótér, **E.** 2006. Recent developments in extreme weather forecasting. *ECMWF Newsletter No. 107*, 8–17.

Forecasting the severe flooding in the Balkans

LINUS MAGNUSSON, FREDRIK WETTERHALL, FLORIAN PAPPENBERGER, IVAN TSONEVSKY

Weeks of wet conditions followed by exceptionally intense rain from 13 to 16 May 2014 led to disastrous and wide-spread flooding in the Balkans, in particular in Bosnia-Herzegovina and Serbia. Critical flooding was also reported in other regions including southern Poland, Slovakia, and the Czech Republic. The event in Bosnia-Herzegovina and Serbia was reported to be the worst for more than 100 years, with more than 80 fatalities reported from the flood-affected regions and a significant loss of livestock. More than a million inhabitants were estimated to have been affected by this flood event and both Bosnia-Herzegovina and Serbia activated the EU Community Civil Protection Mechanism for help.

During the month leading up to the main precipitation event, precipitation had already been double the average. The main precipitation event itself lasted about three days, beginning on 13 May. On that day there was an eastward-moving cold front. Thereafter an upper-level, cut-off low formed, together with a deep surface low over south-eastern Europe. Later the low moved north-westwards, bringing further heavy rain over Serbia as easterly winds on its northern flank hit the upslope of a mountainous region between Serbia and Bosnia-Herzegovina. Finally, on the 16th the low pressure system started to fill. At the end of the episode heavy rain was also observed in Slovakia and Austria.

Panel a of the figure shows the observed three-day accumulation of precipitation starting at 06 UTC on 13 May. The highest values were in a band from Tuzla in the west to Belgrade in the east, with more than 160 mm over three days. The four most extreme reports were Tuzla (264 mm), Loznica (213 mm), Valjevo (190 mm) and Belgrade (174 mm).

Panel b shows the three-day accumulation of precipitation from the high-resolution forecast (HRES) initialised at 00 UTC on 13 May. The location of the precipitation is good. The values are underestimated in the worst-affected area, although forecast totals did reach 140 mm. An underestimation of the largest precipitation totals by HRES was also seen for the flooding in central Europe at the beginning of June 2013 (see *ECMWF Newsletter No. 136*).

For severe weather events, having accurate predictions well in advance can be very valuable. The Extreme Forecast Index (EFI) compares the ensemble forecast (ENS) distribution with the model climate distribution derived from a set of re-forecast data. Panel c shows the EFI for three-day precipitation accumulation starting at 00 UTC on 13 May from the forecast issued on 00 UTC on 8 May.

Already at this very early stage, the ENS suggested there was likely to be extreme precipitation in the Balkans. This early signal of extreme precipitation was connected to a relatively confident forecast of the aforementioned cut-off low.

The European Flood Awareness System (EFAS) uses ECMWF precipitation forecasts to drive its flood forecasting model. EFAS produces medium-range probabilistic flood forecasts for Europe and the computations are executed at ECMWF as part of the Copernicus services. The forecast from the 9th (which was the earliest forecast that covered the day of peak flow) already had ensemble members indicating a risk of a very severe event (not shown). Panel d shows the forecast from the 13th for the return period of the stream flow for the river Sava for a point close to Belgrade. This forecast had more than 50% probability for an event with

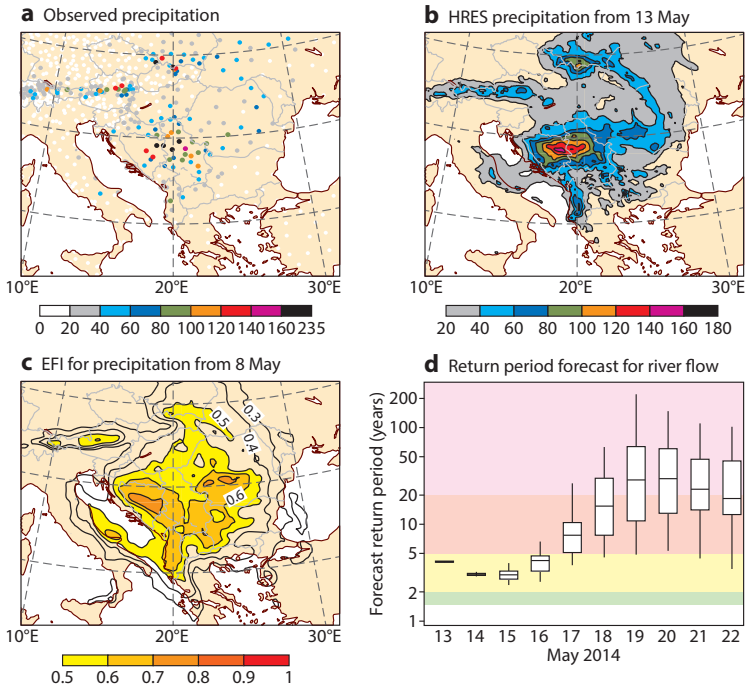

Observations and forecasts covering the period of 13 to 16 May 2014. (a) Observed precipitation between 06 UTC on 13 May and 00 UTC on 16 May and (b) HRES for precipitation accumulated for the same three-day period from 00 UTC on 13 May. (c) Extreme Forecast Index for three-day precipitation accumulation valid for 00 UTC on 13 May to 00 UTC on 16 May issued on 00 UTC on 8 May. (d) Return period forecast for the flow in river Sava for a point close to Belgrade from the forecast initialised on 13 May.

a return period of greater than 20 years. You can also see in the figure that even on the 13th the river flow was already higher than normal, due to the wet conditions in the region during previous weeks.

To summarize, the EFI and the EFAS flood forecast system gave an early warning of the Balkan flooding. This was based on a well-predicted cut-off low that gave persistent precipitation over the region for three days coupled with already-saturated soil from precipitation during the previous weeks. Precipitation amounts from HRES were generally too low for the areas where the largest totals were measured (although values above 140 mm were predicted) and the precipitation amounts in the ENS were in general less than in HRES.

The problem of extreme precipitation amounts being under-forecast was also identified for the flooding in central Europe in 2013 and is presented in *ECMWF Tech. Memo. No. 723*. In the investigation of that case, a number of experiments were conducted with different resolutions and changes to the model physics. The conclusion is that both improved physics and increased resolution could lead to better representation of precipitation extremes. In the next model cycle (to be introduced operationally later in 2014) the cloud physics will change and this should provide a general improvement in the precipitation extremes. The next increase in horizontal resolution is planned for 2015.

Recent cases of severe convective storms in Europe

IVAN TSONEVSKY,
LINUS MAGNUSSON,
TIM HEWSON

Summer 2014 was characterised by a widespread negative anomaly of 500 hPa geopotential height centred over Western Europe (first figure). The whole season has been very active in terms of severe convection. Three cases of major convective storms over Europe are presented. The study of these cases, along with user feedback, indicates that there would be benefit in developing severe weather products focussed on forecasting deep convection.

9 June

On 9 June, following a period of hot weather, a severe convective outbreak affected Western Europe. In Germany six people were killed, mainly by falling trees. Deep moist convection developed along the western fringe of a hot air mass.

Strong wind gusts were reported from many sites in France, Belgium, the Netherlands and Germany, widely exceeding 20 m/s, in a few cases exceeding 25 m/s and with a peak of 42 m/s at Düsseldorf airport (second figure). The ECMWF ensemble forecast (ENS) failed to give a signal of strong winds: probabilities of wind gusts exceeding the 95th percentile of the model climate (M-climate) are fairly small. As a reference, the values of the 95th percentile of the M-climate are in the range 14 to 17 m/s. However, looking at the Convective Available Potential Energy (CAPE) as a predictor of the convective instability of the atmosphere, the ENS shows a very high chance of CAPE exceeding the 95th percentile of the M-climate.

Instability is one of the three key ingredients of severe convection and the high values in this case are a good indicator of the risk of severe thunderstorms and thus of possible strong convective wind gusts. Heavy rain associated with convection was much better captured by both the ECMWF high-resolution forecast (HRES) and ENS. This case illustrates the need to complement the ECMWF severe weather products (e.g. the Extreme Forecast Index, EFI), with a parameter that is suitable for forecasting severe convection.

19 June

Severe thunderstorms developed over south-eastern Europe on 19 June. More than 100 mm of rain fell in north-eastern Bulgaria in just a few hours causing a number of fatalities, most of them during a deluge in a residential area of the coastal city of Varna. Convective storms developed underneath an upper-level trough with active surface cyclogenesis simultaneously occurring over the western part of the Black Sea.

The convective nature of the precipitation makes forecasts of its location and intensity particularly difficult. The uncertainty in the forecast remained large even in the short range. In such situations, high-resolution limited-area ensembles can help in assessing the uncertainty by showing, for example, the probability of precipitation greater than a particular threshold (third figure). These ensembles form part of the TIGGE-LAM project and are available through the ECMWF archive system – they are a valuable source of data for case studies and for forecast evaluation.

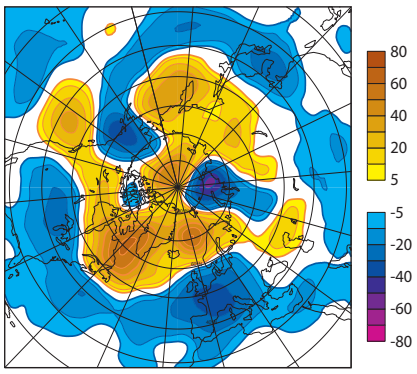

1: Anomalies of 500-hPa geopotential height for June to August 2014 (in m). This shows that a widespread negative anomaly of 500 hPa geopotential height was centred over Western Europe during the summer of 2014. The anomalies are with respect to ERA-Interim. Note that a simple normalisation has been applied to ensure a zero mean anomaly over the domain; without this positive anomalies would look much more prominent, due to a general increase in 500 hPa height over recent decades.

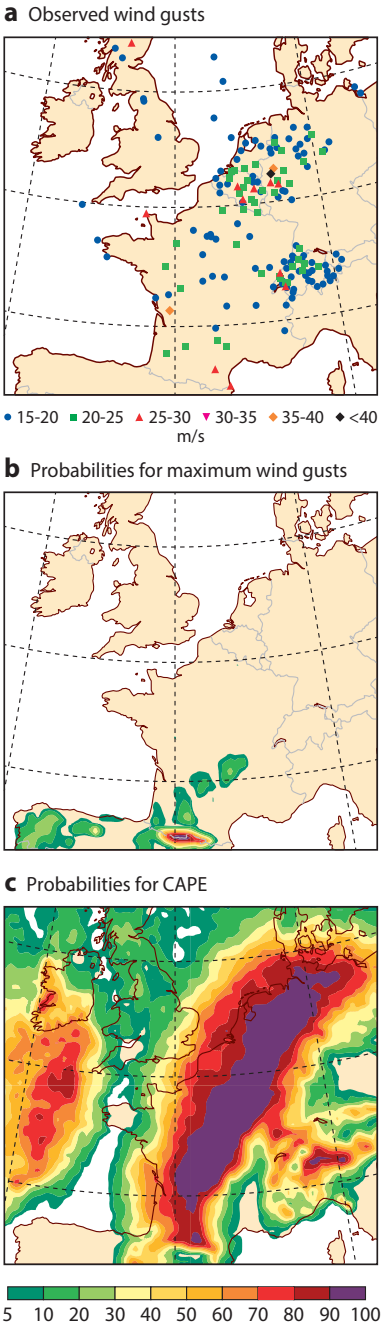

2: Observed wind gusts and ENS probabilities for 9 June 2014. (a) Observed maximum wind gusts (in m/s) on 9 June 2014. (b) Probability of maximum wind gusts in the 24- to 48-hour forecast exceeding the 95th percentile of the M-climate – this did not give a signal that strong winds might occur even in the very short range. (c) Probability of CAPE in the 72- to 96-hour forecast exceeding the 95th percentile of the M-climate – this gave a strong signal that high values of CAPE might occur over a large area well in advance.

TIGGE-LAM is a high-resolution, limited-area model extension of the TIGGE initiative (THORPEX Interactive Grand Global Ensemble), which involves the regular archiving of weather forecasts from ensembles.

31 August

Quasi-stationary convective storms caused significant flooding in Copenhagen and Malmo on 31 August. Roads were closed and buildings flooded. Convection occurred in the vicinity of an occluded front.

High-density observations around Copenhagen, provided on the Danish Meteorological Institute (DMI) website, show some massive precipitation totals in excess of 100 mm, but with large spatial variations across the city. Over 100 mm was also recorded locally in Malmo. These variations occurred within an HRES grid box (~16 km) and as such cannot be captured directly. For the same reason, one should not expect the probability of heavy rain as measured at individual points to be given directly by ensembles either, particularly those run at lower resolution.

As shown in the fourth figure, high-resolution ensembles (COSMO-LEPS ~10 km, DMI-HIRLAM ~5.5 km, COSMO-DE-EPS ~2.8 km) show more detail and generally higher probabilities compared to the ECMWF ENS (~32 km). The ENS can, however, be compared to its own model climatology, via the non-dimensional metrics that ECMWF uses for this purpose, namely the EFI and the complementary Shift of Tails (SOT) (for more details see *ECMWF Newsletter No. 107*). The EFI and SOT for this event are plotted on the fifth figure. Evidently the ENS did provide signals in advance that an extreme precipitation event was possible.

Current status and future developments

The active convective season in Europe this summer, and indeed user feedback, have both highlighted a need to put more effort into developing severe weather products focused on forecasting deep convection. With these we will be able to take full advantage of recent improvements in the Integrated Forecasting System (IFS) and the resolution upgrade planned for next year.

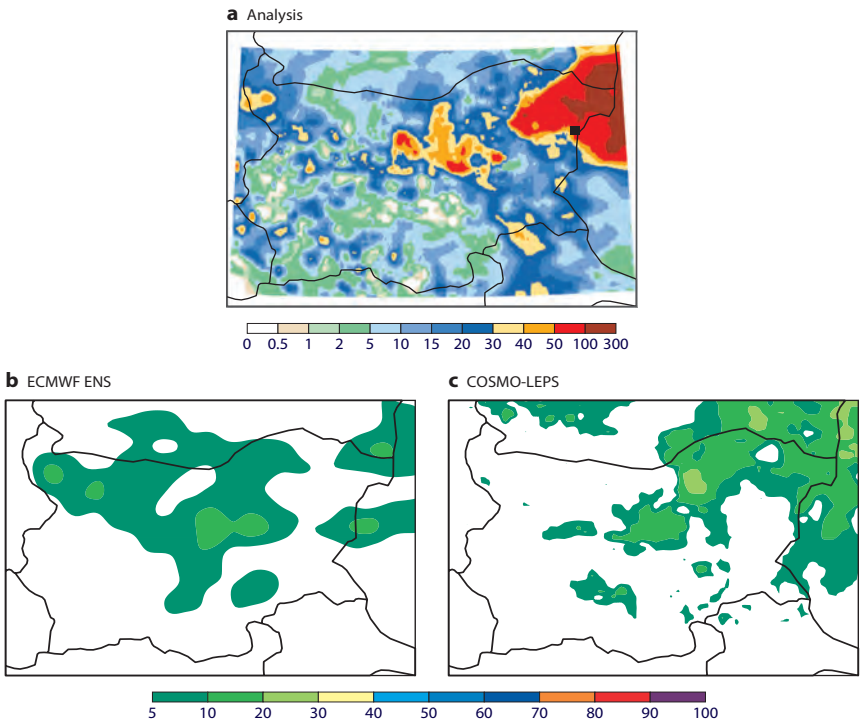

3: Analysis and probabilities of precipitation exceeding 50 mm/24 hours for 19 June 2014. (a) Analysis of precipitation from 06 UTC on 19 June to 06 UTC on 20 June 2014 obtained by ALADIN LAM Bulgaria in combination with a high-density rain-gauge network (courtesy of the National Institute of Meteorology and Hydrology, Bulgaria). (b), (c) Forecasts of the probability of precipitation greater than 50 mm/24 hour from ECMWF ENS and COSMO-LEPS respectively. The high-resolution ensemble forecast from COSMO-LEPS provided more details and could help assess the uncertainty in the short-range forecasts. Both forecasts show probabilities higher than the climatological probabilities. All the forecasts are for 54- to 78-hour lead times. The grid spacing of ECMWF ENS is about 32 km and for COSMO-LEPS it is about 10 km. The black square on the precipitation analysis map denotes the coastal city of Varna that suffered floods and fatalities.

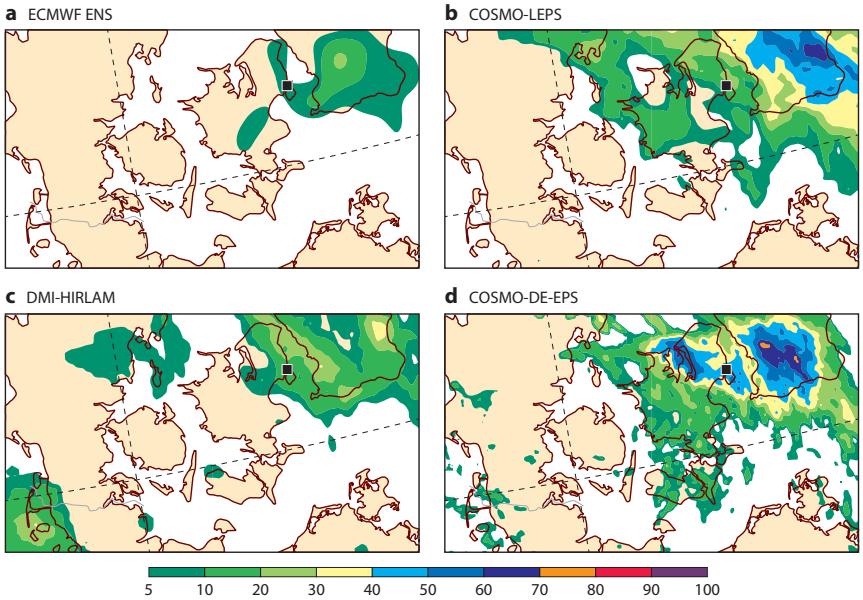

4: Probability of precipitation above 20 mm/12 hours for 31 August 2014. Forecasts are valid from 00 to 12 UTC on 31 August 2014 from ensemble runs at 12 UTC on 30 August from (a) ECMWF ENS (~32 km grid spacing), (b) COSMO-LEPS (~10 km), (c) DMI-HIRLAM (~5.5 km), and (d) COSMO-DE-EPS (~2.8 km). The high-resolution ensemble forecasts show details and generally higher probabilities compared to the ECMWF ENS. The black square is Copenhagen.

The TIGGE-LAM archive helps us evaluate the performance of the IFS in severe weather by allowing us to compare its performance directly with that of limited-area ensembles.

The above discussion has focussed on lead times up to about three days, and has shown that the IFS can provide some very useful pointers for forecasters. For the three cases we have also assessed IFS products, such as the EFI, for longer lead times. These products also contain some signals pointing to the possibility of severe weather, and for the first case a strong CAPE signal was in the right place up to 5 or 6 days in advance. But for the other cases the signals were quite weak and would not have provided much assistance in pinpointing the most vulnerable areas. For other types of extreme weather, EFI signals tend to be more useful than this at longer leads. We believe that these differences in performance simply reflect the fact that certain types of weather extreme are more difficult to predict than others.

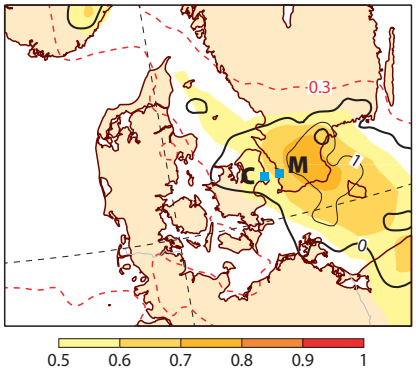

5: EFI and SOT for total precipitation for 31 August 2014. The 48- to 72-hour forecast from 00 UTC on 29 August shows that ENS provided a signal of extreme precipitation. The EFI shadings highlight the areas that are most vulnerable to a heavy precipitation event, whilst the SOT contours indicate that in some regions at least 10% of ensemble members show an outcome that is particularly extreme. Blue squares with the letters are Copenhagen (C) and Malmö (M). Note that the innermost contour in southern Sweden indicates an SOT value of 2.

For those with suitable ECMWF web access credentials, information about more severe weather cases around the world and particularly across Europe can be found via: https://software.ecmwf.int/wiki/display/FCST/Forecast+User+Home.

On these web pages users can also find out about some known issues with and limitations of the ECMWF forecasting system. There is also an opportunity for users to provide feedback and share additional information about the performance of the IFS, and any case study material, such as high density observations, that they have.

Forecasts for a fatal blizzard in Nepal in October 2014

LINUS MAGNUSSON, TIM HEWSON

On 14 October 2014 a blizzard hit the Annapurna massif in north-central Nepal. The snowfall had a devastating impact, killing more than 40 people, mainly trekkers trapped on popular hiking routes (at altitudes around 4,000 to 5,000 m). Part of the area is believed to have received 1.8 metres of snow (source: Wikipedia article '2014 Nepal snowstorm disaster'), but unfortunately we are missing official observations of precipitation for the event. Instead, the top-left panel of the figure shows the short-range precipitation forecast (accumulated for 14 October). The position of Annapurna is marked with an hourglass symbol. The precipitation amount in the region is in excess of 130 mm, which broadly agrees with the reported snowfall. To put this into perspective, in the (model-based) climatology for this region, the threshold for an unusual 24-hour total (1 in 100 chance) at this time of year is only about 20 mm.

The intense precipitation was caused by the remains of tropical cyclone Hudhud. The cyclone formed on 8 October close to the Andaman Islands in the Bay of Bengal. The bottom-left panel shows the cyclone tracks from the ensemble forecast from 00 UTC on 8 October. After making landfall on the Indian eastcoast most of the ensemble members predicted a turn to the north towards the Himalayas. The actual track until landfall (from the Best Track database) overlaid shows that this forecast verified well.

The top-right panel shows the Extreme Forecast Index (EFI, shaded) and Shift of Tails (SOT, contours) for snowfall on 14 October from the same forecast as above (6–7 days in advance). The SOT index complements EFI by providing information about the extreme tail of the ensemble distribution compared to the model climate distribution. Considering the long lead time, the signals in both EFI and SOT are unusually strong for extreme snowfall on the Nepalese

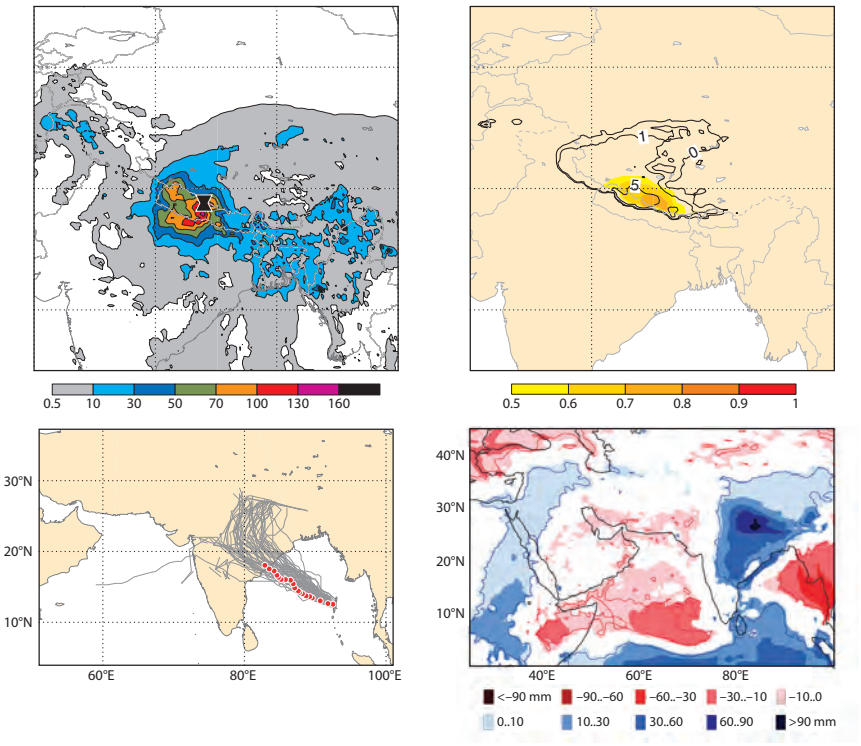

Forecasts associated with the blizzard in Nepal in October 2014. Top-left: 24-hour accumulated precipitation for 14 October from the last forecast before the snowfall event (Annapurna marked by hourglass symbol). Top-right: EFI (shading) and SOT (black contours: 0, 1, 5, 10, 15) for snowfall for 14 October from 00 UTC on 8 October. Bottom-left: Tropical cyclone tracks from the ensemble forecast from 00 UTC on 8 October (reported track until landfall in red circles). Bottom-right: Weekly precipitation anomaly for 13–19 October from the monthly forecast starting on 6 October. The interpretation of these charts is given in the main text.

mountains. The SOT reaches values above 5 for the Annapurna region. The strong signal for snowfall is closely linked to the track of Hudhud.

Finally, the bottom-right panel shows the weekly anomaly of precipitation in the forecast from 6 October, two days before the genesis of Hudhud. The forecast is valid for the week of 13–19 October. The forecast has a strong anomaly for wetter than normal conditions along the track of the cyclone, especially over Nepal.

Whilst determining the precise causes of the snowfall may warrant further investigation, it is clear that the track of Hudhud favoured a strong northward flux of moisture into a very-high-altitude region. At the same time an eastward-moving upper-level subtropical trough is believed to have provided assistance to snow-generation (from this moisture) through dynamically-driven uplift. It also seems that this event is not without precedent; another with very similar synoptic-scale characteristics, and a similar death toll, occurred near mount Everest (about 300 km away) on 11–12 November 1985 (thanks to Lance Bosart of the University of Albany-SUNY, USA, for this insight).

To summarize, the forecasts gave a strong indication of extreme snowfall in the Annapurna region more than a week in advance. This extreme event was caused by tropical cyclone Hudhud. Its track was consistently well predicted, even in forecasts initialised during its early stages, and this led to the high predictability of the snowfall event.

Forecasts for US east coast snow storm in January 2015

DAVID RICHARDSON,
ERVIN ZSOTER,
LINUS MAGNUSSON,
TIMOTHY HEWSON,
FLORENCE RABIER

A severe snow storm caused major disruption to parts of the north-east USA on 27 January. ECMWF forecasts consistently predicted the development of a major snow storm, but small changes in the predicted track led to large differences in snowfall forecasts for New York City.

On 27 January 2015, a blizzard hit north-eastern parts of the USA. The storm was expected to affect an area extending from the state of New Jersey north-eastwards, which includes New York City (NYC) and Boston, and preventive actions were taken (closing subways, motorways etc.). However, New Jersey and NYC only received relatively little snow, with the worst affected areas being in a band from eastern Long Island towards Boston and further north. This was the beginning of one of the snowiest periods on record for Massachusetts.

The snowfall was caused by a cyclone that formed close to Florida early on 26 January and then rapidly developed over the Atlantic late that day as it moved northward close to the US east coast. Both the actual and the predicted areas of heavy snowfall exhibited sharp gradients on the western side that were close to NYC, as seen in the top panels of the figure. Around NYC itself, 10–25 cm of snow was observed (e.g. Newark airport – 16 cm, Central Park – 24 cm, La Guardia airport – 28 cm), though Islip on Long Island, 40 km to the east, recorded over 50 cm. Further northeast many stations reported more than 75 cm of snowfall with the worst affected areas being in Massachusetts. It is not at all unusual to see large gradients in total precipitation in the area to the left of a cyclone's track; this can occur throughout the extra-tropical regions of the northern hemisphere.

The first indication in ECMWF forecasts of a potential major snow storm affecting the north-east USA appeared over a week ahead, although

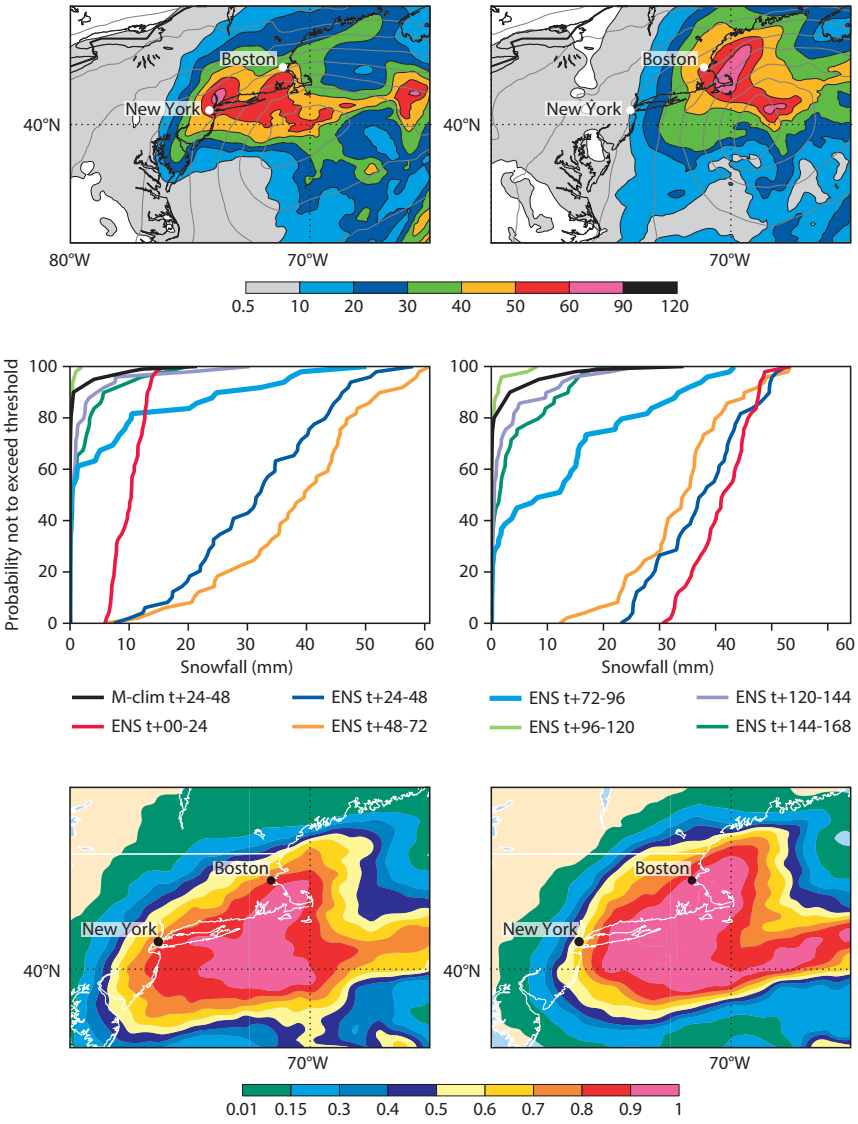

Top panels High-resolution forecast (HRES) of 24-hour precipitation (mm of rainfall equivalent) valid 27 January (shade) and mean sea level pressure valid at 12 UTC on 27 January (contour) from 00 UTC on 25 January (top-left) and 00 UTC on 27 January (top-right).
Middle panels Ensemble forecast (ENS) cumulative distribution functions (CDFs) for snowfall (defined as mm of rainfall equivalent, diagnosed as snow) from forecasts valid 27 January for NYC (middle-left) and Boston (middle-right).
Bottom panels Probability for more than 30 mm of precipitation on 27 January in ENS forecasts from 00 UTC on 25 January (bottom-left) and 00 UTC on 26 January (bottom-right).

the next few forecasts generally kept any developing systems out in the Atlantic, with limited impact on coastal areas. From Saturday 24 January onwards, successive ECMWF forecasts consistently predicted the development of a major snow storm that would affect the north-east coast of the USA on 27 January. However, whilst there was high confidence in the occurrence of a severe storm, its precise track remained less certain.

The lines in the middle panels of the figure represent ECMWF ensemble forecasts (ENS) from different initial dates for snowfall on 27 January for NYC (left) and Boston (right). Early forecasts (dark green, lilac, light green lines) suggested a high probability of at most small amounts of snowfall.

Later forecasts (light blue and yellow lines) indicated a greater probability of larger amounts of snowfall. For Boston this assessment remained stable in the very latest forecasts (dark blue and red lines), but for NYC the latest forecasts moved back to the left in the chart, suggesting once again a much smaller probability of large snowfall amounts.

On 25 January, most ENS members were taking a slightly more westerly track than the forecasts from the previous day. A change of 100–150 km in position (only 3–5 grid-lengths of the model) had a very large impact on the snow forecasts for NYC in particular: the probability of 'substantial snow' (more than 30 mm of precipitation, say, equivalent roughly to 30 cm or 1 foot of fresh snow) was over 80% for both NYC and Boston. This outcome was reinforced by the HRES (high resolution) forecast (top-left panel), which was predicting over 40 mm precipitation widely in north-eastern coastal regions, with over 50 mm in NYC. Although these totals were towards the upper end of the range predicted by the ENS, the overall signal was that a major event was likely to occur in both NYC and Boston. The ENS probabilities (bottom-left panel in the figure) show a sharp gradient over the New York area. Those ENS members that did maintain a track further to the east showed that significantly less snow could occur over NYC even though that was a less likely outcome.

Later forecasts from 25 and 26 January consolidated the likely outcome for Boston: the probability of an exceptional snowfall event increased with each new forecast, as shown by a rightward shift and a steepening of the lines in the right-hand chart of the middle panel. In contrast, the situation for NYC remained uncertain. Indeed the likelihood of 'substantial snow' decreased from 80% to 60% and then 40% as more ensemble members predicted the storm to pass slightly further to the east (bottom-right panel).

NYC was consistently predicted to be near the edge of the area forecast to be affected by the storm. Because of the very sharp gradients in precipitation, a relatively small change of less than 100 km in the storm's track could have a very large impact on the snow forecast for NYC. The ENS has a grid spacing of 32 km, and an uncertainty of perhaps one or two grid lengths has to be expected on some occasions.

This was one such occasion where the uncertainty persisted until the last minute: only in the forecast from 00 UTC on 27 January (top-right panel) was the uncertainty in the ECMWF ensemble finally resolved and the chance for severe snowfall in NYC eliminated, which was too late for operational use.

This case highlights the importance of using the full range of forecast information available, and the challenges in communicating this information to users. The ECMWF forecasts predicted potential extreme snowfall for both NYC and Boston. For both cities the forecast 2–3 days ahead indicated that this was highly probable, though not certain.

The ensemble approach is essential to provide forecast users with information about the range of future weather scenarios and the likelihood of high-impact weather events. The ensemble aims to account for all sources of uncertainty in the forecasting system, and ECMWF is continuing to improve its forecasting system, including by increasing its horizontal resolution. The aim is to both reduce and reliably quantify the uncertainty.

ECMWF forecasts for tropical cyclone Pam

LINUS MAGNUSSON,
SIMON LANG,
FERNANDO PRATES,
FRÉDÉRIC VITART

On 13 March 2015 tropical cyclone Pam hit the islands of Vanuatu in the south Pacific, with devastating effect. Around 15 people were killed and many buildings were destroyed. The cyclone was the second strongest on record in the southern Pacific, second only to Zoe (2002). It is regarded as the worst natural disaster in Vanuatu's history.

The cyclone formed on 6 March east of the Solomon Islands and was classified as a tropical storm on 9 March. The formation is believed to have been influenced by a strong Madden-Julian Oscillation (MJO) event and a connected westerly wind burst in the western tropical Pacific. During the lifetime of Pam, three more cyclones formed in the western Pacific and the south-eastern Indian Ocean: Olwyn west of Australia, Nathan north-east of Australia, and Bavi north of the equator. The MJO event itself was one of the strongest in recent decades.

Tropical cyclones are more likely to occur during the 'active' phases of the MJO, when the frequency and intensity of deep convection are enhanced compared to the climatological mean. The impact of the MJO on tropical storms can be explained by the MJO changing the environment in multiple ways. For example, in an active MJO event relative humidity increases, and vorticity is increased by the westerly wind burst. Since the MJO is to some extent predictable, its modulation of tropical cyclone activity makes it possible to forecast changes in that activity on the intraseasonal (monthly) timescale.

In this case, the MJO and the westerly wind burst were predicted by the monthly forecast more than two weeks in advance. Several ensemble members in the MJO forecast from 26 February showed a strong event in the western Pacific 15 to 20 days into the forecast. The forecast of normalised tropical cyclone energy from 26 February for the week 9 to 15 March predicted cyclone energy levels 2.3 times the normal value in the south-western Pacific and 1.3 times the normal value north-west of Australia. In subsequent forecasts, the ensemble mean cyclone energy increased as the week during which Pam struck approached (to a factor of 3.5 on 2 March, 4.0 on 5 March, and 5.0 on 9 March for the south-western Pacific).

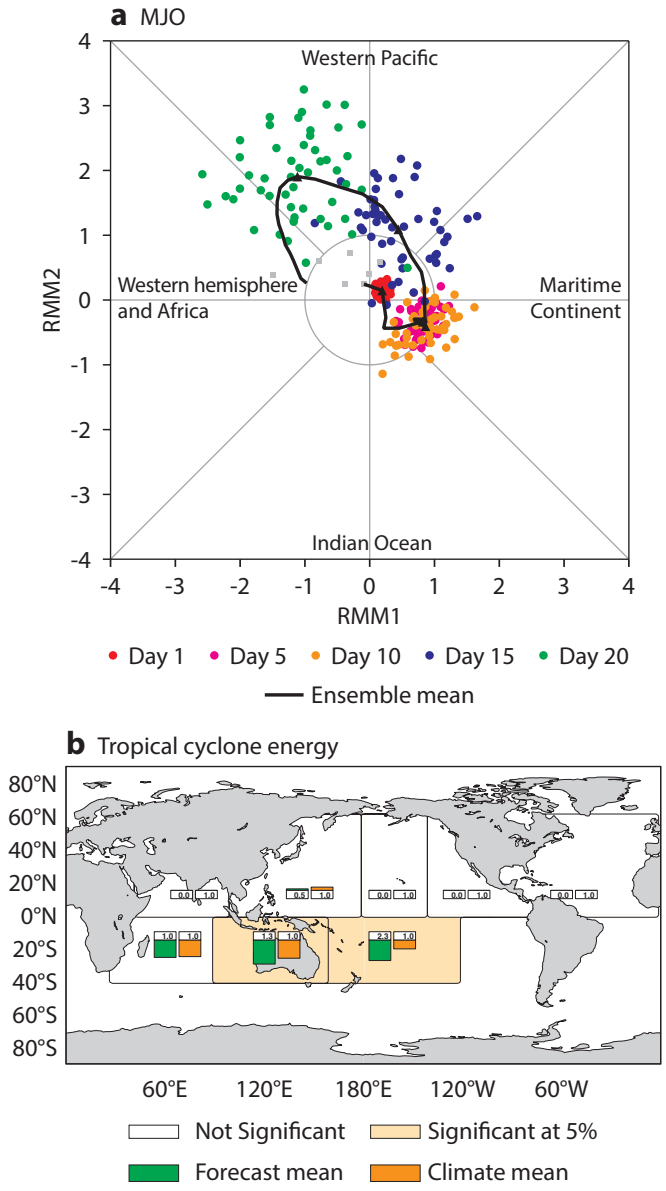

MJO and tropical cyclone energy forecasts. Monthly ensemble forecast from 26 February for (a) the MJO and (b) normalized accumulated tropical cyclone energy for 9–15 March. The dots in (a) show the progression of the active phase of the MJO over a period of 20 days as predicted by different ensemble members. The quadrants indicate the location of the active phase, and the distance of the dots from the centre represents its predicted strength. The solid line, which represents the ensemble mean forecast, suggests that the active phase of the MJO will strengthen as it moves from the maritime continent (comprising Indonesia, the Philippines and Papua New Guinea) into the western Pacific, before subsiding again as it moves over the western hemisphere.

The ensemble (ENS) and high-resolution (HRES) forecasts from 10 March 1200 UTC for the track taken by Pam were somewhat shifted to the east compared to the observed track. Still, a landfall on Vanuatu was inside the ensemble plume.

No in situ measurements of the intensity of the cyclone are available, but estimates from satellite images suggest a core pressure in the range of 896–915 hPa on 13 March. The HRES forecast from 10 March 1200 UTC predicted a minimum pressure below 900 hPa while the ensemble median minimum pressure was a much higher 950 hPa.

Tropical cyclone intensity forecasts are sensitive to the spatial resolution of the forecasting system. In the coming year the horizontal resolution of both HRES and ENS will be increased. An early test with the ENS at 17 km resolution for tropical cyclone Pam (the currently operational resolution of the ENS is 32 km) resulted in an increase in the predicted peak intensity of Pam. The median core pressure of the ensemble changes from 950 hPa to 915 hPa for this case. This corresponds quite well to the estimated observed intensity of Pam. The spread of the intensity among the ensemble members is also increased, especially during the phase of rapid intensification of the cyclone.

The example of Pam illustrates how tropical cyclones can be predicted on different timescales. In the extended range (two weeks ahead), increased tropical cyclone activity was forecast over the south-west Pacific in connection with a strong MJO event. For medium-range forecasts, we have given an example of the potential impact of increasing the resolution of the ensemble forecasts. Moreover, pre-operational experimentation with new IFS Cycle 41r1, introduced in May 2015, suggests that forecast performance for tropical cyclones will improve, both for the track and intensity. However, for this type of case, we have to appreciate that a small error in the track may drastically change the impact and that a reliable measure of forecast uncertainty is very important.

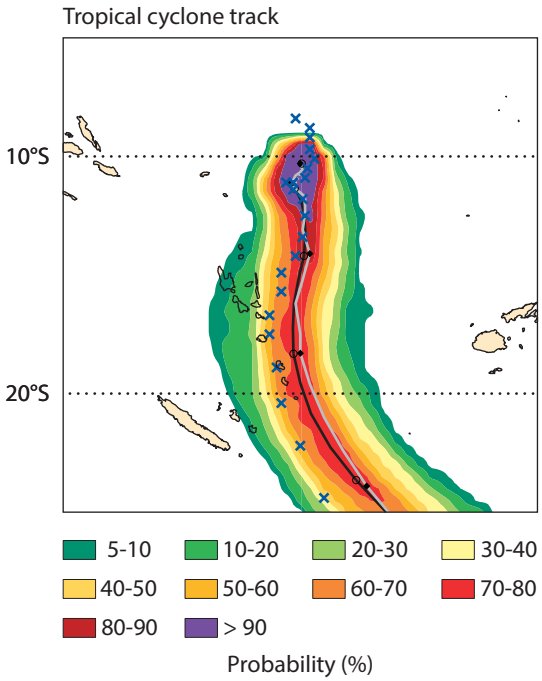

Tropical cyclone track forecast. The shaded areas show an estimate of the probability of Pam passing within a 120 km radius over the next 240 hours, starting from its position about 10° South and 170° East at 1200 UTC on 10 March. The crosses show the observed track, the black line represents the ensemble mean forecast and the grey line the high-resolution forecast.

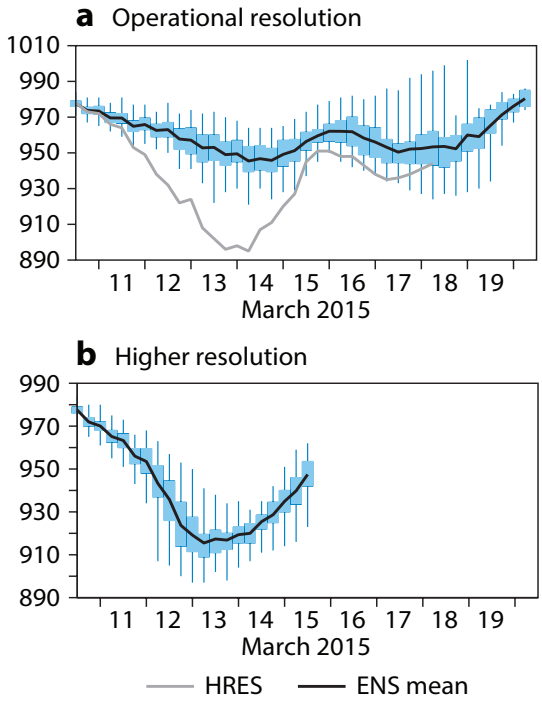

Core pressure forecasts. Forecasts of Pam's central pressure at mean sea level from 10 March 1200 UTC, showing (a) the operational high-resolution forecast (HRES) and the operational ensemble mean forecast (ENS mean) with vertical lines indicating the extreme members and blue bars representing the 25th to 75th percentile of the ensemble distribution, and (b) a higher-resolution (17 km) ensemble mean forecast.

Predicting this year's European heat wave

LINUS MAGNUSSON,
ALAN THORPE,
ROBERTO BUIZZA,
FLORENCE RABIER,
JEAN NICOLAU (Météo-France)

A heat wave affected large parts of Europe during the summer of 2015. Records include an all-time high for Germany (5 July), an all-time high for Switzerland north of the Alps (7 July), a June record for Madrid (29 June) and a July record for the UK (1 July). The 2-metre temperature anomaly from ERA-Interim for the period 1 July to 15 August was more than 3 °C for large parts of central Europe as well as Spain. In this article we examine how successive ensemble forecasts for Paris picked up the onset of the heat wave increasingly well. On 1 July, the observed temperature at 12 UTC was between 35.5 °C and 36.8 °C among SYNOP stations in Paris, and later that day one station reached 39.7 °C, the second warmest temperature on record for the city. There are, of course, many other aspects of the heat wave worth discussing but not covered in this article.

Synoptic situation

The onset of the heat wave was associated with a ridge over western Europe, bringing hot tropical air from Africa. The amplification of the ridge started on the last days of June and coincided with the arrival of a Rossby wave train over western Europe. This Rossby wave had propagated from the west and could be traced back in the analysis to the Western Pacific, where it originated around 22 June.

Another synoptic-scale element was a cyclone that developed on 26 June over the eastern US and propagated eastward over the Atlantic. These dynamical ingredients probably contributed on different timescales to the establishment and predictability of the heat wave.

Ensemble visualisations

The ECMWF ensemble is designed so that its 51 members provide a set of scenarios consistent with our knowledge of the initial conditions and the laws of physics, bearing in mind the associated uncertainties. The ensemble forecast is typically represented in the form of probability distributions, based on the relative frequency of ensemble members making particular predictions. This can take the form of a probability distribution function (PDF), shown for Paris in the top-left panel, or of a cumulative distribution function (CDF), shown in the top-right panel, or of box-and-whiskers diagrams, as shown in the mid-left and mid-right panels. We also show 2-metre temperature anomaly forecasts for Europe initialised on 18 June (bottom-left) and 22 June (bottom-right) for the week starting on 29 June to highlight the spatial pattern of the anomaly.

The different PDFs and CDFs for 2-metre temperature in Paris at 12 UTC on 1 July represent consecutive forecasts. Each PDF has been estimated by calculating a histogram of ensemble members using bins of 1 °C and applying a smoothing function with a weight of 0.5 for the central bin and 0.25 for the neighbouring bins. We have also included the distribution for the model climate, which is a useful reference as it includes the same systematic errors as the forecasts.

Results

The longest lead time illustrated here is the forecast issued one month before the event, on Monday 1 June. For this lead time – the so-called monthly forecast – it is expected that, to isolate a predictable signal, it is necessary to average in time over periods such as a week (as shown in the mid-right and lower panels). However, it is interesting to ask at which lead time the extended-range forecast for a specific time (such as 12 UTC on 1 July) acquires predictive skill. In answering this question, it is important to consider the range of scenarios predicted within the ensemble forecast.

At a lead time of a month (and certainly for point values) we expect to see only very weak evidence of predictive skill if any, and indeed there is no visible distinction between the climate and forecast PDFs and CDFs. In the forecast from Thursday 18 June, the ensemble PDF is shifted towards warmer conditions, although the chance of near-record-breaking temperatures is still rather small. The shift in the PDF was due to a large-scale warm anomaly (covering most of Europe) for a longer period, and this anomaly put its stamp on the local PDF for Paris. The forecast from Monday 22 June has a peak in the PDF close to 34°C, indicating that several members are picking up the risk of extreme temperatures, although a cold tail is still present in the distribution. At this stage forecasters in France started to pay attention to the risk of a heat wave. In the weekly temperature anomaly map for this forecast, the strongest anomalies are present over Western Europe. One could speculate that this signal is connected to the presence of the Rossby wave packet in the initial conditions.

Forecasts change substantially from around 26 and 27 June: the signal of extreme temperatures is dominating and the cold tail in the distribution has vanished, although the predicted temperatures are still a little cooler than the observed 36 °C. From 27 June, the forecast is sufficiently sharp for the coolest ensemble members to exceed the 90th percentile of the climatology. As early as 26 June, Météo-France was able to put warnings on its website for the extreme temperatures. Synoptically, at this time the cyclone had formed over the eastern US and its further development was probably less uncertain than in earlier forecasts. Finally, the 12-hour short-range forecast from 1 July 00 UTC has a very sharp distribution as little uncertainty remains for this short lead time.

To summarize the evolution, the forecast PDF peak progressively shifts towards higher temperatures and the distribution sharpens and loses its asymmetric cold tail. These are characteristics that one would hope to see in an ensemble forecast that has increasing levels of skill relative to climatology as the event approaches.

'Ready-set-go'

This case illustrates rather well how the concept of 'ready-set-go' could be used by forecasters to warn users. The ensemble distribution evolves from a

broad distribution indistinguishable from the climatology towards a very sharp distribution as the day of interest approaches. As valuable information is added to the initial conditions, the sharpness of the distribution increases, reducing uncertainty and increasing confidence. At the longer time range (2–3 weeks ahead), the ensemble provides an indication that the distribution is shifted towards warmer values – the forecaster can tell users to be ready for the possibility of an extreme weather event. At the medium range (e.g. ten days ahead), the forecaster can tell users that they are now more confident about the forecast and can suggest that they get set, i.e. start taking appropriate action that could help to manage the forthcoming weather conditions. Finally at short range (e.g. a few days ahead), forecasters can tell users that they are now very confident about the forecasts and can issue the warning: it is time to go and take action, since the extreme weather is coming.

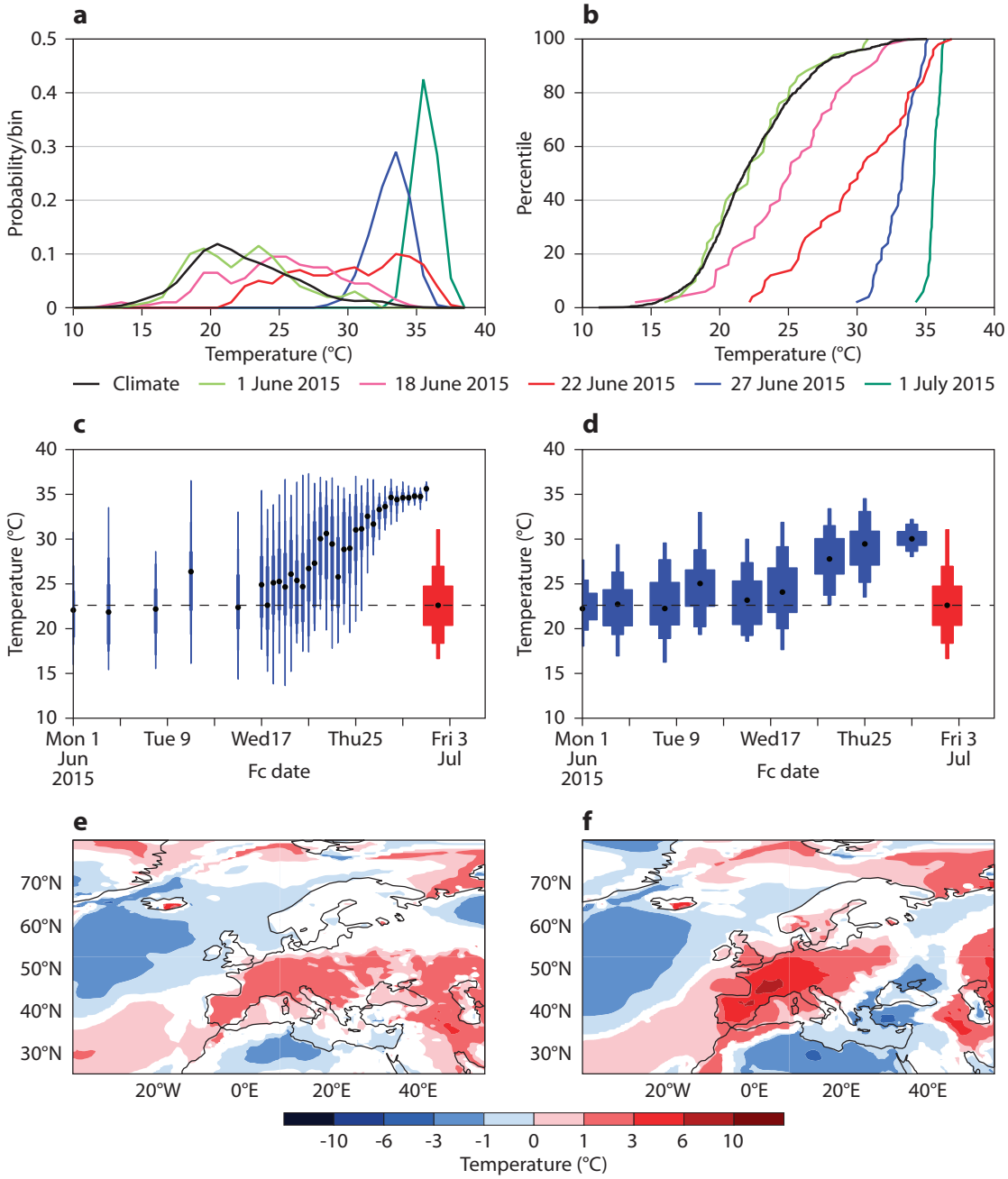

Two-metre temperature forecasts. Ensemble forecasts valid 12 UTC on 1 July in Paris visualised by (a) probability density functions (PDFs) for forecasts initialised at 00 UTC on 1 June, 18 June, 22 June, 27 June and 1 July, (b) cumulative distribution functions (CDFs) for forecasts initialised at the same times and (c) a box-and-whisker plot for forecasts initialised at different times as shown, and for the model climate shown in red; also shown are (d) a box-and-whisker plot for ensemble forecasts of the average 2-metre temperature at 12 UTC for 29 June to 5 July in Paris, and for the model climate shown in red; and 2-metre temperature anomaly forecasts for 29 June to 5 July (shading in areas where the ensemble distribution is significantly different from climatology, significance level of 10%), initialised on (e) 18 June and (f) 22 June. The box-and-whisker symbols mark the 1st, 10th, 25th, 75th, 90th and 99th percentile and the median is marked with a dot. The dotted line represents the median of the model climate.

Forecasting flash floods in Italy

LINUS MAGNUSSON, CALUM BAUGH, FLORENCE RABIER, FEDERICO GRAZZINI
(ARPA-SIMC, Bologna, Italy)

After the very warm summer in southern Europe, the autumn brought a series of severe flash floods along the French and Italian coasts. On 13 September 2015, the Emilia-Romagna region in north-western Italy was hit by a convective storm. The severe weather caused flash floods in the north-west Apennines and record discharges for the Nure and Ceno rivers as well as the Trebbia, the largest river in the region. The precipitation was generated by a single V-shaped mesoscale convective system (MCS), which formed upstream of the Apennines in a warm and humid upper-level south-westerly flow. The persistence of the low-level convergence over the Ligurian Sea maintained the convective system and it was almost stationary for 12 hours. The precipitation intensity was extreme, with four stations recording more than 110 mm/hour and almost 10 stations recording more than 80 mm/hour during the most intense phase.

Ten weather stations which are part of a high-density regional network recorded more than 250 mm/24 hours and three stations more than 300 mm/24 hours. Relying on WMO exchange observations alone without this regional input, the evaluation of ECMWF's forecasts would have missed this event. An ongoing project at ECMWF aims to collect data from national high-density networks to increase the quality of verification work and better support model development.

Farini village after the Nure stream flood. The Nure stream rose to a record level of about 5 metres. (*Photo: Federico Grazzini*)

Forecasts

The Extreme Forecast Index (EFI) and Shift of Tails (SOT) from 9 September (4 to 5 days before the event) indicated the potential for extreme precipitation along the coasts of north-western Italy and southern France on 13 September. An ensemble forecast (ENS) relatively close to the event (from 12 September 12 UTC) put the highest probabilities of more than 100 mm/24 hours along the coast, while further inland, in the flash flood region, the predicted probabilities were lower. The HRES forecast from the same time gave a similar picture as the ensemble with the main precipitation over sea (not shown).

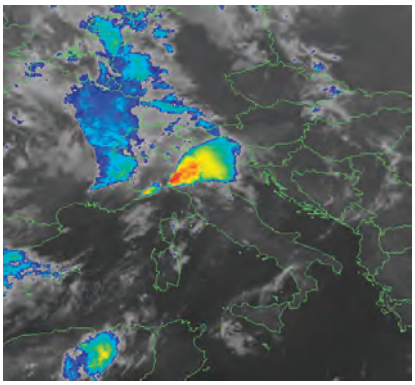

Satellite precipitation image. MSG-3 satellite enhanced infrared picture showing the V-shaped system in its mature phase at 00 UTC on 14 September.

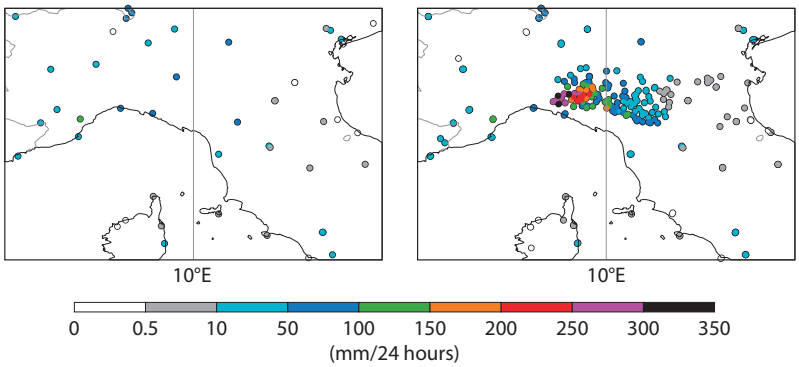

Twenty-four-hour precipitation accumulation. Observations for 13 September 06 UTC to 14 September 06 UTC from WMO exchange (left) and including some regional network stations (right).

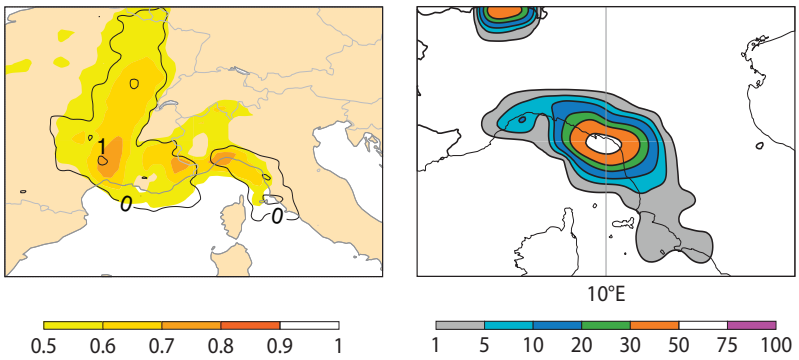

ECMWF forecasts for 13 September. EFI forecast (shading) and SOT forecast (contours) from 9 September 00 UTC (left) and ENS forecast from 12 September 12 UTC of probabilities of more than 100 mm/24 hours (right).

In the Copernicus Emergency Management Service – Early Warning System (Floods), formerly known as EFAS, additional products targeting flash floods are produced using the Enhanced Runoff Index based on Climatology (ERIC) method. Ensemble precipitation forecasts are taken from COSMO-LEPS and combined with soil moisture forecasts from the LISFLOOD hydrological model to estimate the amount of surface runoff. COSMO-LEPS is a limited-area ensemble provided by ARPA-ER SIMC (Italy) that uses the global ECMWF ensemble for initial and boundary conditions. For the flash flood event in Emilia-Romagna the ERIC forecast on 12 September 2015 00 UTC predicted only a low probability of major flash flooding within the affected area. A flood forecast for a point on the upper part of the River Trebbia (where the maximum precipitation was observed) indicated a 15% risk of exceeding a five-year return period, a relatively low but non-negligible probability.

The large-scale atmospheric flow was captured in ECMWF's medium-range forecasts (even up to a week in advance) but the severe mesoscale convective system was missed even by the shortest-range HRES and ENS forecasts. COSMO-LEPS had a few members with a precipitation pattern similar to the observed one, but the resulting probability was low. The low probability was due to the local nature of the convective storm and the fact that only a few members predicted intense precipitation in the right place.

Outlook

It is anticipated that these events will be better simulated with higher model resolution, and that additional observations of moisture over the sea, such as data from the Meteosat Third Generation (MTG) programme, will produce better initial condition estimates. This should in turn improve precipitation and flood forecasts. However, small differences between forecasts and outcomes in the position of convective cells may still lead to relatively low probabilities from the ensemble forecasts, and post-processing of the raw data might still be needed.

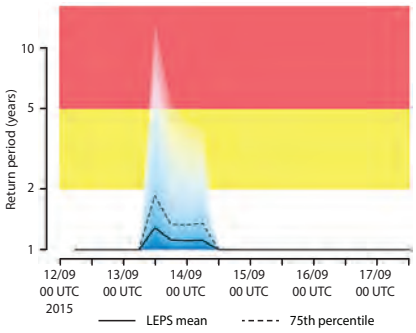

Copernicus forecast for 12 to 17 September. Copernicus probabilistic flash flood return period forecast for a point on the River Trebbia from 12 September 12 UTC. The blue-shaded area shows the predicted probability distribution of an event with a return period of more than a year for 6-hour intervals. According to the forecast, there is a 24% chance of an event with a return period of more than 2 years and a 15% chance of an event with a return period of more than 5 years in a 6-hour interval on 13 September.

Wind and wave forecasts during Storm Gertrude/Tor

LINUS MAGNUSSON,
JEAN BIDLOT

ECMWF forecasts provided early indications of a windstorm that hit north-western Europe at the end of January 2016. Predicted winds and waves were slightly lower than those observed at North Sea oil platforms, but ensemble wave forecasts produced using ECMWF's new higher-resolution model matched observations reasonably well.

The winter 2015–2016 started with a positive phase of the North Atlantic Oscillation (NAO), resulting in warm, windy and rainy weather in north-western Europe during December. The central and northern parts of the British Isles experienced two episodes of severe flooding after storms Desmond and Eva. In January, the weather turned colder in northern Europe with a weaker westerly flow. However, the positive NAO phase returned in the last days of January, bringing a severe windstorm to this part of Europe.

The cyclone, named Gertrude in the UK and Tor in Norway, formed south of Iceland late on 28 January. It rapidly deepened by 30 hPa during the next 24 hours and reached 948 hPa late on 29 January. Red warnings for extreme winds and high waves were issued for Shetland and the southern half of Norway, and amber warnings for Scotland. In Scotland, wind gusts of up to 50 m/s were measured. When the storm made landfall on the Norwegian coast, a new record mean wind speed for Norway was measured at Kråkenes fyr (lighthouse): a 10-minute average of 48.9 m/s, with gusts of up to 62 m/s. Fortunately, the storm did not cause any fatalities, and only limited damage was reported. This can partly be attributed to early warnings. ECMWF forecasts gave a clear indication of extreme winds six days in advance.

The band of the strongest winds stretched from Shetland towards the western part of Norway and passed the oil fields in the North Sea. Many of the oil platforms submit meteorological and wave observations every hour. This provided an opportunity for a

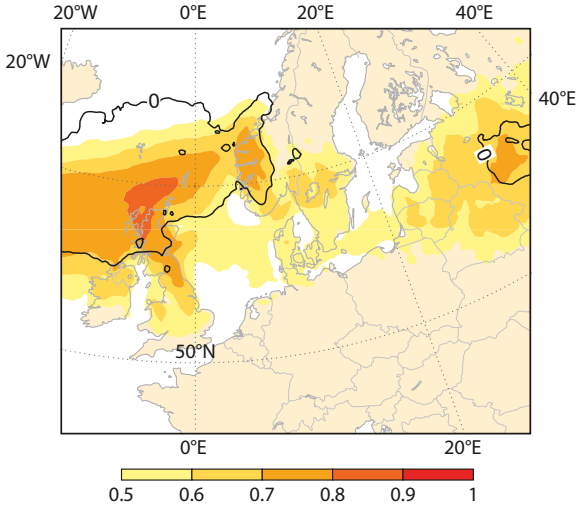

Extreme Forecast Index (EFI) and Shift of Tails (SOT). The chart shows the EFI (shading) and SOT (contours) for 10-metre wind gusts for the forecast from 00 UTC 24 January valid on 29 January (00-24 UTC).

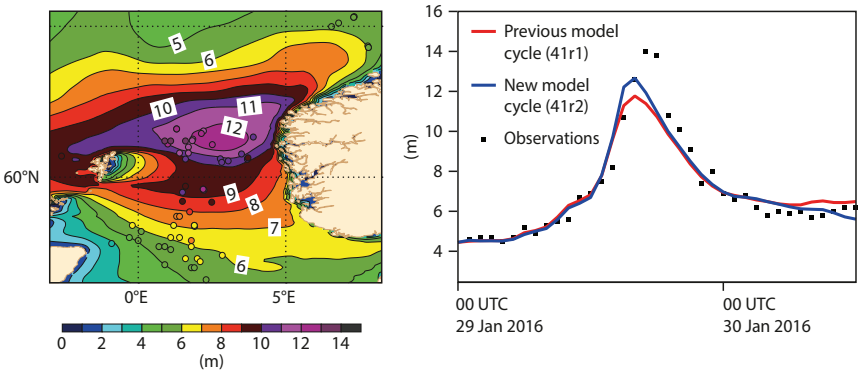

High-resolution wave forecasts and observations. The left-hand panel shows ECMWF's 18-hour high-resolution significant wave height forecast from 00 UTC on 29 January (shading) produced using the new model cycle 41r2, and raw observations (circles). The right-hand panel shows observations from an oil platform located at 61.2°N, 1.1°E, and high-resolution forecasts (HRES) for the nearest grid point from 00 UTC on 29 January produced using the previous model cycle 41r1 and the new model cycle 41r2.

detailed evaluation of ECMWF's wave forecasts produced by the new model cycle 41r2 under extreme conditions, with significant wave heights up to 14 metres. With hourly data from the model, we can compare both the model cycle operational at the time (41r1) and the new model cycle (implemented on 8 March 2016) with observations from an oil platform located at 61.2°N, 1.1°E.

All of the last three forecasts before the peak of the event (28 Jan 12 UTC, 29 Jan 00 UTC and 12 UTC) underestimated the intensity of the peak in the mean wind at the oil platform (28 m/s compared to 38 m/s in the most extreme observation – not shown). However, one has to bear in mind that the measurements are probably made at a height greater than 10 metres and would have to be calibrated for a proper comparison with 10-metre wind forecasts produced by the model. For the wind speed, both model versions give similar values. The maximum significant wave height is also somewhat underestimated (12 metres in the forecast from 29 Jan 00 UTC compared to 14 metres in observations). Comparing the forecasts

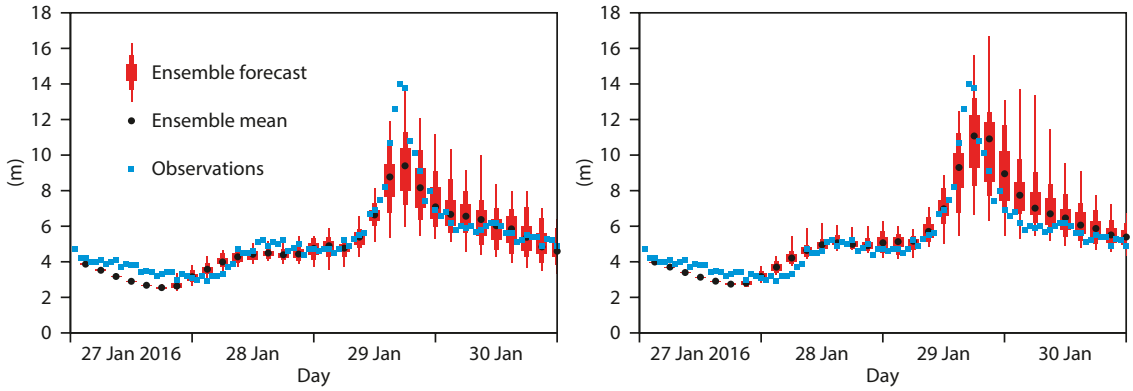

Ensemble wave forecasts and observations. Ensemble forecasts of significant wave height from 00 UTC on 27 January 2016 for 61.2°N, 1.1°E, from the previous model cycle 41r1 (left) and the new model cycle 41r2 (right), and observations.

from the two model cycles, the wave forecast produced by the new model was about 1 metre higher at the peak of the event despite predicting similar wind speeds. This is due to the increased horizontal resolution both in the atmospheric model (9 km grid spacing instead of 16 km) and in the wave model (14 km instead of 28 km), as previously demonstrated for a severe storm that hit the Faroe Islands in November 2011.

The ensemble forecast from the new model shows more extreme scenarios than that produced by the old model, and observed waves are within the range of uncertainty indicated by the forecast from 27 January 00 UTC. For this part of the North Sea, ensemble forecasts are essential as a small difference in the cyclone path can make a large difference in wave fields because of the sheltering effect of the Shetland Islands.

Forecasts showed Paris flood risk well in advance

LINUS MAGNUSSON, FREDRIK WETTERHALL, FLORIAN PAPPENBERGER

At the end of May 2016, large parts of Europe were affected by severe convective precipitation. Flash floods in several places in southern Germany led to fatalities. Further to the west, the River Seine burst its banks. The peak flow in Paris, which was reached in the early hours of 4 June, was the highest since 1982.

ECMWF's forecast index for extreme weather showed the risk of extreme precipitation in the affected regions several days in advance. The Centre's precipitation and temperature forecasts feed into flood forecasts issued by the EU's Copernicus Emergency Management Service (EMS). These indicated the possibility of an event with a 20-year return period in Paris as early as 25 May.

Record precipitation

According to the French national meteorological service, Météo-France, May 2016 was the wettest since 1960 in the Île-de-France region. At the Paris-Montsouris weather station, the monthly total reached 179 mm, about three times as much as the climatological average, beating the previous record of 133 mm reached in May 1992. In the catchment area for the Seine, the soil was wet even before the most intense rainfall, which occurred around 30 May. As part of the ongoing project to collect high-density observations from national networks for verification purposes, ECMWF receives precipitation data from about 1,100 weather stations in France, a much higher number than the 190 SYNOP stations from which data is received through the Global Telecommunication System. These data enable ECMWF to better understand the spatial structure of precipitation events such as this. For 30 May 06 UTC to 31 May 06 UTC, almost all stations in northern-central France reported more than 20 mm accumulated precipitation, with a number of stations reaching 40 mm and a few more than 60 mm, which is equivalent to about a month's worth of rain. The precipitation was caused by an upper-level cut-off low that had a destabilising effect on the atmosphere and brought warm air northwards on its eastern side.

Extreme Forecast Index

ECMWF produces the Extreme Forecast Index (EFI) and the Shift of Tails (SOT) to help identify areas at risk of extreme weather. Both products compare the probability distribution function (PDF) derived from the ensemble forecast with the climatological PDF derived from a reforecast dataset. While the EFI measures the integrated shift of the PDF in the forecast, the SOT focuses on the extreme tail of the distribution. The forecast from 25 May 12 UTC indicated an increased risk of extreme precipitation for the 3-day period 29–31 May. High SOT values indicate

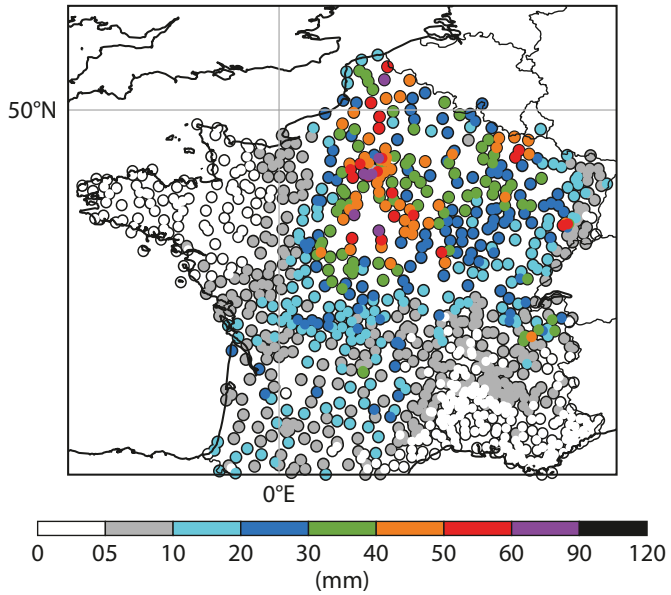

High-density network. Observed precipitation between 30 May 06 UTC and 31 May 06 UTC from high-density observations received from France.

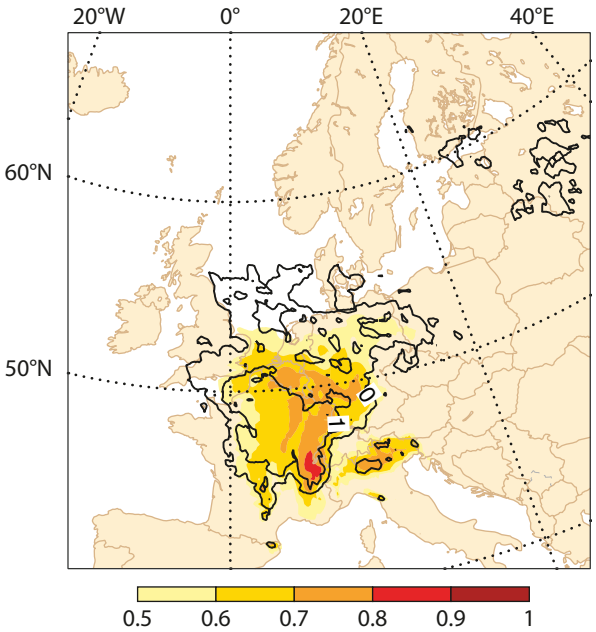

Risk of extreme precipitation. Extreme Forecast Index (EFI) (shading) and Shift of Tails (SOT) (contours) for precipitation accumulated between 29 May 00 UTC and 1 June 00 UTC in the forecast from 25 May 12 UTC.

that a few ensemble members predict extreme precipitation. The early detection of the risk of extreme precipitation was due to the large-scale forcing. Although the forecasting system is not able to correctly predict individual convective cells, the increased probability of such cells is predictable.

Flood forecasts

The European Flood Awareness System (EFAS) uses precipitation and temperature forecasts from ECMWF, the German national meteorological service (DWD) and the COSMO consortium (COSMO Limited-Area Ensemble Prediction System forecasts) as forcings for its flood forecasts (https://www.efas.eu/user-information.html). EFAS produces medium-range probabilistic flood forecasts across Europe as part of the Copernicus Emergency Management Service – Early Warning Systems. In the figures presented here, the ECMWF ensemble forecast and high-resolution (deterministic) forecast are presented together with the DWD's deterministic forecast. COSMO-LEPS short-range forecasts were similar to ECMWF's predictions in this case.

The EFAS forecast system indicated the possibility of river discharge levels with a return period of more than 20 years as early as 25 May. By 26 May, a flood notification for a 1-in-20 year event was issued by EFAS for the Loing River (a tributary of the Seine). On 28 May, the warning was extended to the Seine in Paris.

As the event drew nearer, the magnitude of the predicted river discharge fluctuated between 30 May and 31 May depending on the expected rainfall for the event, but the timing was very stable, with the peak flow centred on Friday 3 June. Overall, the DWD deterministic forecast showed a more stable performance. Forecasts closer to the peak flow, for example from 2 June, showed a much smaller spread in the ensemble forecasts. This was mainly due to the fact that the major precipitation event occurred on 30 May, and the hydrological model propagated the flood wave down the Seine. The 2 June ensemble forecast generally slightly overpredicted discharge levels for the following few days. This was true for all ensemble members, indicating that the forecasts were not diverse enough to capture the observed intensity of the event. Although the ensemble spread cannot be assessed on the basis of a single case, we expect the ensemble to be over-confident as the EFAS system does not yet represent initial and model uncertainties in the hydrological model.

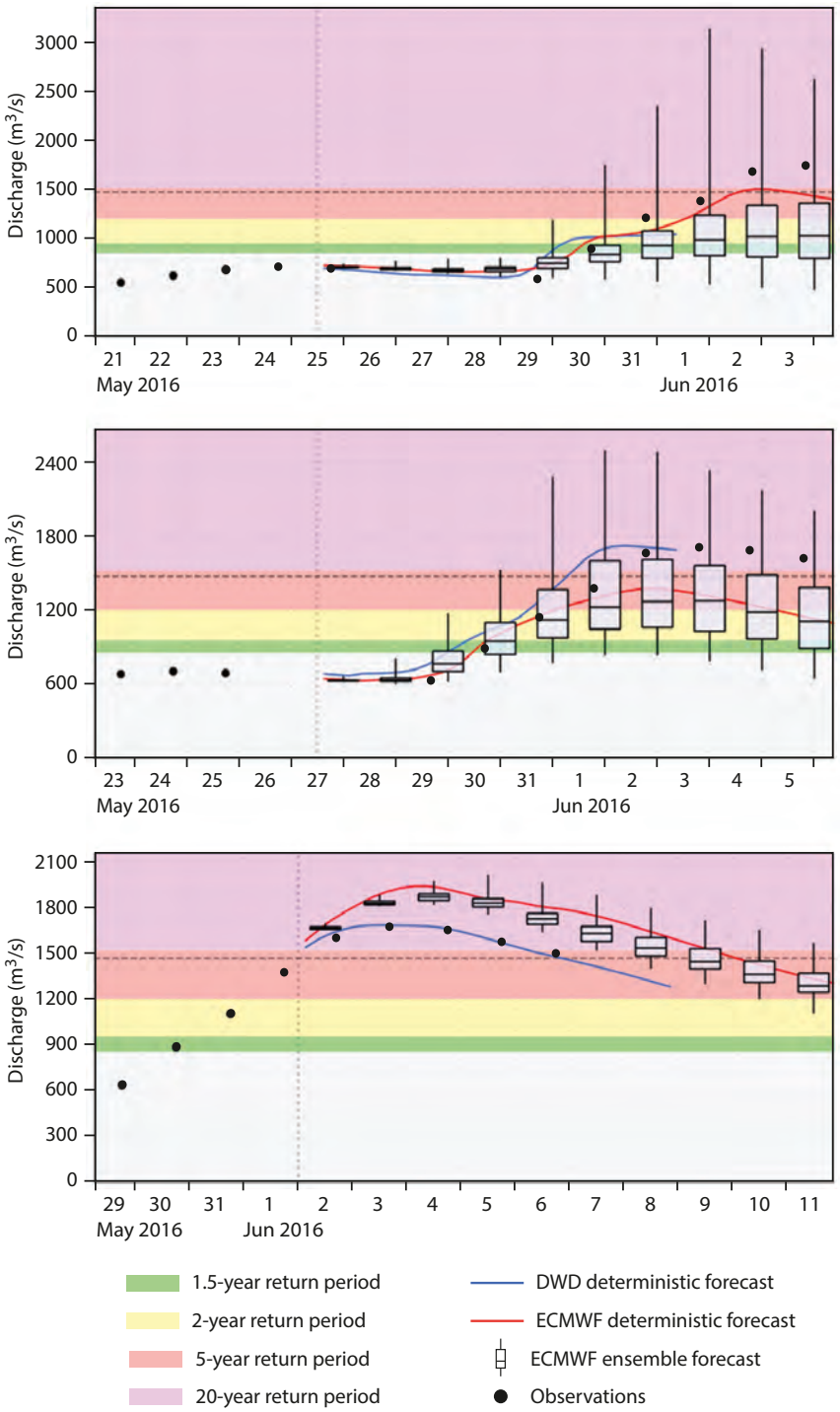

EFAS forecasts. The charts show EFAS forecasts issued on 25 May 12 UTC (top), 27 May 12 UTC (middle) and 2 June 00 UTC (bottom) for the Seine in Paris. The box-and-whisker plot represents the ECMWF ensemble forecast and shows the median (horizontal line), the 25th and 75th percentiles (box), and the minimum and maximum values (vertical lines).

Predicting heavy rainfall in China

LINUS MAGNUSSON, THOMAS HAIDEN

On 19 and 20 July, severe rainfall hit central and north-eastern China. ECMWF's forecasts three to five days ahead of the event performed reasonably well, but the quality of earlier forecasts was geographically uneven.

The rainfall was connected to a low pressure system that formed over southern China and moved northward. The cyclone generally resulted in more than 50 mm of rain in 48 hours along its way, with some stations in central China receiving more than 200 mm. Further north, the precipitation in Beijing reached almost 300 mm over the two days, but local variations were large. ECMWF's high-resolution forecast (HRES) from 19 July 00 UTC predicted rainfall in excess of 300 mm locally south-west of Beijing in the first two forecast days, which shows that the forecast system is capable of simulating such extreme rainfall, although one should not expect it to capture the exact location of the extremes.

In the last forecast before the start of the accumulation period, the HRES and ensemble forecast (ENS) median gave around 150 mm for a grid point in Beijing. Ensemble members ranged from 50 to 300 mm, which indicates a large uncertainty in the local severity even in the shortest forecasts. Looking at earlier forecasts, a risk of 25% or higher for more than 100 mm was predicted by ENS from 16 July onwards, which corresponds to a forecast range of 3–5 days.

In forecasts produced before 16 July, the southern part of the rainfall was captured well, but the extension to the north, where the most severe rainfall occurred, was missed. This is apparent when we compare EFI (Extreme Forecast Index) and SOT (Shift of Tails) values for 3-day accumulated rainfall (19–21 July) in the forecasts from 15 and 19 July.

This event was one of several episodes of extreme rainfall in China this summer. At the beginning of July, central China was hit by severe rainfall that resulted in flooding of the

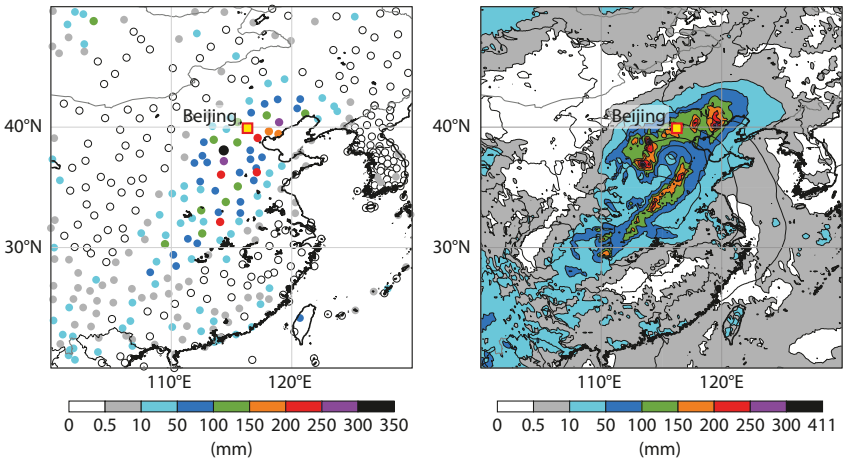

Observations and short-range forecasts. Forty-eight-hour observed precipitation 19 July 00 UTC to 21 July 00 UTC from SYNOP observations (left) and predicted 48-hour precipitation from the HRES issued 19 July 00 UTC (shading) together with mean sea-level pressure (contours) valid 20 July 00 UTC (right).

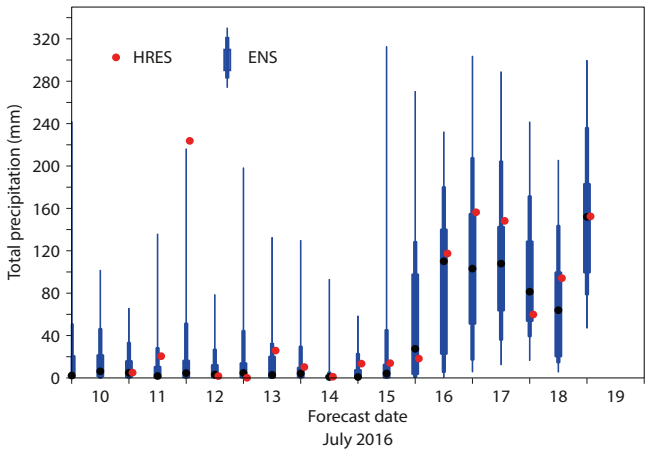

Ensemble and high-resolution forecasts. ENS and HRES 48-hour precipitation at a grid point in Beijing valid 19 July 00 UTC to 21 July 00 UTC for a range of starting dates. Black dots in the box-and-whisker plot represent the ENS median, the wide boxes represent the 25th and 75th percentile, the narrower boxes represent the 10th and 90th percentile, and the vertical lines show minimum and maximum values.

Yangtze River. In this case, the short-range (1–2 days) ECMWF forecasts placed the rainfall somewhat too far north. Although the location error was only in the order of 100 km, it was big enough to have presented a substantial challenge to forecasters trying to predict rainfall levels for specific river catchments.

Cooperation agreement

In 2014 ECMWF concluded a cooperation agreement with the China Meteorological Administration (CMA). Their local knowledge and the availability of high-density observations will help us to better assess and understand the performance of our forecasts. One of the areas of cooperation will be the evaluation of ECMWF's forecasts in China using high-density observational datasets. This will enable ECMWF to obtain more detailed results on model performance in this area.

If insights gained from these studies lead to improved forecasts in the region, then that will not only be of importance for forecasters in China but may also be beneficial for Europe. Forecast errors can propagate with the group velocity of Rossby waves, so that initial and short-range errors

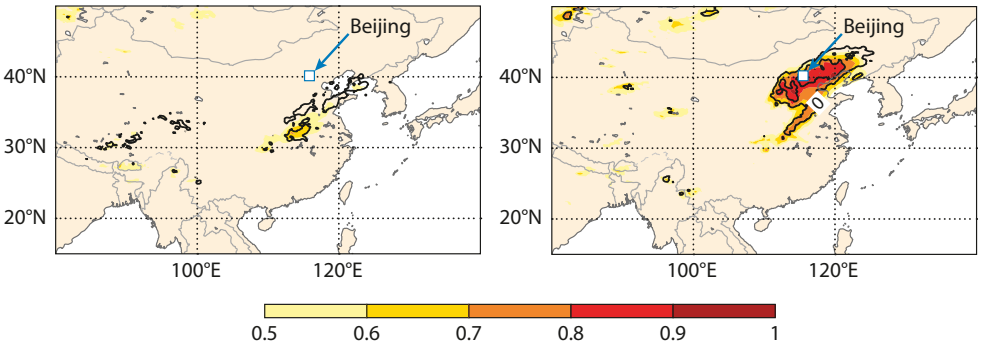

Extreme Forecast Index and Shift of Tails. EFI (shading) and SOT (contours) for 3-day precipitation (19–22 July) from 15 July (left) and 19 July (right).

originating in the area of China could reach Europe eight to ten days into the forecast. Therefore, one of many ingredients for achieving ECMWF's strategic goal of predicting risks of extreme weather over Europe two weeks in advance may be improved analysis and forecast performance over South-East Asia.

Other recent events

On 6 August, Skopje, the capital of the former Yugoslav Republic of Macedonia, was hit by severe flash floods that killed at least 21 people. The location of this event was not well predicted by ECMWF's forecasts.

In the second week of August, the US state of Louisiana was hit by severe rainfall over a period of three to four days. The large-scale features of this event were well predicted around a week in advance, while capturing the local details was a challenge even in the shortest-range forecasts due to its convective nature.

Evaluations of all the events mentioned in this article can be found in the ECMWF Severe Event Catalogue at https://software.ecmwf.int/wiki/display/FCST/Severe+Event+Catalogue.

Flash floods over Greece in early September 2016

TIM HEWSON,
IVAN TSONEVSKY

Between about midday on 6 September and midday on 7 September 2016, extreme rainfall affected parts of Greece, most notably in the southern part of the Peloponnese and also much further north, over and just south of Thessaloniki. According to media reports, the resulting flash floods caused four fatalities, invaded properties, closed roads, and caused cars to be piled up and locally swept out to sea. Rainfall reports are limited, though Kalamata airport recorded more than 130 mm in 24 hours, whilst various unofficial reports from nearby suggest 24-hour totals of the order of 200 mm, most of which fell in two or three hours. Meanwhile a report in the ESSL (European Severe Storms Laboratory) database indicates that over 300 mm fell locally near Thessaloniki. Experience from similar extreme rainfall events suggests that spatial variability can be very high. This means that even larger amounts may have accumulated very locally in each case, even in the absence of topographic forcing. In the figure showing observed rainfall totals there is evidence of such variability near Thessaloniki and also in the high-density observations over the heel of Italy, in a relatively flat area. One current project at ECMWF aims to automatically predict the degree of sub-grid variability in precipitation totals, in recognition of how important this is to users interested in flood risk, and because raw model output provides only a grid-box average.

Synoptic situation

The synoptic situation over Greece on 6 and 7 September was characterised by moist and very unstable south to south-easterly flow, ahead of upper and surface low pressure systems situated to the west. The mean 500 hPa geopotential height field from the 96-hour ensemble forecast (ENS) shown in the figure is quite accurate compared to the analysis; most notably the cut-off upper vortex – the driver of the bad weather – was well positioned over southern Italy. The equivalent high-resolution forecast (HRES) for the same time (not shown) was very similar, just marginally worse. Getting features of the large-scale flow pattern reasonably correct is a necessary but not sufficient condition for accurate predictions of severe surface weather. The cold front shown in the inset was also a key player – extreme convective activity would lie on and ahead of it. In the model sounding in the second inset one can see evidence of extreme convective instability, given triggering by sea-surface temperatures of about 26°C, and the copious low-level moisture supply, both of which would help to generate very large rainfall totals.

Aftermath. The floods left cars piled up in the streets of Kalamata on 7 September. (*Photo: EPA/ Nikitas Kotsiaris*)

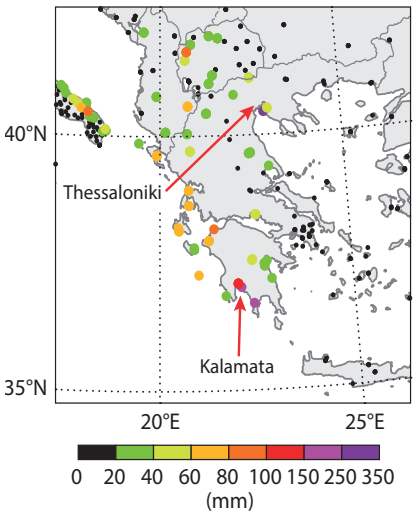

Rainfall totals. Observed 24-hour rainfall totals up to 06 UTC on 7 September 2016, compiled from both official and unofficial sources.

Rainfall forecasts

The remaining figures show HRES and ENS rainfall forecasts, respectively, for a lead time of three to five days, spanning the event. This relatively long window was used to be sure to capture the passage of any extreme rainfall related to the front, and also because it is a standard time window used for the EFI/SOT (Extreme Forecast Index and Shift Of Tails) products provided to forecasters on the web. HRES shows a lot of local detail, correctly signalling a potential for very large totals around Thessaloniki. However, the forecast for Kalamata does not look that extreme relative to other areas (41 mm spot total for the town). ENS as represented by ECMWF's extreme weather indices, on the other hand, correctly highlights both Thessaloniki and Kalamata as being at risk. The EFI is high in both locations (0.8 to 0.9), suggesting that *very large rainfall totals are likely*, whilst the SOT is also high (>2), suggesting that a *truly exceptional event is possible*. This case is a good example of the benefits of using ECMWF output and products for severe weather prediction. It also illustrates that, in the medium range at least, ENS is the main tool to use by forecasters when it comes to identifying areas at risk. HRES is more prone to provide unreliable local detail and similarly to jump between successive runs in its

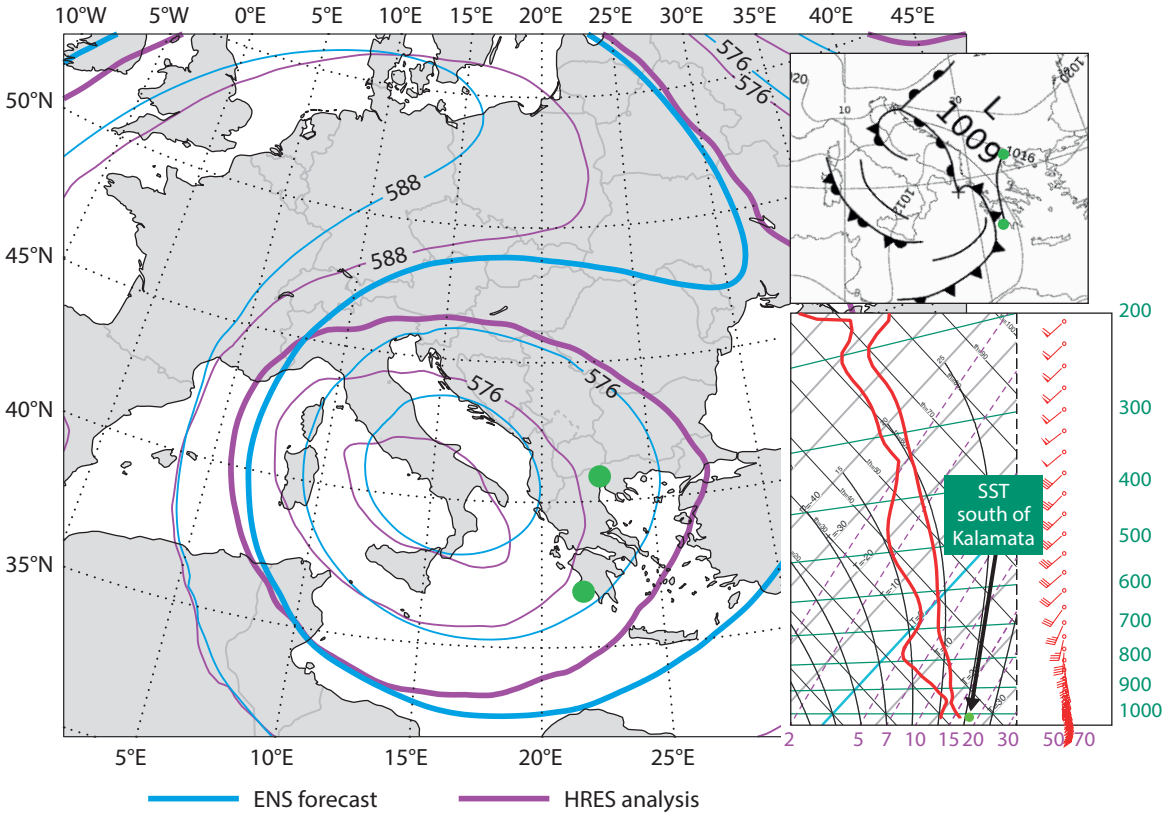

Synoptic situation. The main panel shows the ENS mean 96-hour forecast of 500 hPa geopotential height valid at 00 UTC 7 September 2016 and the HRES analysis for the same time. The top inset shows the UK Met Office surface analysis for the same time. The green dots show the location of Kalamata and Thessaloniki. The bottom inset shows a model T+0 sounding from HRES for the same time, for a marine area just south of Kalamata.

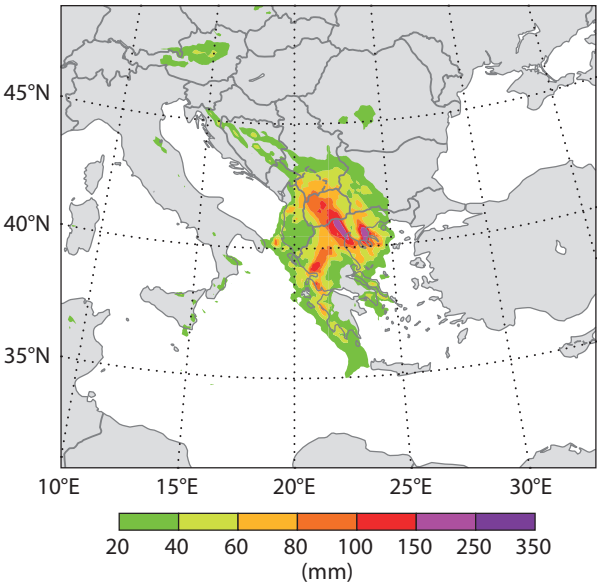

HRES rainfall forecast. HRES forecast of 72-hour rainfall total initialised at 00 UTC on 3 September 2016, valid from 00 UTC on 5 September to 00 UTC on 8 September.

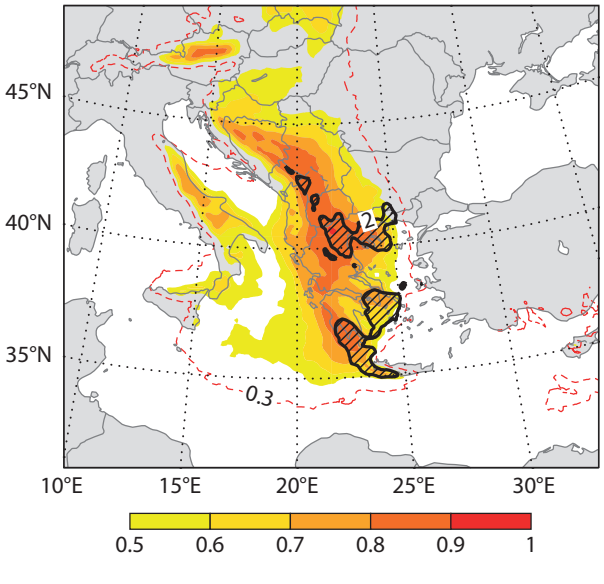

EFI and SOT for rainfall. EFI (shading) and SOT (hatching for SOT>2) for 72-hour rainfall from the ENS run initialised at 00 UTC on 3 September 2016, valid from 00 UTC on 5 September to 00 UTC on 8 September.

indications of where extreme weather may be. This is especially true when the situation is dynamically and/or thermodynamically unstable, as is the case with most severe weather events, including the one illustrated here. It is for such reasons that ensemble prediction lies at the heart of ECMWF's new ten-year Strategy.

ECMWF acknowledges the use of some rainfall data from ESSL, from the Remote Sensing Department and the Department of Meteorological Stations in the Hellenic National Meteorological Service, and from the Weather Underground website.

The cold spell in eastern Europe in January 2017

LINUS MAGNUSSON

A significant part of the winter 2016/2017 was dominated by blocking conditions over Europe bringing warm air towards north-western Europe and cold air into southern Europe. For large parts of eastern Europe the second week in January was the most extreme of the winter. Russia experienced the coldest Orthodox Christmas in 120 years, and temperatures dropped to almost -30°C in Romania and the former Yugoslav Republic of Macedonia. In Sofia, Bulgaria, ECMWF's Extreme Forecast Index (EFI) for short-range (1-day) forecasts reached -1 for three consecutive days (8–10 January). The 3-day average temperature in the city over that period was -12°C, which is 10 degrees below normal. At the same time a lot of snow fell in various parts of southern Europe, including southern Italy and Greece.

Synoptically, the wintry weather was caused by the advection of a pool of cold air from northern Russia to the southwest. This development was linked to the amplification of a ridge over the north-eastern Atlantic and of a trough downstream. Later the trough formed a cut-off low over south-eastern Europe.

Forecast quality

How well was the cold spell predicted? Focusing on the average temperature in Sofia between 8 and 10 January, no signal was present in forecasts issued before the last day of December (including monthly forecasts). During that time, the ensemble forecast distribution was close to the climate distribution. However, from 1 January (8 to 10 days before the event) all members predicted colder than normal temperatures, and from 4 January (4 to 6 days before the event) all ensemble members predicted temperatures below the 10th percentile of the model climate. The broad geographic area where cold temperatures were predicted is evident in the EFI and SOT (Shift of Tails) plots from the same date.

The short-range forecasts (1 to 3 days before the event) were clearly outside the 1st percentile of the model climate for 3-day average temperature. However, the predicted 3-day averages (around -17°C) are much lower than the observed average of -12°C.
A plausible reason is that the local conditions around the observation station were influenced by the heat created in the city. A possible solution to this issue is to include an urban tile in the model, which is part of ECMWF's long-term plans. More rural observation stations showed considerably lower temperatures at the same time (not shown).

Model climate

The cumulative distribution functions of the observed climate and the model climate (derived from re-forecasts) for midday (12 UTC) temperatures in January for Sofia are very similar in normal and warm conditions. In cold conditions, on the other hand, the model climate is colder than the observed one. The difference might be related to the urban setting of the station (as mentioned above) and/or systematic model errors. The discrepancy shows the benefit

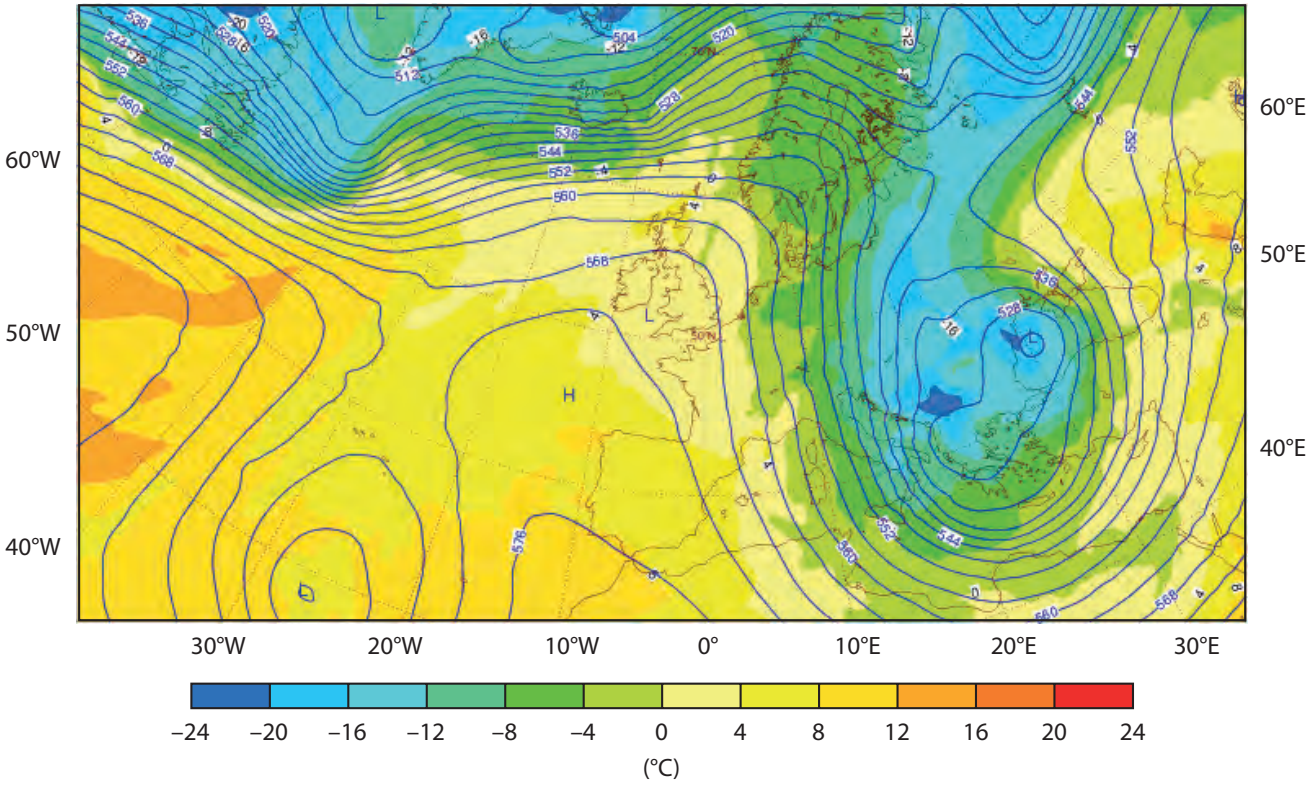

Synoptic situation. Analysis of 500 hPa geopotential height (contours, in decametres) and 850 hPa temperature (shading) on 8 January 00 UTC.

of using the model climate instead of the observed climate when calculating anomalies and points to the need for calibration under certain circumstances. It is worth noting that in other locations the opposite difference can be seen: the model is too warm in cold conditions during winter, especially in rural regions in northern Europe.

To summarise, the extended-range forecasts failed to predict the cold period in the second week of January in eastern Europe, while it was well captured in medium-range forecasts. In short-range forecasts the predicted temperatures were too low, probably because they failed to take into account local conditions, pointing to the need for post-processing.

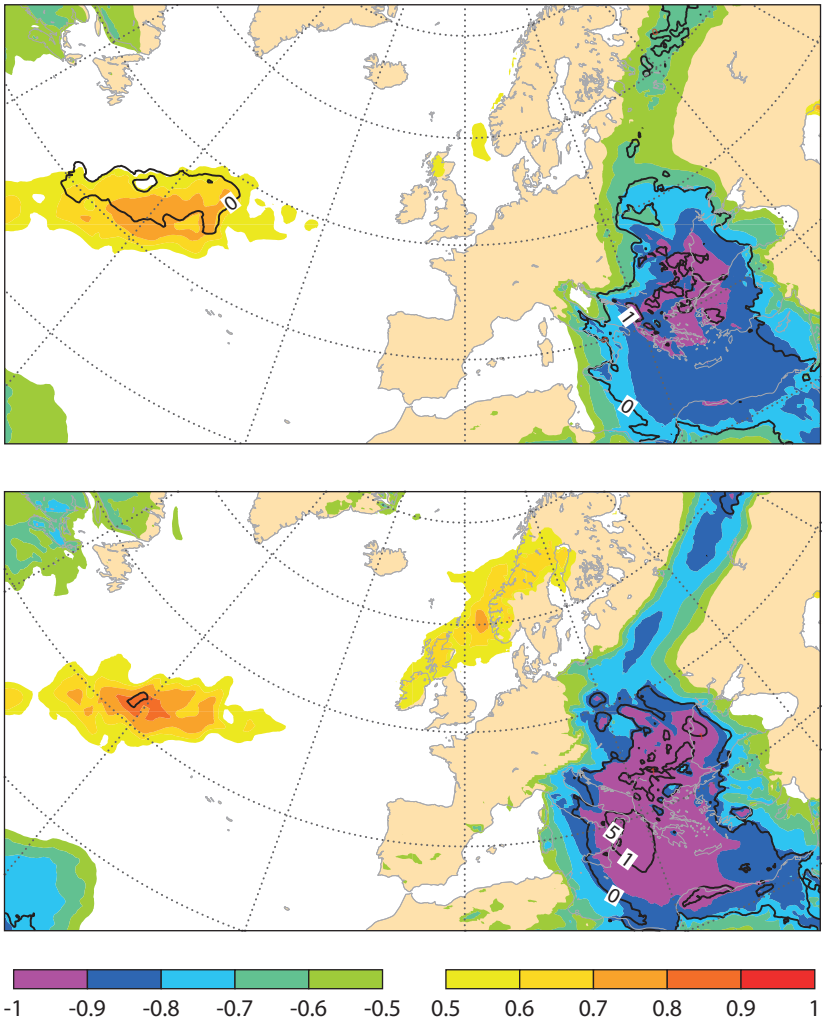

Extreme Forecast Index and Shift of Tails. EFI (shading) and SOT (contours) forecasts for average 2-metre temperature from 8 to 10 January starting from 00 UTC on 4 January (top) and 00 UTC on 8 January (bottom).

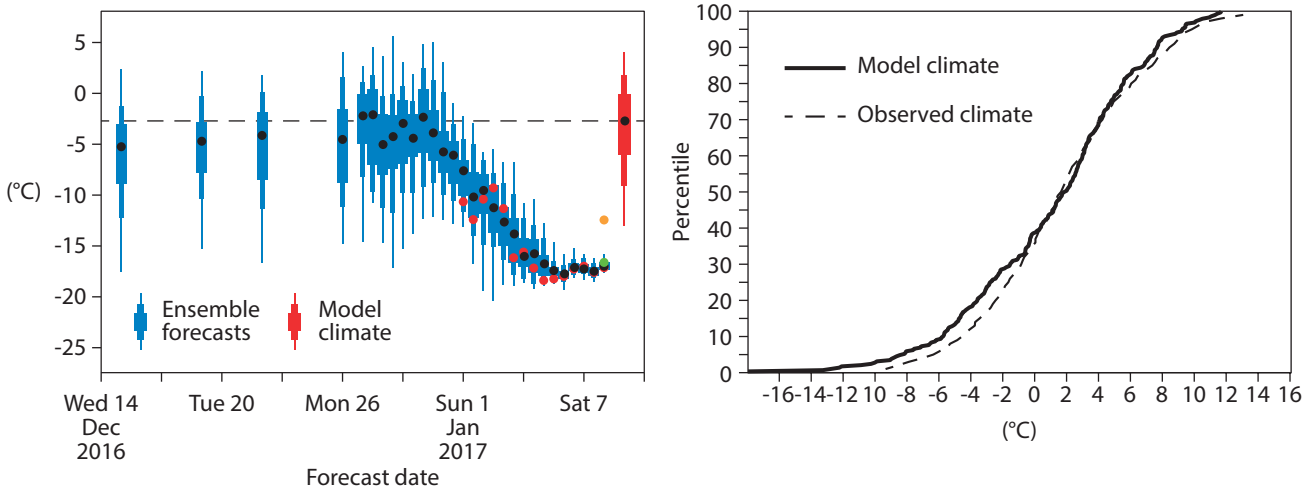

Forecasts and climatologies for Sofia. The box-and-whisker plot (left) shows ensemble forecasts of the average 2-metre temperature from 8 to 10 January in Sofia at successively shorter forecast ranges. The model climate is shown in red. High-resolution (HRES) forecasts are shown as red dots, the analysis is indicated by a green dot and the observed value by an orange dot. The box-and-whisker symbols mark the 1st, 10th, 25th, 75th, 90th and 99th percentile and the median is marked with a black dot. The dotted line represents the median of the model climate. The cumulative distribution functions (right) show the model climate (solid line) and the observed climate (dashed line) for 2-metre temperature at 12 UTC in January in Sofia.

ECMWF supports flood disaster response in Peru

FATIMA PILLOSU, UMBERTO MODIGLIANI, LINUS MAGNUSSON (all ECMWF), **MARTI BONSHOMS CALVELO** (SENAMHI, Peru), **LUISA STERPONI** (consultant for Peruvian Defence Ministry), **MARIA-HELENA RAMOS** (Irstea, France), **PATRICIO VALDERRAMA** (COEN, Peru)

From March 2017, ECMWF provided Peru with its forecast products for a limited period of time to help the country deal with the exceptionally heavy rainfall it experienced in the first few months of the year. As early as 3 February, the government declared a state of emergency in all coastal regions. The most affected areas were in the north (Tumbes, Lambayeque and Piura). In Piura, several records for daily precipitation were broken: on 3 March in El Partidor, 258.5 mm was recorded; 121.6 mm was measured on 21 March in San Miguel; and between February and March in the area of Morropon 150 mm was exceeded on three occasions. In this area, in the past similar amounts have only been recorded during exceptional El Niño events, such as those seen in 1983 and 1998.

The rainfall led to rising waters in coastal ravines. In more southern mountainous regions, this led to what is known in Peru as 'huaicos', which are a mixture of water, mud and rocks. Several rivers burst their banks causing flooding and damage to housing and infrastructure in urban and rural areas; the failure of drainage systems; and disruption of the electricity supply and sewage treatment plants. As of 31 March, the disaster had left 101 people dead, 353 injured and 19 missing, while more than 200,000 homes had been destroyed or had become uninhabitable (figures from COEN, Centro Operaciones de Emergencia Nacional of the Peruvian Ministry of Defence).

Seasonal forecast

This anomalous rainfall is believed to be connected to warm sea-surface temperatures along the coast (a phenomenon called El Niño Costero), which were probably caused by an equatorial Kelvin wave in the ocean. This feature propagated from the Western Pacific, where it was first observed in the autumn of 2016 as a positive sea-surface height anomaly. Probably as a result of capturing the Kelvin wave early on, ECMWF's seasonal forecast was able to predict the anomalous rainfall along the equatorial coast of South America. The forecast from 1 November 2016 showed a wet anomaly over the region in the February to April average.

ECMWF's response

On 26 March, ECMWF received a request for rainfall forecasts from the environmental expert deployed from France (Institut national de recherche en sciences et technologies pour l'environnement et l'agriculture, Irstea) to Peru by the European Union Civil Protection Mechanism (EUCPM) through the European Civil Protection and Humanitarian Aid Operations (ECHO). Due to the exceptional circumstances, ECMWF agreed to provide its forecast products to the Peruvian Meteorological and Hydrological Service (SENAMHI) and COEN for a limited period of time, in accordance with our rules for the distribution of real-time data.

Access to all web products and ecCharts was granted and experts with previous knowledge of ECMWF products facilitated the uptake by local services. ECMWF established technical contacts with staff at SENAMHI and provided access to binary data in GRIB format in order to allow local services to process the information through their visualisation and impact models. Access to a new test product, Point-Rainfall, was also granted. It consists in statistical post-processing of ECMWF ensemble forecasts (ENS) to produce probabilistic rainfall forecasts for points. The idea is to provide better guidance in cases of localised extreme rainfall.

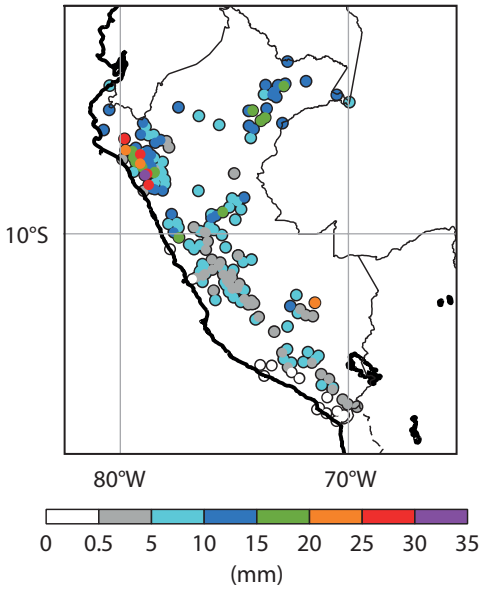

Precipitation observations. Average daily precipitation during March 2017 according to observations received from SENAMHI.

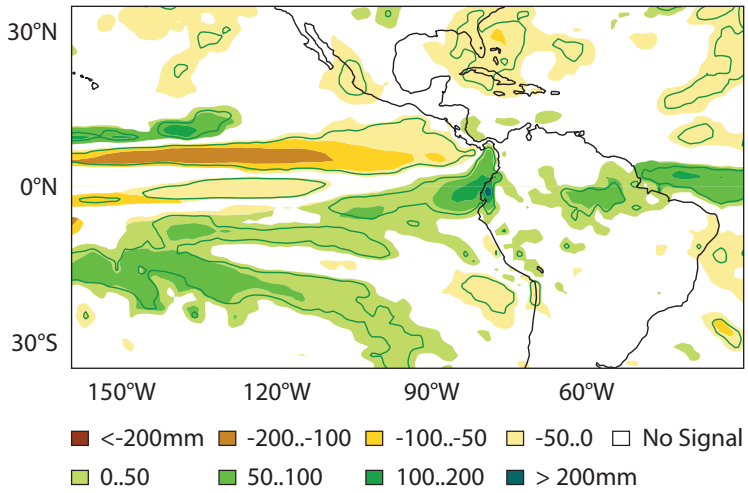

Seasonal forecast. Ensemble mean anomalies for precipitation in the period February–April 2017 in the ECMWF seasonal forecast from 1 November 2016.

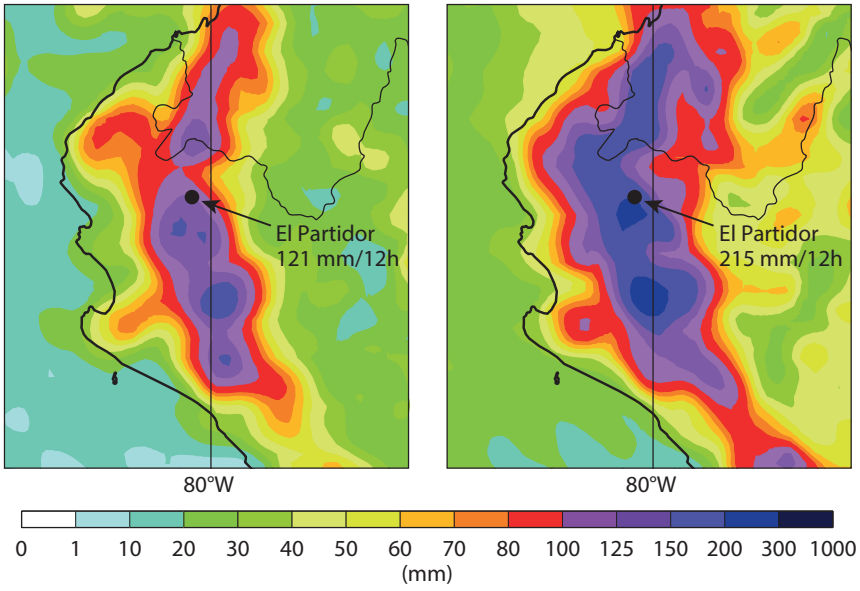

Probabilistic rainfall forecasts for points. El Partidor in the Piura region saw 258 mm of rain on 3 March 2017, most of which fell between 4 p.m. and 10 p.m. local time. The charts relate to ECMWF forecasts of 12-hour precipitation issued on 27 February 2017 at 00 UTC (t+114 to t+126). They represent the 98th percentile for total precipitation from the raw ensemble forecast (left) and from the Point-Rainfall product (right). The risk area for heavy rainfall was well identified in both forecasts even five days in advance, but the raw ensemble did not suggest the possibility of the observed amount of 258 mm. The Point-Rainfall product, on the other hand, suggested that there was a chance, albeit a small one, of such an event occurring.

Weather warning. Example of a meteorological warning map issued by SENAMHI covering the period from 3 to 9 March 2017. The risk levels range from 'one' (no special precautions necessary – white) to 'four' (be extremely cautious – red).

Use of ECMWF products

ECMWF web products helped SENAMHI forecasters to issue warnings of heavy rainfall that was likely to cause new flooding or to exacerbate existing flooding. Special attention was also paid to events that could hinder rescue operations and/or endanger rescuers' lives.

The binary data was used to produce extreme precipitation forecast maps. The daily total precipitation forecast from ECMWF's high-resolution forecasts (HRES) was combined with percentile maps generated from SENAMHI's climatological and hydrological observations (PISCO), which is a gridded database for daily precipitation. The percentile maps showed the areas where the daily accumulated total precipitation (from 12 to 12 UTC) exceeded the 90th, 95th and 99th percentiles of the local climatology. This made it possible to highlight the areas facing a high risk of heavy rainfall and thus to issue corresponding warnings to COEN, the authorities, members of the Peru Disaster Risk Management System, the media and public users.

At the same time, ECMWF products were also used by the scientific team at COEN, who monitored the emergencies triggered by the precipitation and issued alert reports every three hours. ECMWF products were used alongside satellite images and local reports to enhance the accuracy of daily local rainfall forecasts and to enable better warnings of extreme rainfall and river floods. The use of forecast products by emergency teams in the field and during the early recovery phase not only improved preparedness for high-impact events but also helped to devise better-informed response plans. The cooperation with ECMWF has led SENAMHI to evaluate the possibility of acquiring a full NMHS (national meteorological and hydrological service) non-commercial licence to continue to have access to the full range of ECMWF forecast products.

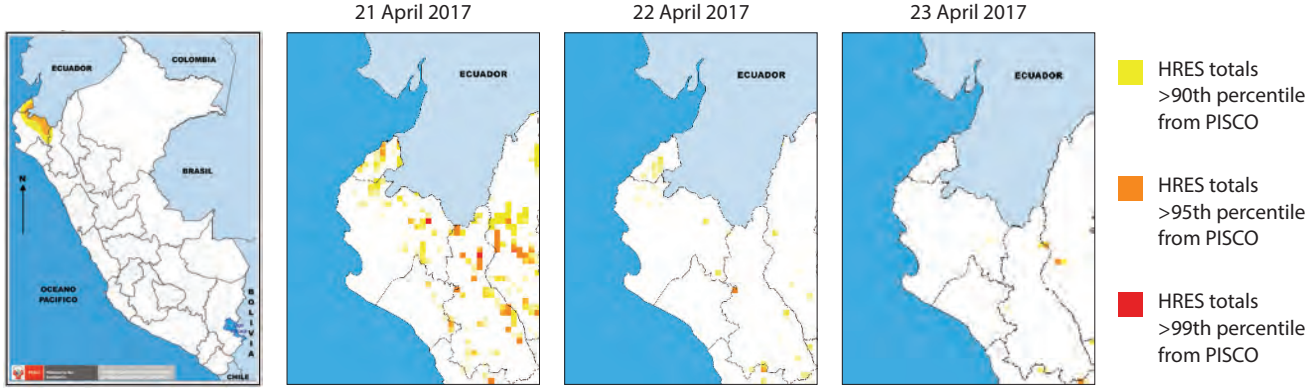

High-resolution forecasts. Meteorological warning map and Categorized Rain Maps (CRM) issued for the warning from 21 to 23 April 2017, using ECMWF HRES (forecast issued on 18 April 2017 at 12 UTC). These charts do not cover days on which the rainfall was at its heaviest. The heaviest rainfall occurred in March, but SENAMHI did not have access to ECMWF data for those days.

Predictions of tropical cyclones Harvey and Irma

LINUS MAGNUSSON,
IVAN TSONEVSKY,
FERNANDO PRATES

At the end of August and the beginning of September 2017, two major hurricanes, Harvey and Irma, were the first in a series to hit the Caribbean and the US. ECMWF forecasts predicted their paths fairly well. In the case of Harvey this helped to predict large amounts of rainfall over Texas. As is common in tropical cyclone (TC) forecasts, the intensity of the hurricanes was less well predicted.

Harvey

On 26 August (25 August local time) TC Harvey made landfall in Texas. Subsequently the cyclone became quasi-stationary and produced more or less continuous rainfall for three to five days. The rainfall totals reached more than 1,000 mm in the worst-affected areas around Houston, where unprecedented flooding occurred.

The cyclone formed from a tropical disturbance east of the West Indies on 18 August and propagated westward as a fairly weak system. On 22 August it made its first landfall on the Yucatán Peninsula (Mexico) and was downgraded to a tropical depression. After reaching the Gulf of Mexico, the system regained its status as a tropical cyclone. Over the next few days, the cyclone rapidly intensified and became a Category 4 hurricane before making landfall in Texas. After landfall, Harvey became quasi-stationary while gradually weakening to a tropical storm. On 29 August it moved out over the Gulf of Mexico again and a day later it made landfall for the third time, in Louisiana.

As early as 18 August, the ensemble forecast was confident about the propagation of Harvey towards southern Mexico. It also indicated that the system might enter the Gulf of Mexico. That risk temporarily decreased on 19 and 20 August when the cyclone was very weak in the central Caribbean Sea. After 21 August, the ensemble was confident that the system would turn into a tropical storm over the Gulf of Mexico but there was considerable uncertainty about where it might make landfall. Between 21 and 22 August, the risk of the cyclone becoming quasi-stationary over Texas increased, and with that came a risk of extreme rainfall. The high-resolution forecast (HRES), in particular, highlighted the risk of extreme precipitation. However, in the short range the predicted area of the worst rainfall was shifted to the southwest compared to the outcome. On 24 and 25 August the cyclone rapidly intensified. This was not captured well by the forecasts before the start of the intensification. However, the total accumulation of rainfall predicted by HRES over Texas was still in the same range as the observed amount.

Irma

TC Irma hit several countries along its path in the Caribbean. On 5 and 6 September, the Category 5 cyclone made its first landfall on some of the Leeward Islands. The first to be hit was Barbuda, followed by Saint Barthélemy, Saint-Martin/Sint Maarten and Anguilla. All these islands were crossed by the eye of the cyclone and wind gusts up to 70 m/s were reported on Barbuda. The cyclone later hit the Virgin Islands and the Turks and Caicos Islands. It also affected Puerto Rico and Hispaniola. On 8 September the cyclone hit the Bahamas. It made landfall on Cuba on 8 to 9 September as a Category 5 cyclone. Finally the cyclone made landfall on the southern tip of Florida on 10 September. ECMWF Member States with territories in the area have given positive feedback on the Centre's forecasts. Here we will focus on ECMWF's predictions for the Leeward Islands and Florida.

The cyclone formed on 30 August west of Cape Verde in the tropical Atlantic. The cyclogenesis was predicted about a week beforehand. The ensemble from 31 August showed a high risk of Irma passing the Leeward Islands six to seven days later. The ensemble was confident that the group of islands would be hit, but there was some uncertainty about the exact track. However, there were large forecast errors in the intensity and wind speed prediction.

The landfall in Florida was much more unpredictable than the landfall on the

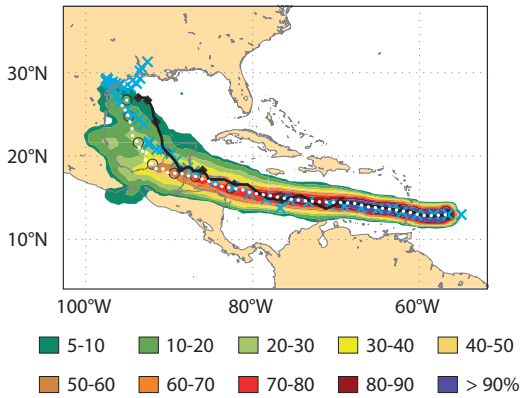

Strike probability map for TC Harvey. The chart shows the probability that Harvey will pass within a 120 km radius during the next 240 hours, according to the forecast from 18 August. The solid line is the HRES, the dotted line the ENS mean, and the crosses show the path as subsequently observed.

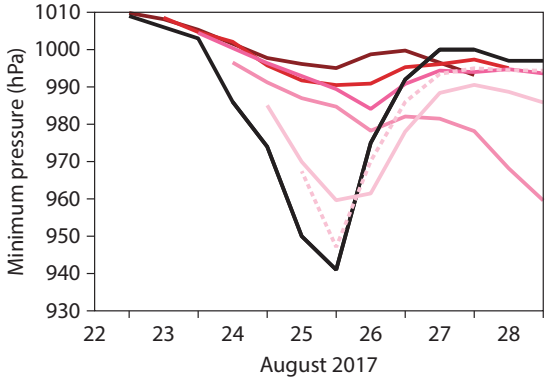

Central pressure forecasts for TC Harvey. The chart shows the evolution of central pressure for TC Harvey during the phase of rapid intensification according to 'best track' data (black) and HRES with different starting times (red).

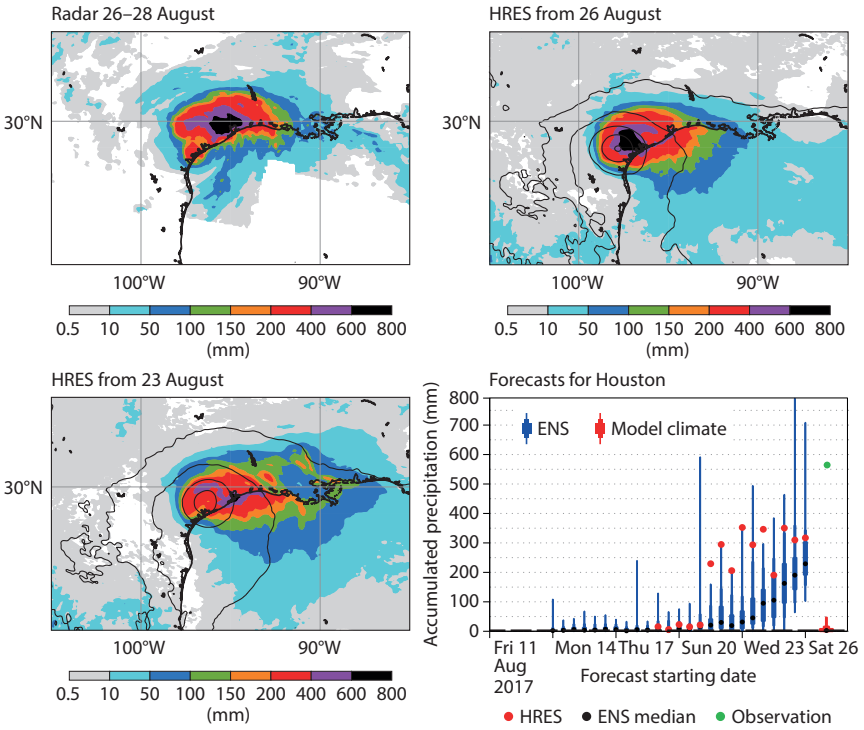

TC Harvey precipitation forecasts. The charts show accumulated precipitation in the period 26 to 28 August from the US radar network NEXRAD (top left), HRES starting from 26 August (top right) and HRES starting from 23 August (bottom left). The bottom-right plot shows the HRES (red) and ENS (blue) predicted accumulated precipitation in the period 26 to 28 August for Houston for different forecast starting dates. The box-and-whisker symbols mark the 1st, 10th, 25th, 75th, 90th and 99th percentile. Contours show mean sea level presssure as predicted for 27 August 12 UTC.

Leeward Islands. Early forecasts indicated a northward turn at some point, but the exact timing of this made a huge difference for the location where Irma would hit the US coast. Five days before the landfall, in the ensemble starting from 00 UTC on 5 September, possible landfall locations ranged from Louisiana in the west to North Carolina in the east. Later the range narrowed, but even three days before landfall, in the forecast from 00 UTC on 7 September, the tracks ranged from west of the Florida peninsula to east of the peninsula. These scenarios meant there was considerable uncertainty over where the impact of the cyclone would be strongest. On the day of the landfall, there were uncertainties in the final details concerning the strength of the cyclone and the exact landfall location. This created large uncertainty in the storm surge prediction. In the end, the cyclone hit Key West and made landfall just west of the tip of Florida. Meanwhile a storm surge caused some flooding in Miami on the east coast.

Summary

Different tropical cyclones pose different types of risks. The primary risk is the winds that damage or destroy buildings, as happened with TC Irma on the Leeward Islands. Another risk is storm surges along coasts, aggravated by waves, as for TC Irma in Florida. A slow-moving cyclone (as in the case of TC Harvey) or a cyclone that hits steep coastlines can also create extreme rainfall accumulations over land leading to potentially devastating flooding. In the case of Harvey the near-stationary nature of the cyclone was the key point to predict.

For both Harvey and Irma, ECMWF forecasts struggled to correctly predict the intensity of the cyclones. This can at least partly be explained by the relatively small scale of tropical cyclones compared to the model resolution. Other phenomena that are difficult to represent and thus limit predictability include eyewall replacements, which temporarily weaken TCs; rapid intensification; intrusion of dry air; and land interaction. These elements are the subject of intense research among tropical cyclone scientists. The processes involved are not yet fully understood and even limited-area models find it difficult to capture them.

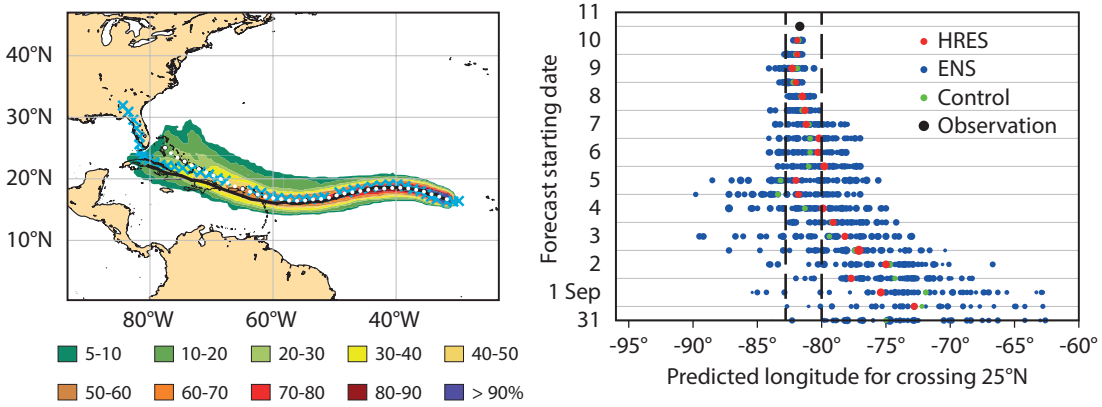

Strike probability for TC Irma. The left-hand chart shows the probability that Irma will pass within a 120 km radius during the next 240 hours, according to the forecast from 31 August. The solid line is the HRES, the dotted line the ENS mean, and the crosses show the path as subsequently observed. The right-hand chart shows the predicted longitude for crossing 25°N (latitude of Miami) in successive ENS (blue), HRES (red) and control forecasts (green). The size of each dot is scaled to the predicted strength of the cyclone at the crossing time. The black dot indicates the observed location and the dashed lines show the width of Florida.

Two storm forecasts with very different skill

LINUS MAGNUSSON, IVAN TSONEVSKY, TIM HEWSON

During autumn 2017, extreme weather events in Europe included the ongoing drought on the Iberian Peninsula, flash floods in Greece, and the landfall of ex-tropical cyclone Ophelia in Ireland. In this article we focus on two devastating windstorms for which the skill level in ECMWF forecasts was very different.

11 August 2017

On 11 August 2017 severe winds hit northern Poland, causing the deaths of five people, significant damage to trees and power disruptions affecting 340,000 households. This severe storm was caused by a mesoscale convective system. Wind gusts of over 40 m/s were reported in the region. However, even the shortest-range high-resolution forecasts (HRES) failed to predict anything near these values, nor did the Extreme Forecast Index (EFI) or Shift of Tails (SOT) for wind gusts show any significant signal, at any time range. This illustrates that directly capturing fine-scale extremes in convective cases is still out of reach for global models. The finer-scale COSMO-EPS from the German national meteorological service DWD (data archived at ECMWF as part of TIGGE-LAM) did predict extreme wind gusts in the region. However, ECMWF has developed a number of products that make the best use of information contained in the medium-range forecast to identify potential fine-scale weather hazards consistent with the large-scale flow. Examples of this are the EFI for convective indices, and also point rainfall (sub-grid) precipitation probabilities. Indeed in this case the risk of severe convective hazards in the affected region was captured in ECMWF medium-range

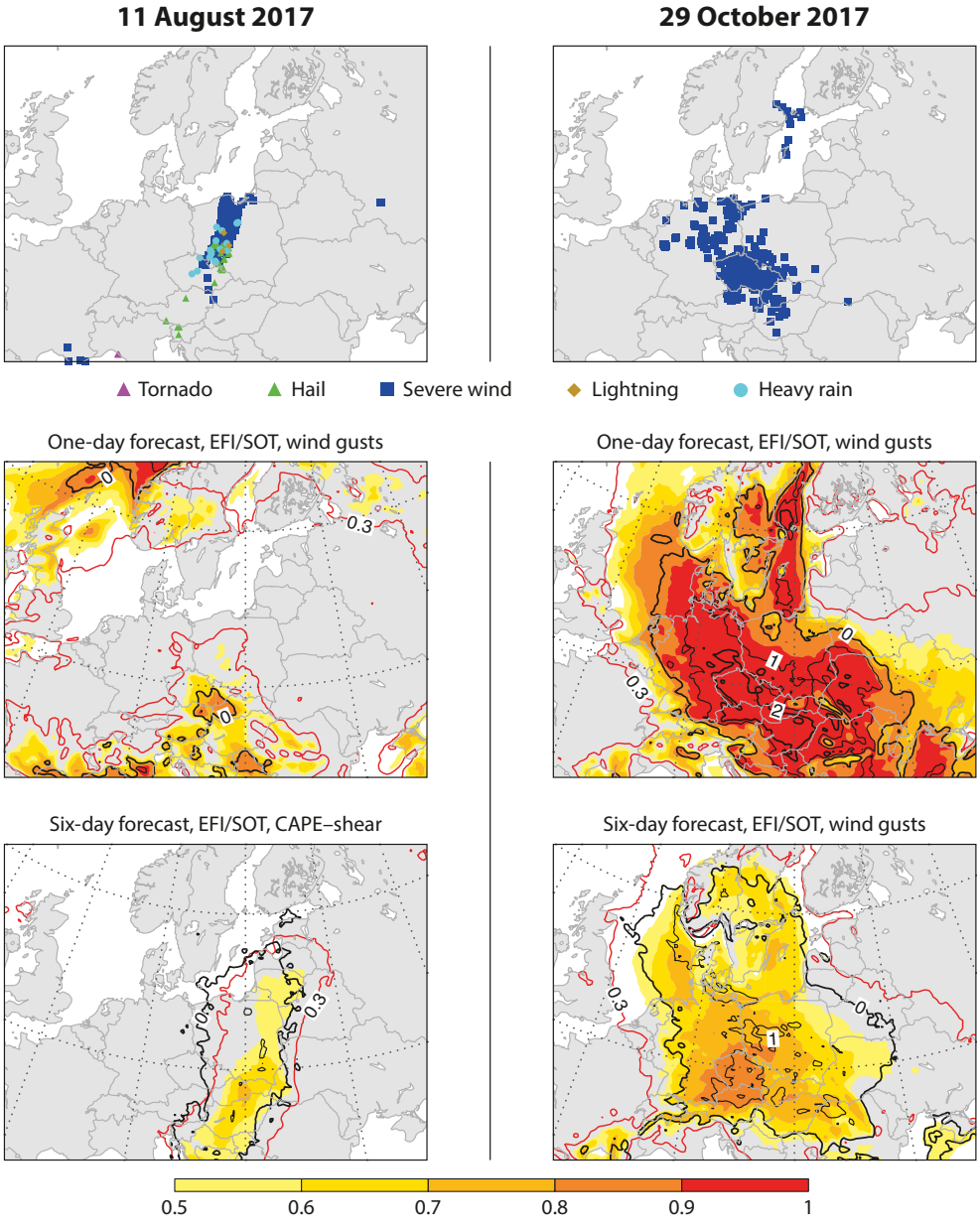

Observations and forecasts for the two windstorms. Reports of severe weather from the European Severe Weather Database (ESWD) for 11 August (top-left) and 29 October (top-right); one-day forecasts of EFI (shading) and SOT (contours) for 24-hour maximum 10-metre wind gusts for the two respective cases (middle); and 6-day forecasts of EFI and SOT for CAPE–shear in the August case (bottom-left) and for 10-metre wind gusts in the October case (bottom-right).

forecasts by the EFI and SOT product for a composite parameter that combines CAPE and wind shear, albeit somewhat too far east in the 6-day forecast.

28–29 October 2017

On the night of 28 October a deepening cyclone, named Herwart by the Free University of Berlin, moved southeastwards across southern Sweden and the southern Baltic Sea. Within the large circulation of this cyclone, very strong winds developed, most notably over Germany, the Czech Republic and Poland. There were at least four fatalities, damage to trees and buildings and disruption to infrastructure. According to reports in the European Severe Weather Database (ESWD), the Czech Republic was probably worst affected. The short-range EFI for wind gusts agrees well with those reports. Even at a lead time of six days, the ECMWF EFI and SOT clearly highlighted a greatly elevated risk of a severe wind event over a large area. Indeed, the strongest signal in the EFI was centred on the Czech Republic. Throughout the lead-up to this event, ECMWF ensemble forecasts (ENS) provided a consistent signal for a dangerous windstorm, which grew stronger with time.

Conclusion

These two cases illustrate very different skill for the same variable (wind gusts). In the first case no skilful forecast regarding the extreme wind was provided directly by ECMWF forecasts, while in the other case the forecast showed skill almost a week in advance. As discussed, the meteorological conditions behind the two events were very different. Such differences should be borne in mind when interpreting verification results for wind gusts as both cases contribute to the statistical sample. Indeed verification over a full year shows significantly lower skill during summer, when the contribution of deep moist convection to cases of severe wind gusts is higher in the sample.

Predicting extreme snow in the Alps in January 2018

LINUS MAGNUSSON, DAVID RICHARDSON

January 2018 saw several episodes of extreme snowfall in the Alps, on both the northern and southern side of the mountain range. In this article we focus on the event that affected the south-western part from 7 to 9 January. Reports on the Web talked about 2 to 3 metres of fresh snow. The ski report for Tignes and Val d'Isère reported 110 to 160 cm of fresh snow in two days. Road links to several villages, such as Bonneval-sur-Arc in France and Zermatt in Switzerland, were cut by avalanches and tourists were stranded in the resorts.

The extreme precipitation in the south-western Alps was caused by a cut-off low centred over the western Mediterranean that stayed in a similar position for several days and brought moist air northward on its eastern side. The cut-off low was well predicted and ECMWF's Extreme Forecast Index (EFI) for total precipitation showed a signal more than a week in advance over the south-western Alps. The median of the ensemble forecast (ENS) starting on 1 January showed precipitation of 40 mm/48 hours in Val d'Isère for 7–8 January, and a risk of up to 100 mm. Between 2 and 3 January, the ensemble forecast became more extreme and the median jumped up to above 80 mm.

For all forecasts issued from 3 January onwards, the high-resolution forecast (HRES) gave higher two-day precipitation for 7–8 January in Val d'Isère than the ensemble median. This suggests a sensitivity to horizontal resolution (about 9 km for HRES and 18 km for ENS), which is expected in steep terrain. From the TIGGE-LAM archive hosted by ECMWF, we have access to eight different limited-area ensembles for evaluation purposes. Comparing the ECMWF global ensemble with the COSMO-LEPS ensemble with 7 km resolution from ARPA-ER SIMC in Italy, we find much higher precipitation accumulations in the limited-area ensemble. This is also true if we compare a short-range forecast from a random ensemble member from COSMO-LEPS with ECMWF HRES.

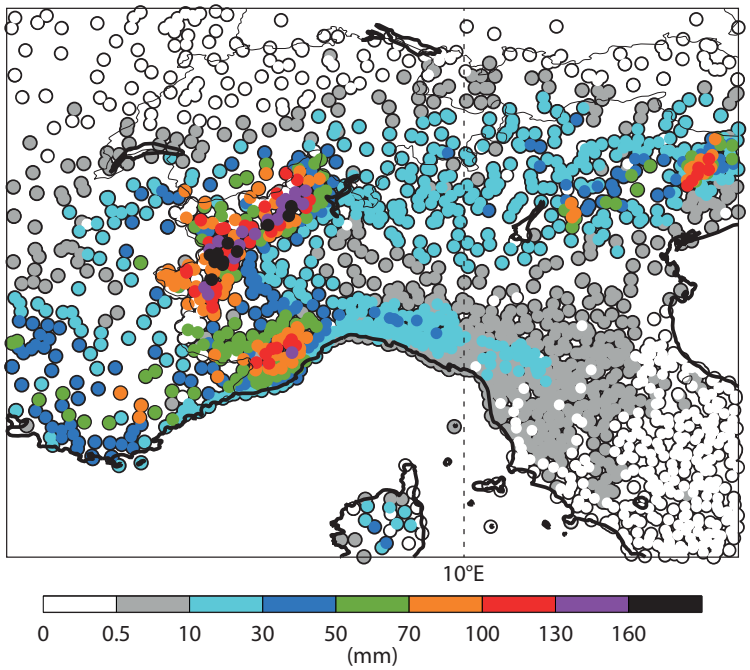

Observed precipitation. Twenty-four-hour precipitation between 8 January 06 UTC and 9 January 06 UTC, according to reports received from regional networks contributing to the high-density observation (HDOBS) project at ECMWF.

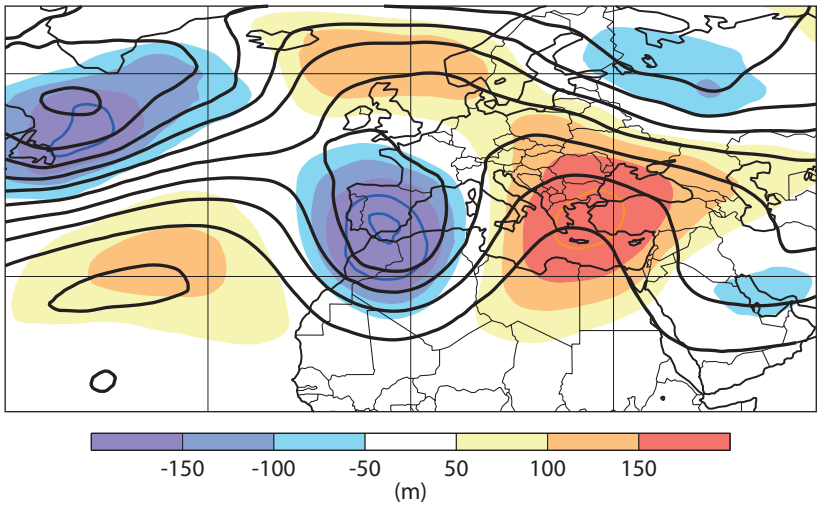

Cut-off low. The analysis of 500 hPa geopotential height (contours) and the corresponding anomaly (shading), averaged for 7–9 January, indicate the location of the cut-off low in the western Mediterranean that brought extreme precipitation to parts of the Alps.

Accurately predicting snow accumulation in complex terrain is difficult for current global models because of their relatively coarse grid spacing. It is impossible to resolve local differences in precipitation due to individual valleys and mountain peaks and local wind patterns. The lack of resolution for the orography also poses difficulties in predicting the freezing level relative to the terrain and whether the precipitation will fall as rain or snow. For verification, observing precipitation accumulation is very challenging during heavy snowfall. During fast accumulations of snow, rain gauge buckets can easily be filled by snow between being emptied, and automatic stations are known to have large errors during

intense snowfall. It is therefore very difficult to judge the performance of the forecasts in terms of total precipitation. What we can say is that the ECMWF forecast gave an early indication of unusually large amounts of precipitation in the Alps. However, with the lower amounts of about 40 cm for Val d'Isère in the earlier forecasts, there could have been an expectation that there would be nice skiing conditions with some fresh snow, while the outcome of probably three times as much or more resulted in closed pistes and tourists being trapped in the resorts.

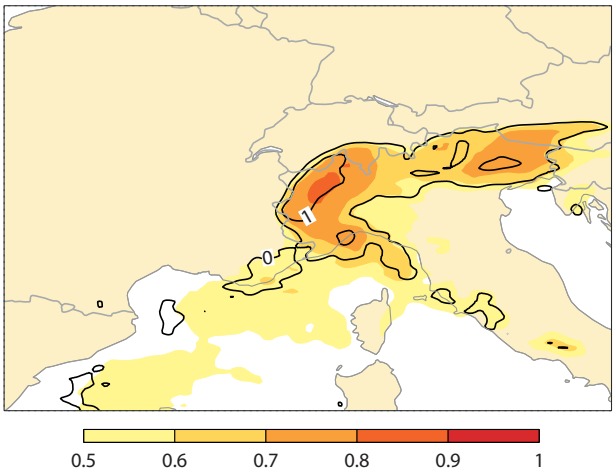

Extreme Forecast Index (EFI) and Shift of Tails (SOT). EFI (shading) and SOT (contours) for three-day total precipitation from 7 to 9 January in the forecast from 1 January.

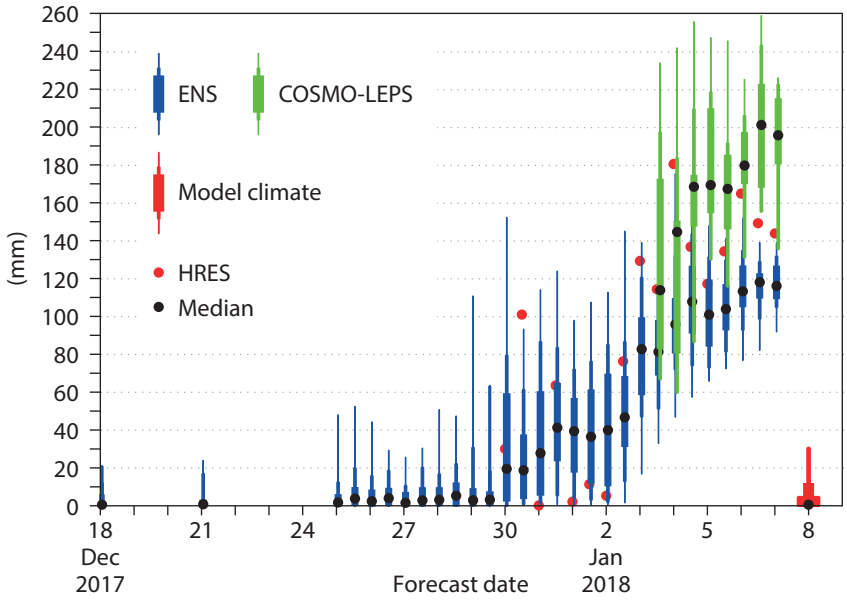

Ensemble forecasts for Val d'Isère. Total precipitation for Val d'Isère on 7 and 8 January as predicted by forecasts from different initial times. The box-and-whisker plots show the 1st, 10th, 25th, 75th, 90th and 99th percentile and the black dots show the median.

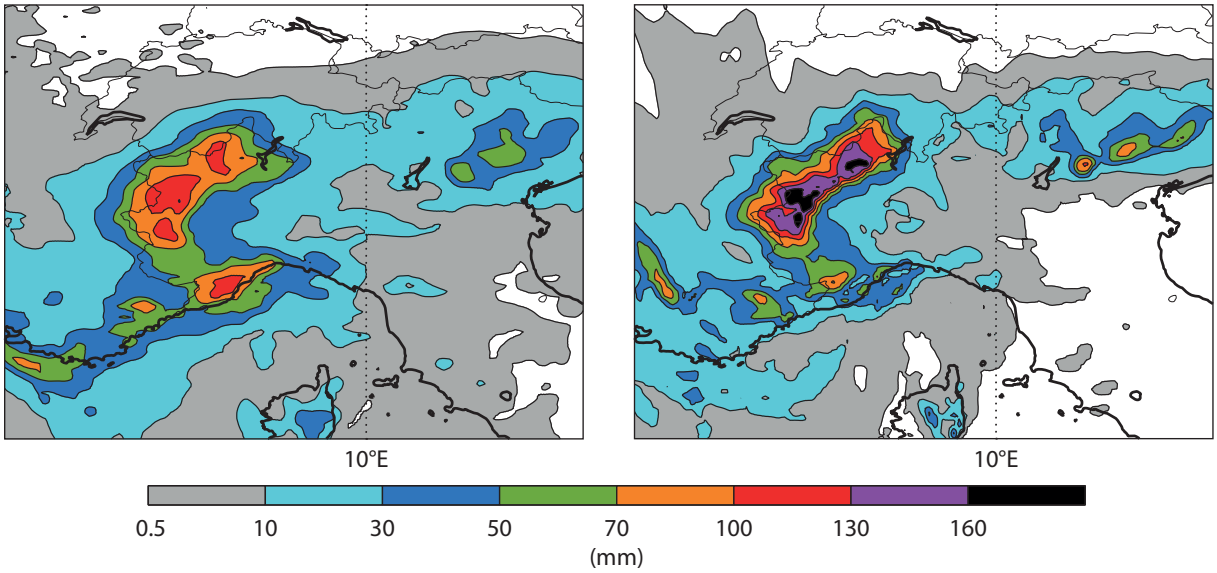

Short-range HRES and COSMO-LEPS forecasts. HRES precipitation forecast initialised on 8 January at 00 UTC for the period 8 January 06 UTC to 9 January 06 UTC (left) and the same forecast from a member of the COSMO-LEPS ensemble (right).

Forecasting convective rain events in late May

LINUS MAGNUSSON, IVAN TSONEVSKY, TIM HEWSON

During most of May 2018, northern Europe experienced a heat wave. The intensity and spatial extent of the event are evident in the monthly mean air temperature summary maps provided by the Copernius Climate Change Service implemeted by ECMWF (https://climate.copernicus.eu/). Many records for May average temperature were broken. For Stockholm, where temperature records go back to 1759, the monthly average temperature reached 16.1°C, which is 2.2°C higher than the previous record of 13.9°C, the Swedish national meteorological service reported. The hottest days were at the end of May and continued into the first days of June. In the warm and humid air and with generally weak synoptic-scale forcing over north-western Europe, severe convective systems developed during these days. Global forecasting systems can struggle to capture such relatively small-scale systems. Here we look at the usefulness of different ECMWF products for this type of event. We will focus on 29 May, when extreme rain and flash floods affected parts of Germany, the Netherlands, Belgium and France, where Paris was hit by intense rainfall. Severe thunderstorms were accompanied by other convective hazards, including large hail, strong winds and lightning.

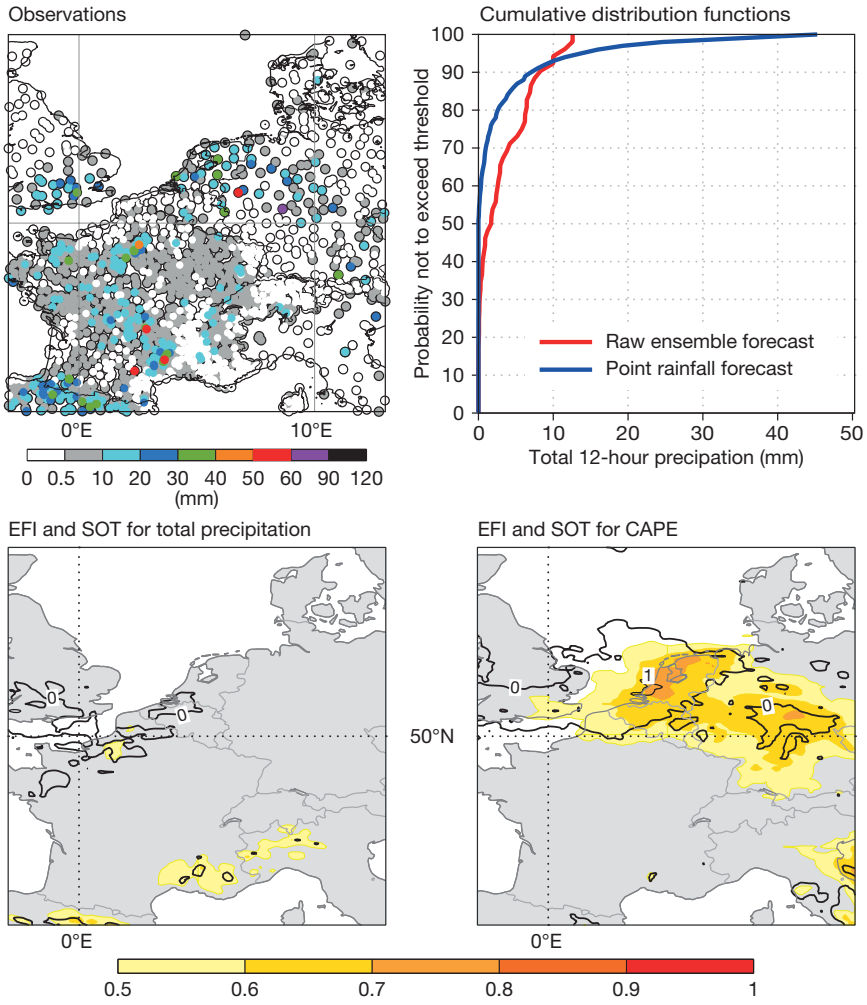

Rainfall and CAPE predictions. The plots show 24-hour observed precipitation between 29 May 06 UTC and 30 May 06 UTC (top left); cumulative distribution functions for raw ensemble and ecPoint-Rainfall forecasts over Paris starting at 00 UTC on 25 May for 12 UTC on 29 May to 00 UTC on 30 May (top right); EFI and SOT of total precipitation for 29 May in the forecast from 25 May 00 UTC (bottom left); and EFI and SOT for CAPE for 29 May in the forecast from 25 May 00 UTC (bottom right).

In global forecasting systems, heavy convective rain events are usually associated with low forecast probabilities due to the high spatial variability of precipitation and uncertainties in convective initiation. As a result, the total precipitation Extreme Forecast Index (EFI) generally provides weak signals of extreme rain even in short-range forecasts in such situations. This was the case with the forecasts for 29 May over Germany. The predictability of heavy rain events in Belgium and the Netherlands was higher, with positive Shift of Tails (SOT) in the medium range, indicating that at least 10% of ensemble members were predicting extreme rainfall. On the other hand, the model is usually quite good at predicting the favourable environment for deep moist convection well in advance. In the case presented here, the CAPE EFI, for example, gave a much stronger signal for convective hazards throughout the short and medium range than the EFI for total precipitation.

ECMWF's recently developed ecPoint-Rainfall product uses an innovative post-processing method to account for sub-grid variability and weather-dependent biases in rainfall totals (Newsletter No. 153, autumn 2017). For cases of severe convection, this product should increase probabilities for extreme rainfall and also for no rainfall, compared to the grid-box average probabilities provided by raw model output. In the case of Paris on 29 May, observations of 24-hour rainfall ranged from less than 5 mm to more than 30 mm within the metropolitan area, most of which fell during the afternoon. The raw ensemble from 5 days before (25 May) indicated a maximum possible value of 13 mm/12 hours (as a grid-box average), while the post-processed ecPoint product indicated that point

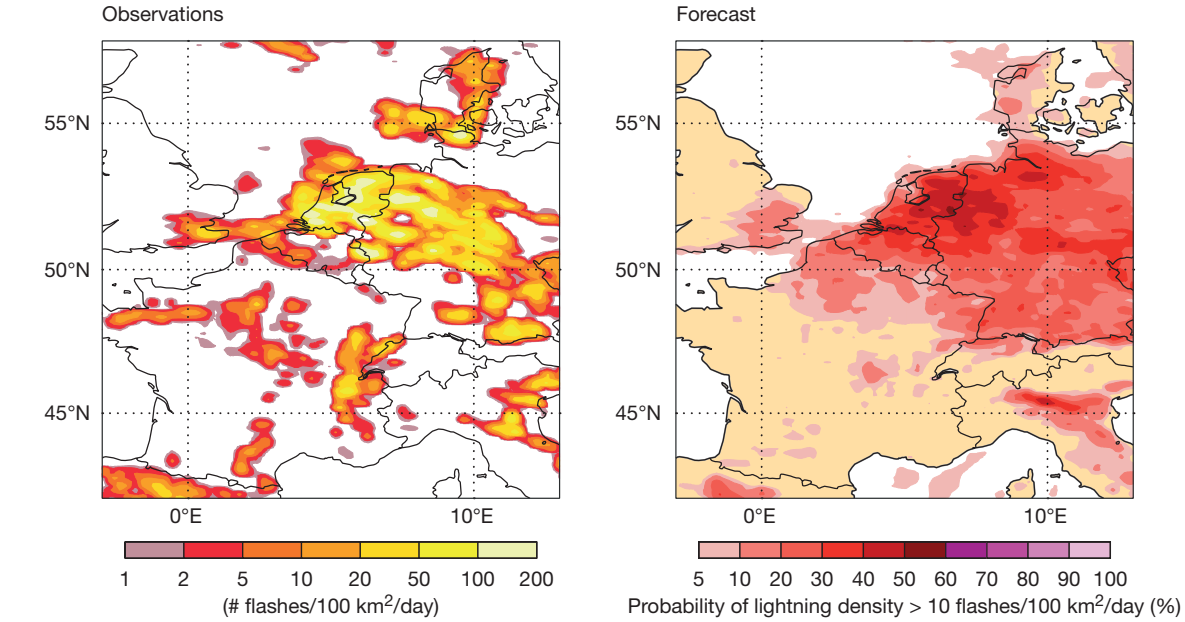

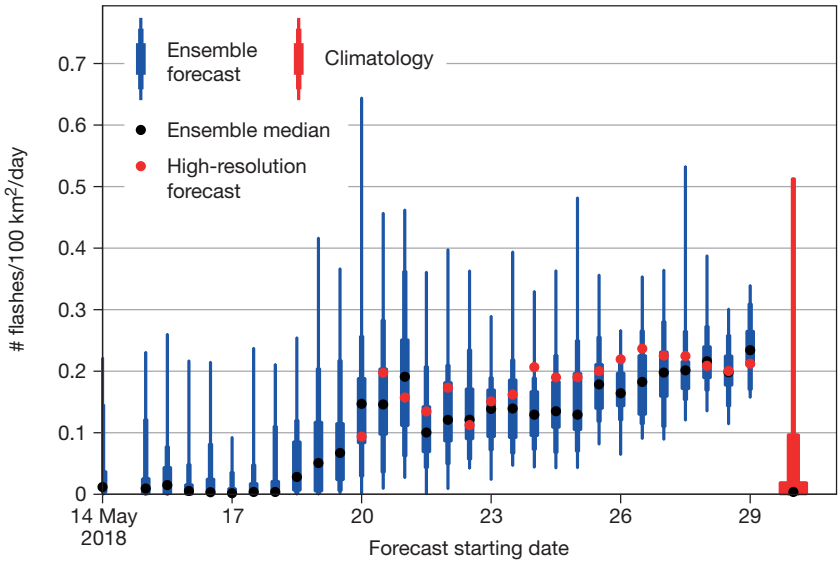

Lightning density forecasts. Lightning density from the UK Met Office ATDnet lightning detection network in flashes per 100 km^2 per day from 29 May (top left); probability of lightning density greater than 10 flashes per 100 km^2 per day in the 5-day forecast from 25 May (top right); and lightning density (# flashes per 100 km^2 per day) over north-western Europe (45°N–55°N, 0°E–10°E) on 29 May as predicted by forecasts from different initial times (bottom). The box-and-whisker symbols show the 1st, 10th, 25th, 75th, 90th and 99th percentiles.

rainfall above 30 mm/12 hours was possible (forecasts valid for 12 UTC on 29 May to 00 UTC on 30 May).

The convection over north-western Europe on 29 May was also associated with intense lightning activity. ECMWF has recently implemented a new parametrization of lightning density (Newsletter No. 155, spring 2018). For the case of 29 May, probabilities of intense lightning in the 5-day forecast from 25 May highlighted the risk over Belgium, Germany and the Netherlands. Note that ATDnet (used here for verification) detection efficiency is much higher for cloud-to-ground (CG) flashes than for intracloud (IC) flashes, whilst the forecast lightning density accounts for both CG and IC discharges, hence we do not expect a perfect match between predicted and observed quantities. Summarising all lightning forecasts valid for 29 May over western Europe (45°N–55°N, 0°E–10°E) in one plot, we find that as early as 10 days before the event the ensemble had a clear signal, with the ensemble median above the 90th percentile of the model climate, and the signal was consistent in all subsequent ensembles.

In summary, ECMWF forecasts captured the risk of thunderstorms in western Europe more than a week in advance. The high predictability was linked to the ability to predict the large-scale environment in which the convective storms developed. Indices such as CAPE and lightning density forecasts are expected to give good guidance on regions likely to be affected by convective hazards. By contrast, there is low predictability for the location and timing of individual convective cells and associated precipitation, although the point rainfall product can better reflect the range of probabilities at particular points than the raw ensemble.

Forecasting the 2018 European heatwave

Linus Magnusson, Laura Ferranti, Freja Vamborg

The late spring and summer of 2018 were among the warmest on record for northern Europe. ECMWF extended-range forecasts predicted warm anomalies weeks in advance, but the northerly extent and intraseasonal variability of the heatwave were only reflected in forecasts up to two weeks ahead.

A chart produced by the Copernicus Climate Change Service (C3S) implemented by ECMWF shows that the near-surface air temperature anomaly in Europe for the period April to August 2018 was far larger than in any previous year since 1979. The strongest anomalies occurred in the Baltic Sea region, while the countries around the Mediterranean experienced close to normal temperatures on average. The heatwave can be divided into three parts: the second half of April, mid-May to mid-June, and the second half of July to the beginning of August, with more normal temperatures in between. While southern Europe had more normal temperatures on average, south-western Europe experienced a surge of heat at the beginning of August, with temperatures reaching 45°C in Spain and Portugal on 4 August.

With these temporal and spatial variations, there are many aspects to verify in ECMWF's forecasts, and not all can be covered here. Focusing on the two main parts of the heatwave, as a first verification we use composites of weekly anomalies from extended-range forecasts covering the period 7 May to 12 August at different lead times (one week, two weeks, three weeks and four weeks). For example, the composite of week-one forecasts issued on Mondays uses forecast days 0 to 7, the composite of week-two forecasts uses forecast days 8 to 14, etc. The predicted anomalies in week-one and week-two forecasts resemble the spatial pattern of the anomalies in the analysis well. Warm anomalies are also present in the week-three and week-four forecasts, but they are weaker and the forecasts did not reflect their northerly extent. It is worth mentioning that, even at the longest time ranges, the

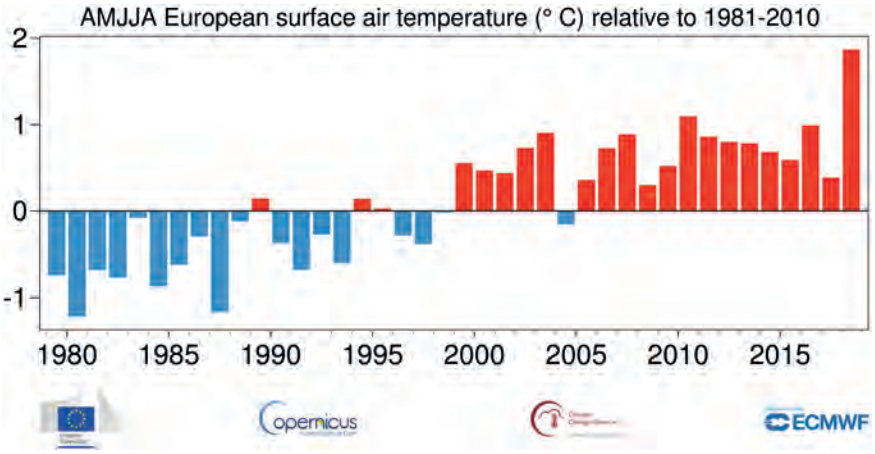

Evolution of near-surface air temperature anomalies. This chart produced by C3S shows that the near-surface air temperature anomaly in Europe in the period of April to August (AMJJA), calculated relative to the 1981–2010 average for those months, was much larger in 2018 than in any previous year since 1979.

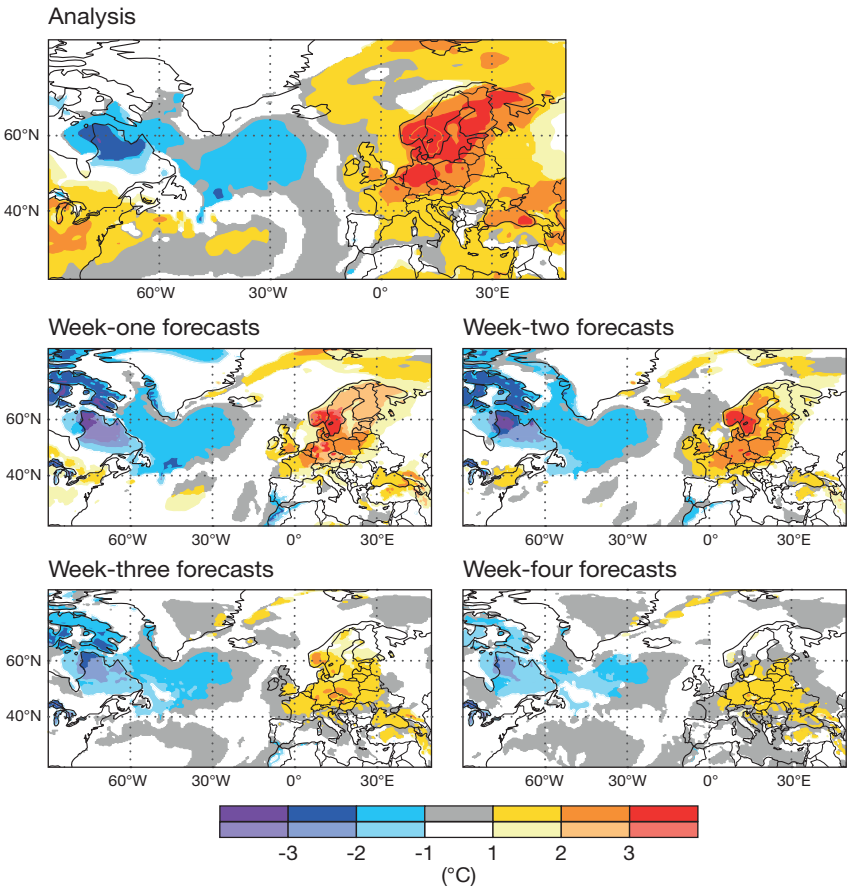

Analysis and forecasts of 2-metre temperature anomalies. The plots show ECMWF's analysis of the average 2-metre temperature anomaly 7 May to 12 August (top) and composites of weekly 2-metre temperature anomalies from extended-range forecasts valid for 7 May to 12 August, based on week-one forecasts (middle left), week-two forecasts (middle right), week-three forecasts (bottom left) and week-four forecasts (bottom right). Saturated colours indicate signficance at the 95% level.

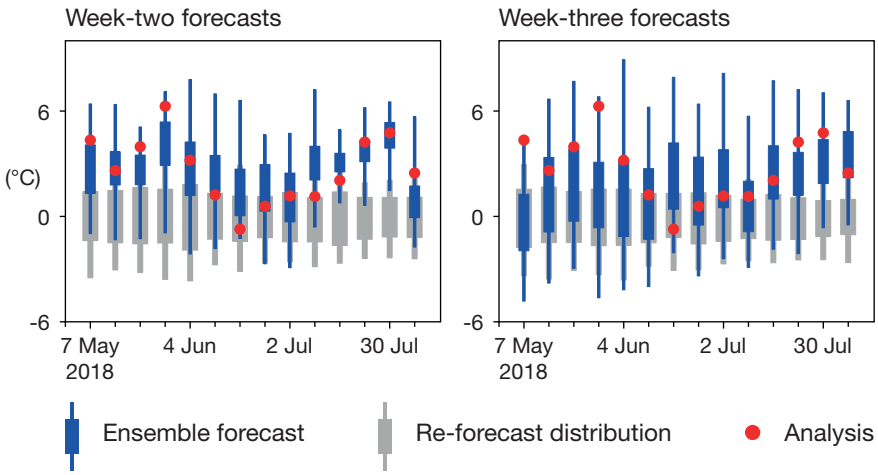

Ensemble forecast distribution of anomalies. Weekly ensemble forecast distribution of 2-metre temperature anomalies for a region in northern Europe (50°N–60°N, 10°E–20°E) for week-two forecasts (left) and week-three forecasts (right). The box-and-whisker symbols show the 5th, 25th, 75th and 95th percentiles.

cold anomaly over north-eastern Canada and the central-northern Atlantic was captured.

The results from this evaluation show that the extended-range forecasts predicted the warm anomaly fairly well on average, but they do not tell us how well the intra-seasonal variability was captured. We have therefore also visualised the week-by-week evolution of 2-metre temperature anomalies averaged over a region in northern Europe (50°N–60°N, 10°E–20°E) in week-two and week-three forecasts, the analysis (used for verification) and the model climate (re-forecast distribution). By definition, the anomalies in the re-forecasts are centred around zero. The plots show that week-two forecasts captured the intra-seasonal variations seen in the analysis reasonably well. Week-three forecasts, on the other hand, showed less variation in the predicted anomalies throughout the summer. They failed to give any indication of the warm peak at the end of May or of the break in the warm weather at the end of June, although they gave some indication of the warm period in the second half of July.

In short-range forecasts, when averaging over the period 7 May to 12 August 2018, a general tendency can be detected across Europe for daily maximum temperatures to have been underestimated and minimum temperatures to have been overestimated. The underestimation of the diurnal cycle in heatwave conditions is one of the topics being explored in ECMWF's USURF project. For more details on USURF, see the article on biases in near-surface forecasts in this Newsletter.

The European heatwave of 2018 poses questions about the driving mechanisms behind the strong anomalies. Evaluating the predictability of heatwaves is part of ECMWF's activities in the subseasonal-to-seasonal (S2S) project sponsored by the World Weather Research Programme (WWRP) and the World Climate Research Programme (WCRP). It will also be part of the newly approved EU-funded Horizon 2020 CAFE project, which starts in 2019 and in which ECMWF is a partner.

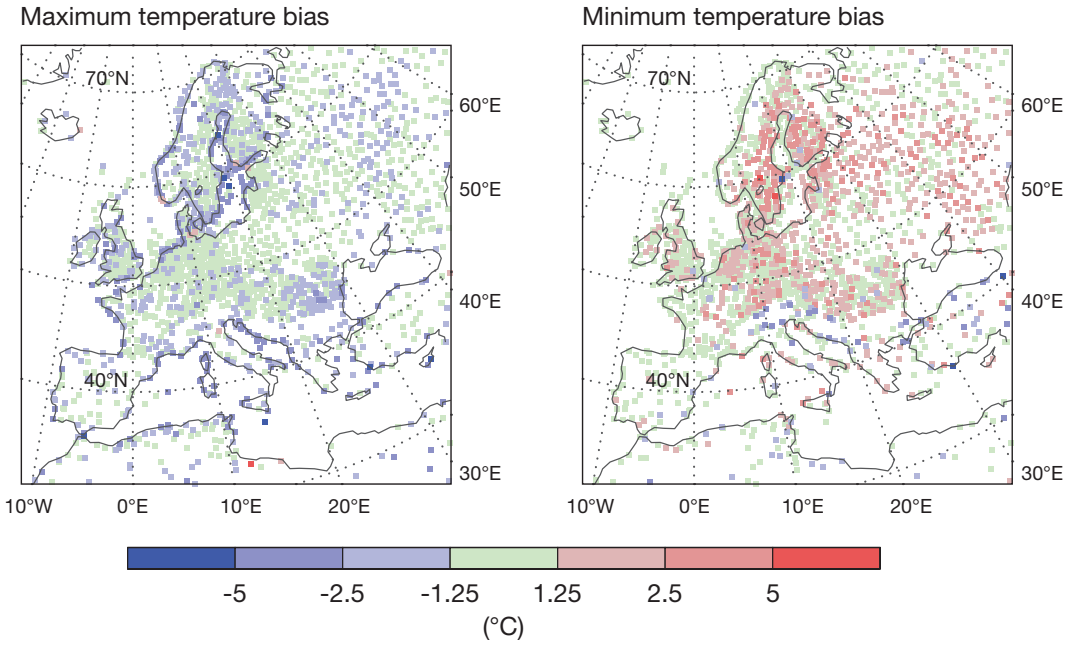

Underestimation of the diurnal cycle. The plots show the bias in maximum (left) and minimum (right) 2-metre temperature for day-two forecasts between 7 May and 12 August 2018, compared to SYNOP weather station observations. Blue colours indicate that on average the forecasts were too cold, red colours that they were too warm.

Predicting multiple weather hazards over Italy

Linus Magnusson, Luigi Cavaleri (CNR ISMAR, Italy)

Autumn 2018 was characterised by a continuation of dry weather in northern Europe while southern Europe experienced several episodes of very wet and windy weather. In this article, we will focus on a cyclone which developed from a large-scale trough over the western Mediterranean. On 29 October, it moved from Sardinia towards the Alps. In Sardinia, severe convection linked to the cyclone brought extreme accumulations of hail. In the Eastern Alps, recorded wind gusts reached 59 m/s. The storm uprooted or broke 11 million trees, and torrential rainfall led to flash floods. Later the Po river experienced moderate flooding. The storm was accompanied by significant wave heights up to 11 m in the Tyrrhenian and Ligurian Seas west of Italy and more than 9 m in the Adriatic. About six metres were recorded at the ISMAR oceanographic tower in the Gulf of Venice. There was a severe surge bringing flooding to Venice, thankfully mitigated by the fact that the meteorological peak occurred during low tide. This is an example of a single weather system bringing multiple hazards, and here we will discuss the predictability of some of them.

For the verification of 24-hour precipitation, we have access to high-resolution observations from many of our Member and Co-operating States thanks to a project to collect high-density observations. For the period 29 October 06 UTC to 30 October 06 UTC, three stations in Italy reported more than 300 mm, and the average precipitation from all observations in a 2°x2° box centred over north-eastern Italy was 100 mm. The maximum precipitation in ECMWF's high-resolution forecast (HRES) starting on 25 October 00 UTC reached 173 mm. Underestimation of orographic precipitation is a known model deficiency even though it has improved in recent years as a result of upgrades in model physics and model resolution. The area average in the 2°x2° box for this HRES forecast was 82 mm based on all observation points and 63 mm based on all grid points, on a similar level to short-range forecasts. The HRES and ensemble median consistently predicted values above the 99th percentile of the model climate from six days before the event and onwards.

The signal of extensive rainfall, violent wind gusts and high waves in northern Italy on 29 October began to appear in the ensemble forecast a week before the event. This resulted in a relatively strong Extreme Forecast Index (EFI) signal, as exemplified by forecasts for the three variables from 23 October 00 UTC. The early predictability was linked to the deep trough over the western Mediterranean.

The ensemble wave forecast gradually became more and more extreme as the event approached. Seven days before the event, the median of all ensemble forecasts was above the 75th percentile of the model climate and three days before above the 99th percentile in the Northern Adriatic. The last ensemble forecast before the event had a median significant wave height of 3 m while HRES gave 3.7 m. This is still significantly below the observed value of nearly 6 m. The discrepancy is not unexpected because of the global model's limited ability to resolve the Gulf of Venice and its bathymetry, and here limited-area wave models play a

Flooding in Venice. Flooding was one of the multiple weather-related hazards over parts of Italy in the last week of October 2018. (*Photo: Luciana Bertotti*)

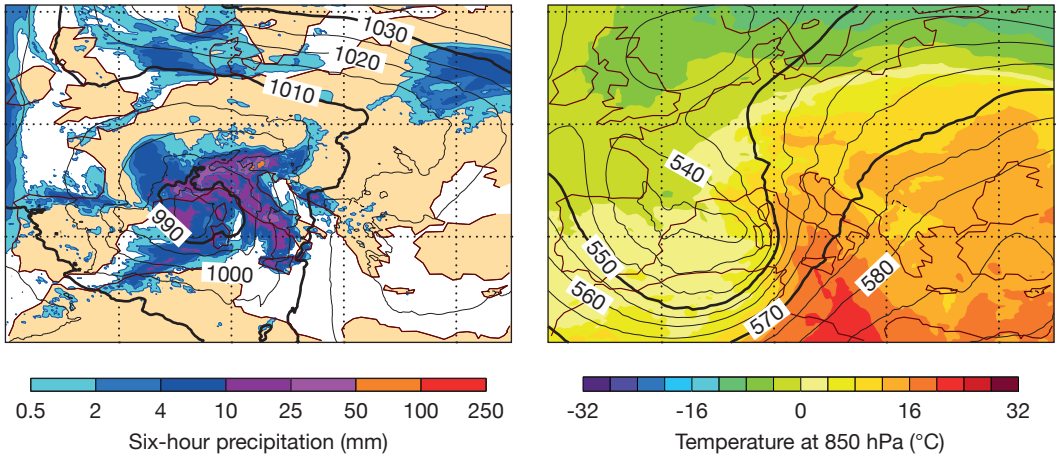

Meteorological situation on 29 October 2018. Analysis of mean sea-level pressure (contours, in hPa) and 6-hour precipitation (shading) (left) and geopotential height at 500 hPa (contours, in decametres) and temperature at 850 hPa (shading) (right) for 29 October 12 UTC.

role. The regional wave forecasts from the Institute of Marine Sciences (CNR ISMAR), Venice, use ECMWF's wind forecasts but adjust them (+16%) for a known underestimation in the Adriatic Sea. This simulation at higher resolution (about 0.08° for the wave model and down to about 100 m for the surge model) led to a very good forecast of wave and surge conditions, both accurately quantified several days in advance. For surge and flood forecasts, a key difficulty is to pinpoint with sufficient accuracy the time of the storm. Small phase differences between astronomical and meteorological components can lead to drastic differences in flooding. In the present case, the timing was sufficiently correct 24 hours in advance.

Overall, ECMWF forecasts provided an early indication of hazardous weather in this case, although they did not always capture just how extreme conditions were going to be. ECMWF is going to work on understanding if this type of event has predictability in the extended range (beyond 10 days) and also to explore how forecasts of extreme surface wind and precipitation can be improved.

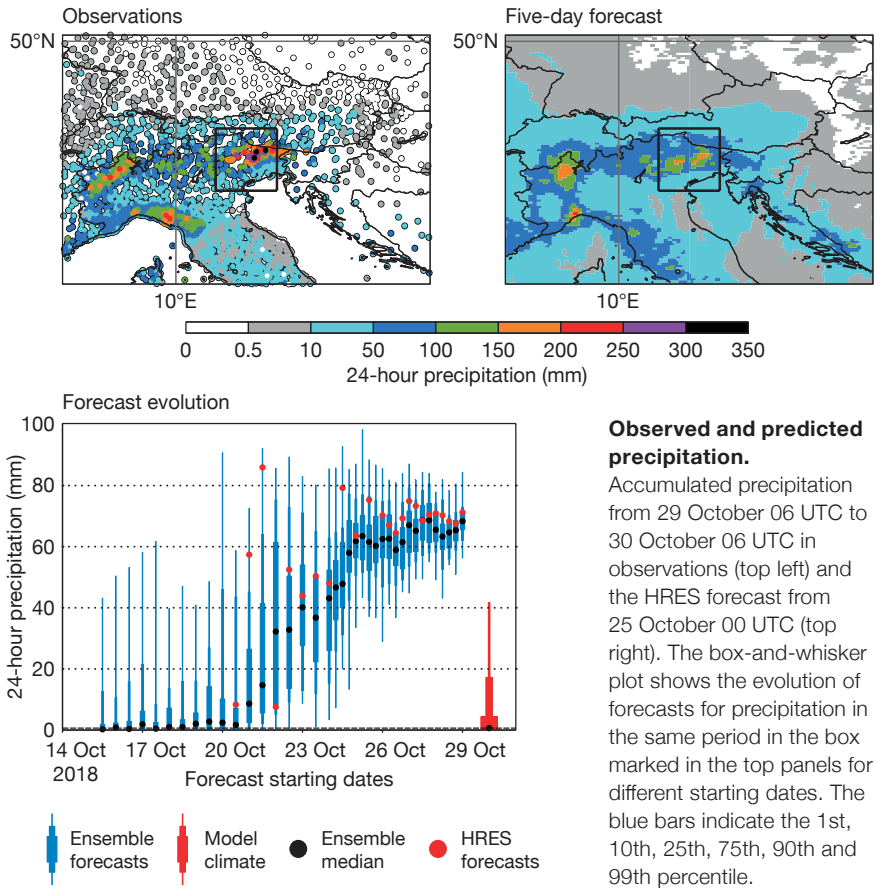

Observed and predicted precipitation. Accumulated precipitation from 29 October 06 UTC to 30 October 06 UTC in observations (top left) and the HRES forecast from 25 October 00 UTC (top right). The box-and-whisker plot shows the evolution of forecasts for precipitation in the same period in the box marked in the top panels for different starting dates. The blue bars indicate the 1st, 10th, 25th, 75th, 90th and 99th percentile.

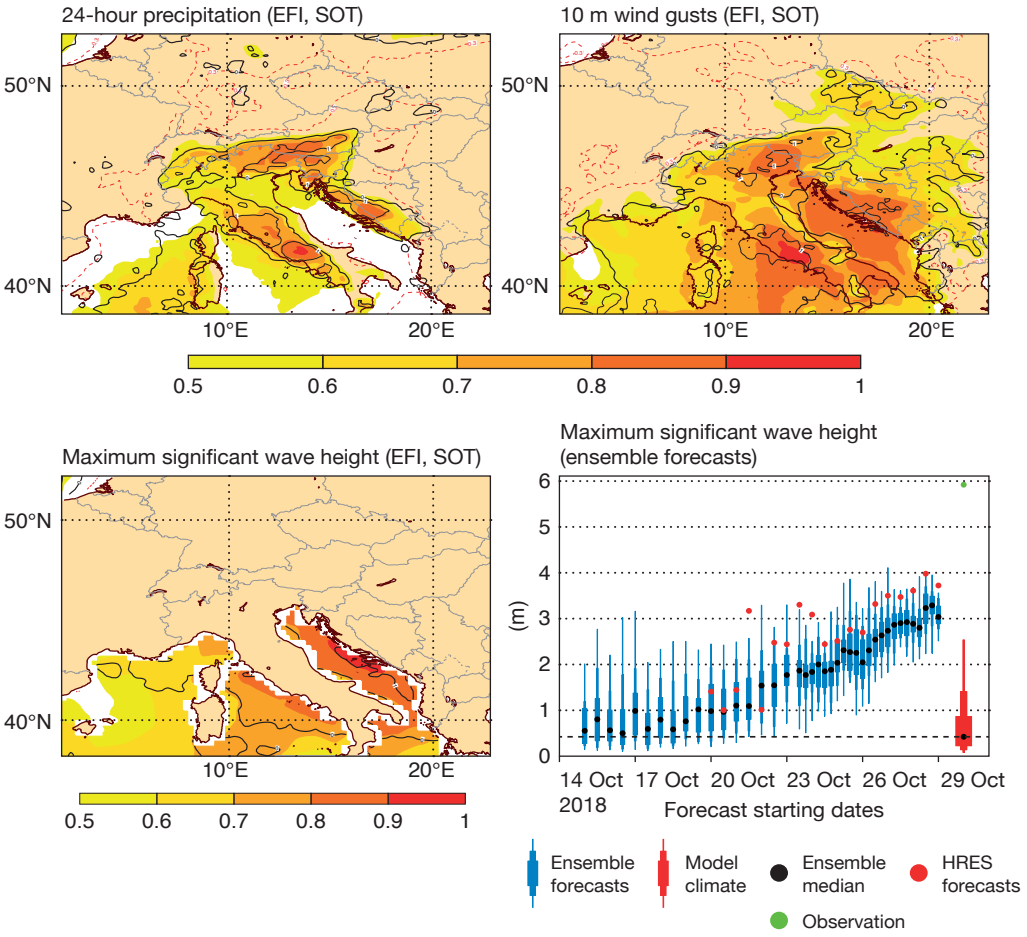

Extreme Forecast Index/ Shift of Tails and wave forecast. EFI and Shift of Tails (SOT) in the forecast from 23 October 00 UTC valid on 29 October for 24-hour precipitation (top left), 24-hour maximum wind gusts (top right) and maximum significant wave height (bottom left). The bottom right panel shows the evolution of maximum significant wave height forecasts for a point off the coast of Venice.